



THE HONG KONG
POLYTECHNIC UNIVERSITY

香港理工大學

Pao Yue-kong Library

包玉剛圖書館

Copyright Undertaking

This thesis is protected by copyright, with all rights reserved.

By reading and using the thesis, the reader understands and agrees to the following terms:

1. The reader will abide by the rules and legal ordinances governing copyright regarding the use of the thesis.
2. The reader will use the thesis for the purpose of research or private study only and not for distribution or further reproduction or any other purpose.
3. The reader agrees to indemnify and hold the University harmless from and against any loss, damage, cost, liability or expenses arising from copyright infringement or unauthorized usage.

IMPORTANT

If you have reasons to believe that any materials in this thesis are deemed not suitable to be distributed in this form, or a copyright owner having difficulty with the material being included in our database, please contact lbsys@polyu.edu.hk providing details. The Library will look into your claim and consider taking remedial action upon receipt of the written requests.

Pao Yue-kong Library, The Hong Kong Polytechnic University, Hung Hom, Kowloon, Hong Kong

<http://www.lib.polyu.edu.hk>

**PREDICTION AND ENHANCEMENT OF THE
SOUND TRANSMISSION LOSS ACROSS
PLENUM WINDOWS**

LI XIAOLONG

Ph. D

The Hong Kong Polytechnic University

2020

The Hong Kong Polytechnic University
Department of Building Services Engineering

**Prediction and Enhancement of the Sound
Transmission Loss across Plenum Windows**

LI XIAOLONG

A thesis submitted in partial fulfilment of the requirements for
the degree of Doctor of Philosophy

MAY, 2020

CERTIFICATE OF ORIGINALITY

I hereby declare that this thesis is my own work and that, to the best of my knowledge and belief, it reproduces no material previously published or written, nor material that has been accepted for the award of any other degree or diploma, except where due acknowledgement has been made in the text.

_____ (Signed)

LI XIAOLONG (Name of student)

Department of Building Services Engineering

The Hong Kong Polytechnic University

Hong Kong, China

May, 2020

ABSTRACT

Noise pollution is an emergent issue to be solved especially in developed cities, as it brings many health problems to citizens, such as high stress level, hypertension, tinnitus etc. Much efforts have been made for the noise control devices, for instance, noise barrier, extended podium, public parks, balconies, plenum windows. Plenum window is an interesting noise reduction device which can provide significant noise attenuation while maintaining a degree of ventilation. Despite the growing popularity of the plenum window, the prediction of its sound transmission loss is not straightforward.

This study firstly tries to propose a prediction model for the transmission loss across the plenum window. Besides, experiments were carried out for the validation of this empirical prediction models. Total of three prediction models were raised for the transmission loss of single plenum window and the second model gives the best prediction of all by comparison. It was also found that the diffracted field and reverberant field inside the plenum window from the theory were weaker than actual experiments. Based on the first part of study, extensive traffic noise transmission loss measurements were carried out inside the residential units of a standalone 30-storey housing block located in an opened environment next to a very busy and noisy main trunk road. Then the prediction and experiment models for the transmission loss of coupling plenum windows and three plenum windows were developed. Results show that the corresponding predictions agree very well with site measurement results.

Besides, lab measurements and simulation was performed on the transmission loss of plenum window installed with rigid cylinder array. Parameters of diameter of rigid cylinder, rigid cylinder array types and gaps of the plenum windows were investigated in present study. Results show that the installment of rigid cylinder array inside the central cavity of the plenum window is effective and can provide significant acoustic protection.

Key words: Plenum windows, Transmission loss, Prediction, Rigid cylinder array.

PUBLICATIONS

Some ideas and figures have appeared previously in the following publications:

Xiaolong Li, S.K.Tang and T. Hung. Sound reductions of plenum windows on the façade of a high-rise residential building in an opened environment. [J]. Building and Environment (Under review).

Xiaolong Li, Y.G. Tong, S.K. Tang, K.K. Lau. Empirical prediction of sound transmission loss across plenum windows chambers [J]. Applied Acoustics. 151 (2019) 45–54.

Li, X., & Tang, S. K. (2019, September). Sound Insulation of Plenum Windows Installed with Rigid Cylinder Array. In INTER-NOISE and NOISE-CON Congress and Conference Proceedings (Vol. 259, No. 8, pp. 1103-1109). Institute of Noise Control Engineering.

Tang, S. K, **Li, X** . (2020, August). In-situ measurement and prediction of traffic noise transmission loss across a residential flat unit façade installed with two plenum windows. The 49th International Congress and Exposition on Noise Control Engineering (INTER-NOISE 2020) Seoul, Korea, 2020

ACKNOWLEDGEMENTS

First of all, my deepest gratitude and appreciation goes foremost to my chief supervisor, Professor Tang Shiu-keung, who offered me the precious study opportunity. High tribute shall be paid to Professor Tang for his patient guidance and fully support on my study and research. He is always so liberal, sagacious and erudite that I have too much to learn from him!

I also owe my sincere gratitude to Professor Zheng Tinghui for her kindness support and generous help on my research and life.

My heartfelt thanks also go to my colleagues in office ZS 801 and friends who always provide good advices during this period.

I should give my hearty thanks to my girlfriend Zheng Ge and her family for their unselfish love and encouragement.

Finally, I am deeply indebted to my parents and my grandma, who always give me the best what they have to unreservedly support my dream at any time. I cannot achieve more without their support, care and love!

Table of Contents

| | |
|--|----|
| Chapter 1 Introduction | 1 |
| 1.1 Background..... | 1 |
| 1.2 Objectives of this research | 5 |
| 1.3 Outline of this thesis | 6 |
| Chapter 2 Literature Review on Noise Insulation Devices with Natural Ventilation | 9 |
| 2.1 Introduction..... | 9 |
| 2.2 Commonly used noise attenuation devices..... | 10 |
| 2.3 Plenum Window..... | 18 |
| 2.3.1 Structure and theory of the plenum window | 19 |
| 2.3.2 Research of plenum window..... | 24 |
| 2.4 Summary..... | 31 |
| Chapter 3 Prediction of Traffic Noise Transmission Loss across Single Plenum Window | 33 |
| 3.1 Introduction..... | 33 |
| 3.2 Sound Transmission Loss Prediction Model | 34 |
| 3.3 Experimental Validation | 36 |
| 3.4 Optimization of Empirical Model..... | 53 |

| | |
|---|-----------|
| 3.5 Conclusions..... | 59 |
| Chapter 4 Sound Reductions Prediction of Multiple Plenum Windows | 62 |
| 4.1 Introduction..... | 62 |
| 4.2 Site Measurement..... | 63 |
| 4.2.1 Building orientation, floor layout and test unit dimensions..... | 63 |
| 4.2.2 Measurement setup | 67 |
| 4.3 Results and Discussions | 70 |
| 4.3.1 Reverberation times | 70 |
| 4.3.2 Traffic noise transmission loss across a plenum window | 72 |
| 4.3.3 Cases of multiple plenum windows | 76 |
| 4.4 Conclusions..... | 83 |
| Chapter 5 Sound Insulation of Plenum Windows Installed with Rigid Cylinder | |
| Array | 85 |
| 5.1 Introduction..... | 85 |
| 5.2 Measurement Setup..... | 86 |
| 5.2.1 Test Chamber | 86 |
| 5.2.2 Scale down model | 88 |
| 5.2.3 Sound Source | 89 |
| 5.2.4 Reverberation Time | 89 |

| | |
|---|------------|
| 5.3 Measurement procedure..... | 91 |
| 5.4 Rigid cylinder array arrangements..... | 93 |
| 5.5 Numerical simulation..... | 97 |
| 5.6 Results and Discussions..... | 99 |
| 5.6.1 TL of the reference plenum windows with different gaps..... | 99 |
| 5.6.2 Effects of regular rigid cylinder array..... | 104 |
| 5.6.3 Effect of rigid cylinder array with single staggered row | 110 |
| 5.6.4 Effect of rigid cylinder array with dual staggered rows | 114 |
| 5.6.5 Effect of the gap of plenum window and the diameter of cylinder. | 118 |
| 5.7 Summary..... | 127 |
| Chapter 6 Conclusions and Recommendations..... | 129 |
| 6.1 Main Conclusions | 129 |
| 6.2 Limitations of this study | 131 |
| 6.3 Recommendations for future work | 133 |
| References..... | 134 |

List of Figures

Chapter 2

| | |
|---|----|
| Figure 2. 1 Commonly adopted plenum windows. (Tang, 2016) | 19 |
| Figure 2. 2 Schematic of a plenum chamber..... | 20 |
| Figure 2. 3 Plenum chamber configuration of Wells (1958). | 21 |

Chapter 3

| | |
|---|----|
| Figure 3. 1 Schematics of a plenum window and the nomenclatures adopted. | 34 |
| Figure 3. 2 Experimental setup and dimension of testing volume..... | 37 |
| Figure 3. 3 Examples of plenum windows tested. | 38 |
| Figure 3. 4 Examples of the spectral variations of TL across plenum windows..... | 46 |
| Figure 3. 5 Improvement of traffic noise reduction across plenum windows by artificial sound absorption. | 47 |
| Figure 3. 6 Spectral variations of $ G_i ^2$ | 48 |
| Figure 3. 7 Comparison between predicted and measured TL_{EN1793} (Eq. (3.13)). | 49 |
| Figure 3. 8 Comparison between predicted and measured TL_{EN1793} ($Q = 4\cos\phi$)..... | 51 |
| Figure 3. 9 Comparison between predicted and measured TL spectra. | 52 |
| Figure 3. 10 Variation of Δ with Q and K (Eq. (3.14) with constant Q_{op} and K_{op})..... | 54 |
| Figure 3. 11 Comparison between predicted and measured TL_{EN1793} (Eq. (3.14) with constant Q_{op} and K_{op}). | 55 |
| Figure 3. 12 Spectral variations of Q_{op} and K_{op} | 56 |
| Figure 3. 13 Comparison between predicted and measured TL_{EN1793} (Eq. (3.14) with frequency dependent Q_{op} and K_{op}). | 57 |

| | |
|---|----|
| Figure 3. 14 Prediction error distributions. | 58 |
|---|----|

Chapter 4

| | |
|--|----|
| Figure 4. 1 Typical floor layout of the surveyed building and its orientation relative to the noise source. | 63 |
|--|----|

| | |
|---|----|
| Figure 4. 2 The surveyed building and its surrounding. | 64 |
|---|----|

| | |
|--|----|
| Figure 4. 3 The four flat layouts and the microphone locations. | 65 |
|--|----|

| | |
|--|----|
| Figure 4. 4 The locations with treatment of sound absorption. | 69 |
|--|----|

| | |
|---|----|
| Figure 4. 5 One-third octave band reverberation times. | 71 |
|---|----|

| | |
|--|----|
| Figure 4. 6 One-third octave band sound levels. | 73 |
|--|----|

| | |
|--|----|
| Figure 4. 7 The measured and predicted $TL_{trafficS}$ of U6, U7 and U13. | 75 |
|--|----|

| | |
|---|----|
| Figure 4. 8 One-third octave band sound levels for U8. | 76 |
|---|----|

| | |
|--|----|
| Figure 4. 9 Comparison between estimated $TL_{trafficS}$ of U8, U10 and U14 plenum windows. | 78 |
|--|----|

| | |
|--|----|
| Figure 4. 10 Comparison between estimated $TL_{overallS}$ of U8, U10 and U14. | 82 |
|--|----|

Chapter 5

| | |
|--|----|
| Figure 5. 1 2-D Layouts of the test chamber (in red). | 87 |
|--|----|

| | |
|--|----|
| Figure 5. 2 Scale down model. (Dimension in mm) | 88 |
|--|----|

| | |
|--|----|
| Figure 5. 3 Line source adopted in this measurements. | 89 |
|--|----|

| | |
|--|----|
| Figure 5. 4 Average reverberation times acquired inside scale down model. | 90 |
|--|----|

| | |
|---|----|
| Figure 5. 5 Measurement devices used for data acquisition. | 91 |
|---|----|

| | |
|--|----|
| Figure 5. 6 Locations of microphones. (Dimension: mm) | 93 |
|--|----|

| | |
|---|----|
| Figure 5. 7 Tested plenum windows and cylinders. | 95 |
|---|----|

| | |
|---|-----|
| Figure 5. 8 Rigid cylinder array arrangement..... | 96 |
| Figure 5. 9 Computational domain and plenum model..... | 97 |
| Figure 5. 10 Computational model with meshing..... | 98 |
| Figure 5. 11 Transmission losses of plenum window with different gaps..... | 99 |
| Figure 5. 12 Sound field of the plenum windows with different gaps..... | 100 |
| Figure 5. 13 Δ TL of the plenum window (gap: 98mm) installed with regular rigid cylinder arrays (cylinder diameter: 19mm) in one-third octave band..... | 104 |
| Figure 5. 14 Sound field of the plenum windows with regular rigid cylinder array.. | 106 |
| Figure 5. 15 Sound field of the plenum windows installed with staggered rigid cylinder array. | 108 |
| Figure 5. 16 Δ TL of the plenum window (gap: 98mm) installed with single staggered row rigid cylinder array (diameter: 19mm) in One-third octave band..... | 110 |
| Figure 5. 17 Sound field of the plenum windows installed with staggered rigid cylinder array. | 112 |
| Figure 5. 18 Δ TL of the plenum window (gap: 98mm) installed with dual staggered rows rigid cylinder array (diameter: 19mm) in one-third octave band..... | 114 |
| Figure 5. 19 Sound field of plenum windows installed with dual staggered rows rigid cylinder array. | 115 |
| Figure 5. 20 Sound field of plenum windows installed with dual staggered rows rigid cylinder array at 630 Hz..... | 117 |
| Figure 5. 21 Δ TL <small>EN1793</small> of the plenum widows installed with rigid cylinder array. . | 118 |

List of Tables

Chapter 3

| | |
|---|----|
| Table 3. 1 Sound transmission across two sample casement windows ($h = 1.35$ m) .. | 43 |
| Table 3. 2 Dimensions of the plenum windows included in the present study..... | 44 |
| Table 3. 3 Sound transmission loss of the plenum windows tested..... | 45 |

Chapter 4

| | |
|--|----|
| Table 4. 1 Flat layout parameters for acoustical calculations.* | 66 |
| Table 4. 2 Positions of microphones relative to lower right hand corner of test unit living room.* | 68 |
| Table 4. 3 Plenum window configurations. | 69 |
| Table 4. 4 Comparison between predicted and measured $TL_{overall}$ (in dBA). | 82 |

Chapter 5

| | |
|--|-----|
| Table 5. 1 Sound transmission loss of the plenum windows. (Gap=98 mm, cylinder diameter= 19 mm)..... | 120 |
| Table 5. 2 Sound transmission loss of the plenum windows tested. (Gap=158 mm, cylinder diameter= 19 mm)..... | 121 |
| Table 5. 3 Sound transmission loss of the plenum windows tested. (Gap=218 mm, cylinder diameter= 19 mm)..... | 122 |
| Table 5. 4 Sound transmission loss of the plenum windows tested. (Gap=158 mm, cylinder diameter= 10 mm)..... | 125 |
| Table 5. 5 Sound transmission loss of the plenum windows tested. (Gap=158 mm, cylinder diameter= 32 mm)..... | 126 |

List of Abbreviations

| | |
|------------|--|
| dB | Decibel |
| dB(A) | A-weighted noise level in decibel |
| $V()^{DS}$ | Rigid cylinder array with upper dual staggered rows |
| $V()_{DS}$ | Rigid cylinder array with lower dual staggered rows |
| EEA | European Environment Agency |
| Eq. | Equation |
| G | Plenum window gap |
| H | Height of the plenum window |
| Hz | Hertz |
| ISO | International Standards Organization |
| l | Length of the plenum window |
| l_o | Overlapping length |
| MLS | Maximum Length Sequence |
| mm | Millimeter |
| MPA | Micro-perforated absorbers |
| NRC | Noise reduction coefficient |
| PML | Perfect Match Layer |
| RT | Reverberation times |
| $V()^S$ | Rigid cylinder array with upper single staggered row |
| $V()_s$ | Rigid cylinder array with lower single staggered row |
| SPL | Sound pressure level; |

| | |
|-------|---------------------------------|
| TL | Transmission loss; |
| W_i | Inlet opening of plenum window |
| W_o | Outlet opening of plenum window |

Chapter 1 Introduction

1.1 Background

Acoustics, one of the physics branches, is the science of sound and concerned with the study of mechanical waves propagating in elastic media, such as solids, gases and liquids. In modern society, the knowledge of acoustics is usually applied in the noise control industries.

Noise is unwanted and unpleasant sound, which is one of the most common and harmful environmental health hazards in the world today (Basner et al., 2014; Jafari et al., 2019). From the point of physics, noise is the sound with irregular frequency and intensity. The intensity of noise is measured in decibels (dB). Human noise response is subjective feeling, which varies from person to person. It generally has local character and decays quickly in air. There will be no leftover noise pollution, once the noise source has been shut down. There are some common noise sources, such as airplanes, ground transportation vehicles, factories, construction sites etc. As noise is one of the most dangerous environment pollutants, statutory authorities enforce laws to control the noise exposure level of their citizens.

In a dense urbanized built environment, residential buildings have to be erected near to major ground transportation lines, such as trunk roads and rail tracks, because of high population density and the shortage of appropriate land for residential purposes. The heavy road traffic then results in serious noise pollution, and such problems

become more and more acute as time goes by. Noise from ground transportation, therefore, affects many people and is a major source of urban pollution.

Traffic noise is the most dominant contributor of noise pollution. Excessive exposure to high traffic noise poses a threat to human health in many ways. According to recent studies, noise contributes to severe hazards, such as cardiovascular disease (Vienneau et al., 2015), annoyance (Hughes & Mabry, 1976), sleep disturbance (Miedema & Vos, 2007), adverse birth outcomes (Wallas et al., 2019), hearing impairment (Gierke, 1990), cognition impairment (Hygge, 2011) and even Alzheimer's disease (Jafari et al., 2019), and could arouse negative emotions (Öhrström, 2006) as well as reduce work efficiency (Khan,2018).

Around the world, tens of millions are affected by excessive noise exposure and suffer from a range of adverse health status (Fritschi, 2011). Statistics from the World Health Organization (WHO) indicates that at least one million healthy life years are lost because of traffic-related noise in western Europe countries every year (WHO, 2018) and traffic noise has been ranked second (the first is particulate air pollution) among the nine environmental stressors reported in Hänninen et al. (2014) in term of health impact. Traffic noise has also been confirmed as the major noise pollution source by the European Environment Agency (EEA, 2013). In Hong Kong, there are ~960,000 people exposed excessively to traffic noise (Hong Kong Environmental Protection Department, 2006). The situation is not expected to improve in the years to come. As a result, protecting people from noise is urgent and necessary. Both legislative and commercial noise control interventions are implemented continuously. The quest for

more effective noise mitigation measures is therefore one of the top priorities of many statutory authorities worldwide.

To mitigate the adverse effects on human and environment caused by noise, there are three ways of noise control. One can control the radiation of the noise source, control the propagation pathway of the noise and apply noise mitigation measures at the receiver. Controlling the noise radiation at source is the best method. By the mechanism analysis of noise source, one can reduce the extra noise level from the source by, for example, modifying the structure of noise source devices, improving machinery precision that lower precision will cause noise pollutant from the mechanical devices, etc. Adding absorption material is a simple option to control the noise from the noise propagation pathway. For the method of noise control from the receivers, reducing the exposure time of noise environment is an effective way to reduce the harmful effects of noise.

In term of the noise control methodology, there are two commonly used methodologies for noise control, passive and active noise control. The passive noise control method is a method that implements with the noise control devices, such as barriers, absorption materials, silencers, dampers, balconies etc. With the application of these devices, noise can be reduced, especially in the high frequency range. While active control technique could reduce the noise level at targeted octave bands. Commonly used active control methods are active noise control and active structural control, which play a key role in the noise reduction at the low frequency range (Liu, 2006).

During the past decades, much efforts have been made by scholars to tackle the noise problems.

The migration of residents to the countryside is an option. However, it does not help much as the original relatively quiet countryside will become noisier as more residents move in. Also, the high demand for residential units in urban areas has forced the statutory authority to re-develop lands for housing estates (both public and private) within these originally noisy areas. This adds to the challenge the government, engineers and academia are facing. A similar situation also exists in other major highly congested cities, such as Tokyo and Shanghai. In consideration of the noise hazard, there is an urgent need for practical noise control method.

The noise barrier is one of the most commonly used noise control devices. It can obstruct the propagation of sound wave between the traffic line and receivers and offer acoustic protection for people.

Increasing the distance between the traffic line and residential buildings with parks and other public building facilities also can provide acoustical protection. Extended podium can act as the noise screen to mitigate noise.

However, the noise control devices mentioned above either require large piece of land for construction or expensive. At the same time, the structure of the device may cause adverse standing wave, which reduces the acoustic protection performance.

Due to the limitation of space and cost, many traditional effective noise attenuation methods cannot be fully applied in congested cities. Thus researchers pay more attention to the weak point of the building façade where noise control device can be

installed in past few decades. The weak points of a building façade include openable parts, mostly balconies and windows. Balcony is an interesting option for noise control and has attracted the attention of researchers. It provides a comfort indoor living space by screening the noise from the outdoors. There have been numerous studies on the acoustical performance of balcony. However, there are limitations. When the distance between the noise source and balcony is short, the acoustical performance will be weakened. The configuration of the balcony also have an effect on the noise reduction.

Certainly, closing the window is the direct way to stop noise. However, it requires mechanical ventilation to maintain comfortable indoor air quality, which costs much electrical energy and has an adverse effect on the environment. Though the double and triple glazing windows can provide significant noise insulation, it also sacrifices the air change of the indoor space.

In order to enable more residential units to be built within relatively noisy urban areas (demand is very strong at least in Hong Kong), a façade device, which has strong sound insulation capacity but at the same time can allow for a reasonable degree of natural ventilation, is in urgent need. This device should also not be bulky so that it can be applied in the congested urban areas of densely populated high-rise cities, where a certain degree of city reverberation may exist.

1.2 Objectives of this research

The present study focuses on the research of the traffic noise transmission loss

across plenum windows. Initiated by Ford and Kerry (1978), the plenum window attracted the attentions of researchers and there are many related studies on this device. The plenum window could provide significant traffic noise reduction while maintaining an acceptable degree of ventilation for the indoor living space. Thus, this device can help reduce energy consumption as less amount of mechanical ventilation will be required. Plenum window has already been implemented in a few residential building in Hong Kong. In order to improve the adaptability of this device, a simple but reliable empirical prediction of the transmission losses of plenum windows is necessary and in urgent need. In view of the current researches of the plenum windows, improving the acoustical performance of this device is also the key point and carries great potential for future development. The main research objectives of the present study are as follows:

1. Development of an empirical prediction model for a standalone plenum window;
2. Development of the transmission losses prediction model for units with multiple plenum windows;
3. Improving the sound transmission loss across plenum windows using add-in rigid cylinder array experimentally.

1.3 Outline of this thesis

A total of six chapters are included in this thesis and brief introduction of each chapter is described as follow:

Chapter 1 begins with a general introduction of noise in cities and its effect on human health. The major objectives of the present study are introduced.

Chapter 2 presents a literature review of the related studies on façade sound insulation devices, which can allow for natural ventilation. At the same time, this chapter especially focuses on the research of plenum windows, which is the key study objective of this thesis. The structure and the studies of plenum window are reviewed in detail.

In Chapter 3, the results of a parametric study on the traffic noise transmission losses across plenum windows are presented. This part of research work is an attempt to develop a practical empirical model for the prediction of sound transmission loss across plenum windows. A total of three prediction models are presented and validated. The prediction accuracy is discussed.

Chapter 4 shows the results of an on-site measurement conducted in a high-rise residential building. This measurement focuses on the traffic noise transmission losses of the plenum windows installed in the tested units. Based on the data obtained, the empirical prediction models proposed in Chapter 3 are further validated and generalized for application to façades with two or three plenum windows. This study proves that the proposed empirical prediction model can provide accurate predictions on the traffic noise reduction across the plenum windows.

Chapter 5 presents a study on the improvement of the sound attenuation of the plenum window using rigid cylinder array experimentally and numerically. Parametric study is carried out with different types of rigid cylinder array, different diameters of the rigid cylinder and different gap widths of the plenum windows. Significant sound transmission losses of plenum windows can be obtained after the installation of the rigid

cylinder array.

In the last chapter, conclusions of this thesis are summarized and presented. Research limitations in present study are addressed and future study recommendations are made.

Chapter 2 Literature Review on Noise Insulation Devices with Natural Ventilation

This chapter reviews the development and study on noise control devices, especially highlighting those devices protecting the indoor cavity from the outdoor traffic noise pollution in residential buildings of high-density cities. The presented noise control devices are meaningful for the sustainable development of cities with high population density, as they can offer significant traffic noise attenuation while maintaining a reasonable level of natural ventilation. The application of these types of equipment should help reduce energy consumption of mechanical ventilation. Plenum window, a recently proposed sound insulation device consisting of a plenum chamber, is particularly discussed in this chapter. In the meantime, fundamental principles and theoretical mechanisms of the sound transmission losses across the plenum window in existing references are also summarised in this chapter.

2.1 Introduction

Noise from the road traffic is one of the biggest threats to public health. In order to eliminate the effects of noise pollution on human health, the migration of residents to the countryside is an option. However, it does not help much as the original relatively quiet countryside will become noisier as more residents move in. Also, the high demand for residential units in urban areas has forced the statutory authority to redevelop lands for housing estates (both public and private) within these originally noisy areas. This

adds to the challenge the government, engineers and academia are facing. A similar situation also exists in other major highly congested cities, such as Tokyo and Shanghai. In consideration of the noise hazard, there is an urgent need for practical sound insulation devices to alleviate the agitation brought by noise problems. To tackle the problem of traffic noise annoyance, much effort has been made by researchers and engineers.

2.2 Commonly used noise attenuation devices.

Increasing the separation between noise sources and residential buildings using public parks is a noise mitigation option (Hong Kong Planning Standard and Guidelines, 1990). The existence of a park can reduce the sound energy reaching the building façade to a certain extent. Trees and other facilities in the parks could serve as sound barriers for traffic noise, which also help reduce the sound pressure level to the residents. However, the construction of public parks or squares requires a large piece of land that is extremely luxurious and infeasible in the main regions of congested cities. So it is not applicable in congested urban areas. The problem can also be political too. The use of extended podium (Hong Kong Planning Standard and Guidelines, 1990) in urban areas is restricted by the limited land supply and is a costly alternative too, as it will result in a substantial loss of residential units within the construction site boundary.

The most commonly used noise control device is the road noise barrier (Kurze & Anderson, 1971) which gives acoustical protection to the residents within its shadow zone by obstructing the direct-line-of-sight between the residents and the ground traffic

lines. The noise barriers could mitigate the effects of traffic noise for residents who are exposed to noise pollution environment. Numerous researches have been carried out for an understanding on the acoustical performance of this kind of device. Okubo & Fujiwara (1998) studied the noise mitigation efficiency of the noise barrier installed with a Waterwheel cylinder whose surface pressure is zero. From the two-dimensional simulation study, results showed that the performance of traffic noise attenuation was better than cases without the Waterwheel cylinder. Improvement by this 'soft' cylinder depended on frequency and was affected by the configuration of the cross section. Hart and Lau (2012) conducted simulation on a noise barrier installed with linear arrays of active noise control sources and found that the noise energy near the barrier was significantly minimized uniformly. However, a barrier can also result in adverse standing wave patterns between its structure and the residential building façade it is supposed to protect (Li & Tang, 2003), reducing the overall acoustical protection.

Noise enclosures or acoustic enclosures can reduce noise pollution and shield noise energy. But noise is emitted from the opening of the enclosures' structure, making these locations inhabitable (Takagi, Miyake, Yamamoto & Tachibana, 2000).

Setbacks and extended podia also can provide protection from noise pollution (Hong Kong Planning Standard and Guidelines, 1990). However, their high construction cost makes it not cost-effective in terms of noise attenuation (in dBA) per dollar spent. Also, the construction of these noise control devices needs a large piece of land such that it is often not an option for application in the already very congested urban areas. Besides, the existence of these structures will have an effect on the vision,

illumination and natural ventilation, which will affect residents' living comfort. Construction of barriers, enclosures, setbacks and extended podia is not suitable in congested urban areas.

Owing to capital and land constraints, the choice of effective noise mitigation measures which can be applied along the sound propagation path in urban areas is limited. Noise mitigation devices that can be attached to the weak points of a building façade have aroused scholar's interest during the past few years. These weak points are openable parts, mostly windows, through which outdoor noise intrudes into the residential units.

The balcony appears to be an interesting alternative for traffic noise reduction. It can serve as a noise barrier and protect the indoor cavity from noise pollution (May, 1979). Apart from noise insulation, the balcony can enhance natural ventilation and illumination of the indoor space, so it is very popular. A balcony can also cut off the pathway of the sound wave and prevent the sound waves from reaching the receiver directly. Its noise screening performance has been extensively studied. Tang (2005; 2017) had summarized the screening effects of different forms of balconies. A balcony can provide some noise attenuation while maintaining significant natural ventilation for indoor space, which makes it a suitable option in the design of green building.

As a common façade noise control device, many types of research were conducted on the acoustical performance of the balcony. These studies tend to find the mechanism of the sound mitigation and enhance its ability of traffic noise reduction by different methods.

Mohsen and Oldham (1977) conducted a parametric study on the acoustical protection of a balcony. This study took detailed parameters, such as balcony configuration, effect of a parapet, locations of the balcony, inlet sound orientation, window configurations, the distance between balcony and sound source, into consideration. Both a 1/10 scale down model test and simulation were carried out in this study. Their results indicate that the enclosure balcony can provide an insertion loss of about 5dB on average. Oldham and Mohsen (1979) also provided an empirical formulation for balcony insertion loss. However, it should be noted that nearly all balconies at the façade of a high-rise building have ceilings, which tend to reflect sound into the balcony void. The overall noise screening capacity of a high-rise building balcony is therefore weak (Hammad & Gibbs, 1983; Tang, 2005; Tang, 2010). The closer the balcony to the noise source, the worse will be the screening performance.

May (1979) carried out a site measurement inside the balconies of a high-rise building next to a busy traffic line. This research indicates that reflections inside the balcony cavity have an effect on the acoustic performance of this device. In order to eliminate the reflection resulted from ceiling reflection, the installation of absorption materials inside the balcony cavity is necessary. Results show that the installation of sound-absorbing material can enhance noise attenuation. Balcony with absorption on the ceiling provides an insertion loss of 4-5 dB. More add-in absorption (around 1/3 surface area of the tested balcony with Sabins) results in 7-8 dB noise reduction.

In another paper, Hammad and Gibbs (1983) conducted a measurement with a 1/10 scale down model. When there is no obstacle between the receiver and noise source,

the acoustic performance of the balcony is not significant and is frequency-independent.

Tang (2005; 2010) carried out a study with a 1/10 scale model to investigate the effect of the adjacent structures of balconies on the insertion loss. There was a total of four different types of balconies included in this study. These balcony types are commonly adopted in residential buildings. The acoustical performance of the front wall and side panels of a balcony were examined. Results show that noise reduction of a balcony presents great difference with and without a front panel. It is due to the presence of the ceiling. Reflection occurs and reduces the noise attenuation ability of this device. This phenomenon becomes more obvious when the noise source is located at a faraway distance from the balconies. Negative insertion loss was also obtained in the test conditions. Incidence angle was considered as a factor in the insertion loss in this study. Without the reflection of top ceilings, the elevation angle of the sound source is closely related to the sound reduction obtained from the balcony. Acoustic modes that occur inside the balcony cavity correlate to the peaks in the insertion losses spectrum.

In order to improve the noise screening performance of the high-rise building balcony, there have been numerical studies and site measurements concerning the sound absorption application inside a balcony. May (1979) have suggested the addition of sound absorption can contribute to the noise reduction of the balcony, but the related transmission loss was not presented.

Hothersall et al. (1996) built a two-dimensional multiple-balconies model with the method of boundary element to investigate the effect of different absorption treatments

inside the balcony. The model just consisted of the front and rear walls without consideration of the sidewall. Results obtained from different floors show that in the presence of the upper ceiling and back wall, the acoustical protection of balconies is not significant. A total of eight different treatments to the balcony structure were calculated in this research work. The upper ceiling and the rear wall are the most efficient location of absorption material installation for noise reduction. Traffic noise reduction ranges between 5 dB and 8dB. The best treatments of absorption inside the balcony provide 10 dB insertion loss. When installed on the ceiling of the balcony, the absorption could provide a more significant insertion loss than other cases, in which the absorption treatment was lined on the surface of the rear wall or the outside surface of the front wall facing the traffic line directly.

Tong et al. (2011) conducted a full scale model experiment on a balcony-like device to examine the insertion loss of this structure. The upper ceiling of this balcony-like device is the prior place for the treatment of absorption material, then is the side panels. Acoustic modes and the resonance inside the balcony void will affect the spectrum characters in 1/3 octave band. Results show that as large as 7dB insertion loss can be achieved.

There have also been investigations that suggested modifying the balcony ceiling and the parapet to control noise propagation. El Dien and Woloszyn (2004; 2005) used a balcony model with an inclined ceiling instead of a horizontal one. Their results indicate that the modified inclined ceiling has an impact on the reflection by changing its propagation pathway. The location, height and depth of the balcony both are in a

positive relationship with noise insulation. This modified structure can produce around 0.5-6 dBA higher insertion loss than the conventional balcony structure.

By the installation of the ceiling-mounted forms, Ishizuka and Fujiwara (2012) investigated the noise attenuation performance of a modified balcony. The modified ceiling structure acts as a reflector to change the pathway of wave reaching the ceiling surface. With these reflectors, an extra 7-10 dBA can be obtained in the condition that the incidence angle is close to the incline angle of the ceiling forms. However, there are incidence angle and balcony height limitations.

Cheng et al. (2000) tried to add a horizontal noise screen on the façade of the balcony and tested the acoustical performance of this designed form. Scale model test was adopted for the validation of theoretical results. However, one does not usually have the luxury of a balcony large enough to implement their suggestions in the congested urban area of a densely populated city. Also, the balcony is only effective if the noise source is located at a lower height than the balcony. It will not be effective inside an urban street canyon, especially at lower floor levels where the noise levels are relatively uniform due to street reverberation (Ko et al., 1978).

There were few types of research on the applications of horizontal lintels (Tadeu et al., 2007) and eaves (Sakamoto, 2008) for noise screening, but the limited lengths of these protrusions and the various reflections make them not so effective as façade noise mitigation devices.

Protrusions installed on the window structures can help screen traffic noise, prevent the noise from entering room directly. At the same time, these devices can direct

sunlight into the residential units. The acoustical performances of different types of protrusive devices are reviewed in Tang (2017).

Lintels, a kind of horizontal flat plate installed on the top and bottom edges of windows, can screen the noise emitted from a lower location, playing the role of traffic noise barriers and flashing board. Tadeu et al. (2007) conducted a simulation to examine the acoustic behavior of the thin rigid screens. Three different types of rigid screen forms were examined and the structure with curvilinear configuration was found to provide the best acoustical performance. More significant noise reduction was obtained on the upper floors.

In terms of the single vertical fin, reflection can reduce the acoustical performance of this device. Adding absorption material can help improve noise reduction. Two vertical fins together will cause multiple reflections and reduce sound insulation severely. Janczu et al. (2011) investigated the reflections inside the region of two fins by simulation. This research tried to present a modified configuration of the façade to achieve acceptable acoustical protection. Simulation results were verified by site measurements and the acoustical benefit for the upper units was obvious. However, a single vertical fin should provide no more than 3 dB noise reduction.

Louvers, eaves and the combination of these structures are another kind of protrusion that can adjust temperature and screen noise. Martello et al. (2015) carried out experiments to test the sound reduction of louvers with absorption treatment. Results show that the presence of sound-absorbing louvers can help reduce the sound pressure level on the glass surface, thereby enhancing sound insulation of this shading

device. Especially at frequency between 1600 Hz and 5000 Hz, the noise reduction of sound absorbing louvers is significant. The adoption of absorbing louvers provide an extra 5 to 6 dB noise reduction on average.

However, reflections from nearby buildings or structures are not taken into consideration in most of the studies abovementioned. Though Janczu's research (Janczu et al., 2011) has included the influence from traffic structure, it misses the effect of neighborhood buildings. The presence of city reverberation will weaken the noise abatement behavior of these noise screen protrusions.

2.3 Plenum Window

Certainly, one can stop the noise intrusion by closing all the windows. However, this is done at the expense of indoor air quality, unless mechanical ventilation is provided (for instance, Asdrubali and Buratti (2005)).

Mechanical ventilation consumes electrical energy and thus is not recommended under the growing concern of sustainability. Therefore, the double and triple glazing windows (Tadeu & Mateus, 2001), though having strong sound insulation capacity, are not applicable in residential buildings unless they are used as 'fixed' (non-openable) windows for daylight utilization. In order to enable more residential units to be built within relatively noisy urban areas (demand is very strong at least in Hong Kong), a façade device, which has strong sound insulation capacity but at the same time can allow for a reasonable degree of natural ventilation, is an urgent need. This device should also not be bulky so that it can be applied in the congested urban areas of densely

populated high-rise cities, where a certain degree of city reverberation may exist. Efforts have been made to explore effective alternatives, which are more acceptable in actual application.

2.3.1 Structure and theory of the plenum window

The plenum window is a window system with a chamber consisting of two staggered glass panes, first adopted by Ford and Berry (1973) in laboratory testing. Based on existing literature, there are two types of plenum window, vertical plenum window and horizontal plenum window, which are classified by the orientation of inlet and outlet openings, as shown in Figure 2.1.

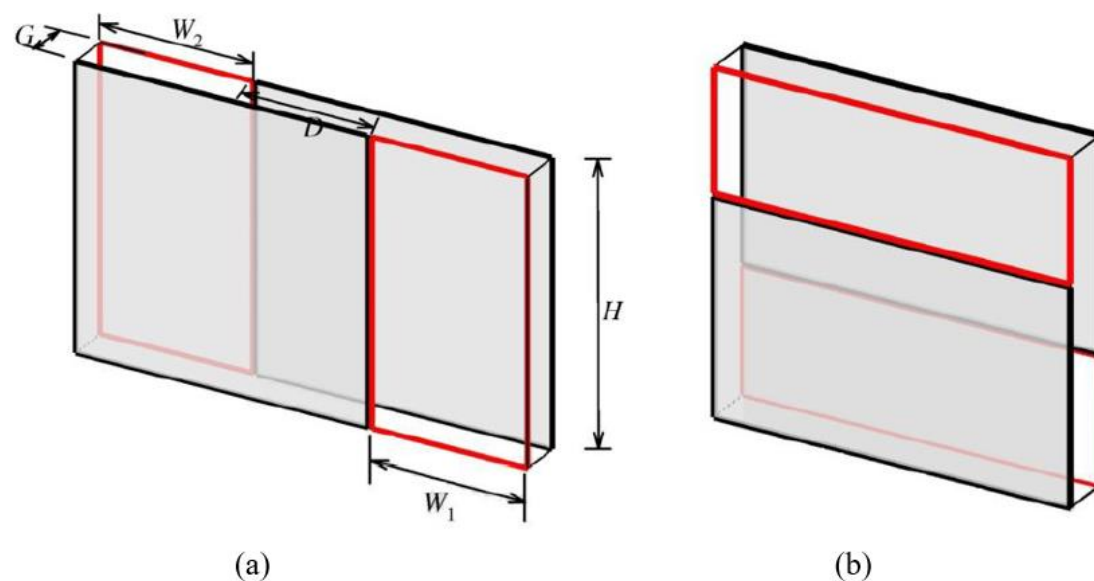


Figure 2. 1 Commonly adopted plenum windows. (Tang, 2016)

(a) Horizontal plenum window; (b). Vertical plenum window.

The plenum window is derived from the partially open double glass window resembling a plenum chamber (Ford & Kerry, 1972). Before further discussing the related researches about plenum window, it is fundamental to have an understanding

on the sound attenuation mechanism of the plenum chamber.

The plenum chamber is one kind of commonly used reactive silencer, which is usually like a large rectangular enclosure with an inlet and one or more outlets

According to the existing literature, the plenum chamber firstly appeared in Dr. Hardy's study on the noise control of jet engine testcells (Hardy, 1952; Wells, 1957). Plenum chamber is usually adopted in the mechanical ventilation system, connected the air ducts and a fan to adjust airflow and attenuate the noise from the mechanical ventilation system (Sharland, 1972). A plenum chamber can take the shape of a cylinder or cuboid, but the most commonly adopted configuration is the rectangular shape.

The plenum chamber, shaped as a rectangular enclosure, consists of an inlet opening and an outlet opening, as shown in Figure 2.2. Sound energy enters into the device through the inlet opening, fills up the chamber cavity, then a portion of it get reflected at the outlet opening while the rest goes out of the chamber via that opening. As only part of the incident sound energy can pass across the chamber, noise reduction is achieved.

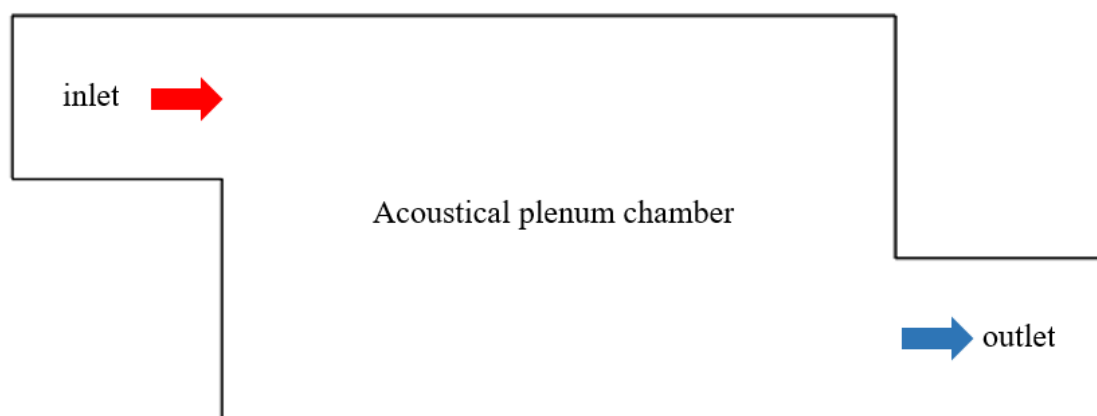


Figure 2. 2 Schematic of a plenum chamber.

In the present study, acoustical performance is the key point of attention. Thus, attention is paid on the noise attenuation of plenum chamber. Documented by the numerous literature, a number of models have been proposed to predict the noise reduction of the plenum chamber.

Wells (1958) proposed a theoretical model for predicting the sound transmission losses of plenum chambers. Based on room acoustics equations, a modified formula (Eq. 2.1) is derived for the estimating the sound transmission loss the model shown in Figure 2.3.

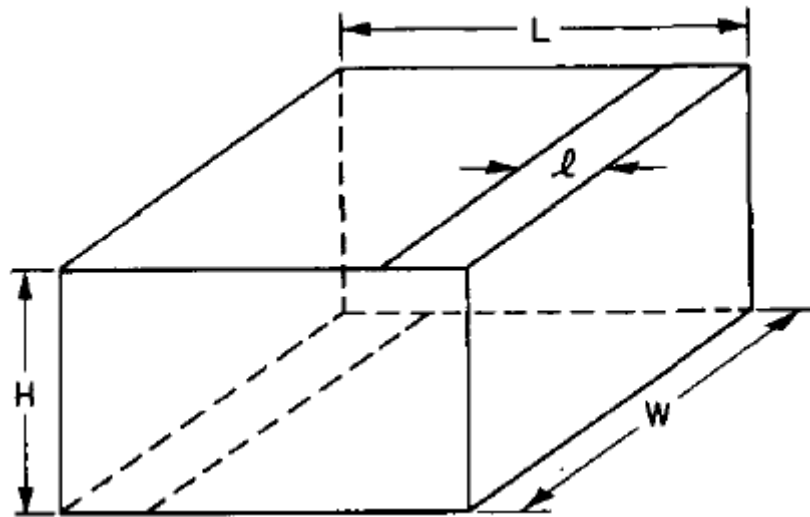


Figure 2. 3 Plenum chamber configuration of Wells (1958).

$$TL = SPL_{out} - SPL_{in} = -10 \log_{10} \left(\frac{A_{out}}{R} + \frac{A_{out} \cos \alpha}{2\pi d^2} \right) \quad Eq. 2.1$$

where TL is sound transmission loss, SPL the sound pressure level, the subscripts 'out' and 'in' refer to the inlet opening and outlet opening respectively, $d^2 = (L - l)^2 + H^2$ the slant distance between the inlet opening and outlet opening, $\cos \alpha = H/d$, A_{out} is

the outlet opening area of the plenum chamber and R is the room constant of the plenum chamber:

$$R = \frac{S_{total}\bar{\alpha}}{1 - \bar{\alpha}} \quad Eq.2.2$$

where S_{total} is the total internal surface area of the plenum chamber and $\bar{\alpha}$ the mean surface area absorption coefficient of the chamber interior in m^2 Sabines.

In Wells (1958), a small scale down model was used for the laboratory measurements to provide a reference for the prediction results. By comparison between predicted and test data, the results indicate that the predicting transmission losses only show acceptable agreement with the test results at high frequency and with small window opening size. At low frequency where the wavelength is larger than the length of plenum chamber, the prediction model overestimates the sound transmission loss by 5 to 10 dB.

In order to predict the sound transmission loss of the plenum chamber integrally, Cummings (1978) proposed two theoretical models. One of the models is suitable for transmission loss prediction at low frequency and the other is applied for the prediction at high frequencies. The prediction results were compared and validated by the measurement data in Cummings (1979).

In terms of the low frequency range prediction model, higher order acoustic modes are excited inside the plenum chamber cavity. The inlet sound field is composed of the incident waves and reflected waves, while there is no reflection at the outlet side from downstream. Inside the plenum chamber, the sound field is assumed to consist of high order modes and direct sound. The linear equations with unknown mode magnitudes

developed through modal matching can then be solved. The process is summarized in Li and Hansen (2005).

For the high frequency model, the incident sound field is assumed to include numerous higher acoustic modes and can be described as (Wells,1958):

$$TL = -10 \log_{10} \left(\frac{A_{out}}{R} + \frac{A_{out} Q(\theta) \cos \alpha}{2\pi d^2} \right) \quad Eq. 2.3$$

where Q is the directivity factor and $Q(\theta) = 4 \cos \theta$. In this prediction model, room constant R is derived by equation 2.2 with statistical absorption coefficient instead of the original coefficient. It is obvious that the high frequency model becomes the low frequency model when $Q=2$.

Compared to the measurement data, the low frequency prediction model could offer an anastomotic transmission loss at frequencies below the first order cut-on frequency of the duct. In the higher frequency range, the theoretical model underestimates the sound reduction.

There are also many studies on the prediction of sound transmission loss in the past few decades. One of the most commonly used classic means is the transfer matrix method. Munjal (1987a, 1987b) proposed a numerical prediction method, which includes four-pole parameters and assumes the inlet and outlet as rigid boundaries. The plenum chamber is delimited by three sections, namely the inlet port, the chamber cavity and the outlet port. A set of linear equations is developed for each section and connected by the boundary relationship. Though the prediction method proposed by Munjal can save computing resources and improve the efficiency of calculation, by

comparing the theoretical method and finite element method, the agreement between both methods is not good at high frequencies.

Huang et al. (2011) also proposed a model with the method of modal matching used by Cummings to obtain a set of linear equations for transmission loss of the plenum window. Yu, et al. (2017) proposed a numerical prediction model was proposed for the noise reduction of plenum windows. Although the prediction results are proved to agree with the measurement results reasonably, the numerical procedure is inapplicable to be applied in practice for engineers.

2.3.2 Research of plenum window

First, a set of experiments conducted by Ford and Berry (1973) was aimed to examine the noise reduction of a partially opened window with staggered glass panes. This test included two types of the staggered double glass windows, one was placed in the horizon and the other was placed in the vertical direction. Both windows were equipped with inlet and outlet openings with a gap between two glass panes. Test results show that a horizontal staggered double glass window provides better acoustical performance than a vertical one. A 2.4m width window, resuming as an elongated chamber with a separation between two glass pane of 0.2 m and the width of the opening is 0.03 m, can produce as large as extra 9 dBA noise reduction compared to a conventional window. However, the partially opening width is 100 mm, which is much smaller than the width of the adopted window.

The study of Ford and Kerry (1973) opens a new direction for the noise attenuation by a staggered double glass window. The simple structure and decent acoustical

performance of this type of window have attracted the interest of scholars. Since then, related experimental researches of this modified window system, which is also known as plenum window or ventilation window, have begun (hereinafter referred to as plenum window).

In order to improve the traffic noise reduction of the plenum window, numerous researches have been conducted. In these studies, measurement method (on-site and laboratory scale model test), computer simulation and theoretical method were partially or totally used.

The introduction of add-in silencers or absorption materials is the direct method for the improvement of the acoustical performance of the plenum window. Kang and Brocklesby (2005) conducted a series of experiments to investigate the acoustical behaviors of plenum window installed with transparent micro-perforated absorbers (referred to MPA hereafter). Natural ventilation and daylighting conditions were considered in their study. MPA was installed inside the chamber cavity or air gap. By changing the width of the air gap and the distance between MPA panes, the noise reduction was investigated. Results show that the plenum window with MPA can provide 2 to 6 dB between 500 and 8000Hz. Higher noise attenuation was found as the width of the air gap increased. However, the light penetration was reduced as a result of the use of multiple MPA layers. When the airflow speed inside the chamber of the plenum window was controlled below 2 m/s, the acoustic protection of MPA was acceptable.

Kang and Li (2007) carried out a numerical study on the plenum window by finite

element method. In this investigation, noise level difference between the two sides of a typical plenum window with and without louvers and MPA was examined. Simulation results indicate that absorbers can effectively improve the sound pressure difference between the inlet and outlet of a plenum window system. Results show that noise reduction provided by this window system is around 20 dB in terms of the average value at 125Hz- 1kHz when there is no absorber. The installation of rigid louvers inside the central cavity of the plenum window contributes slightly to its acoustical performance. Absorption louvers whereas provide higher noise reduction instead. External hood installed outside the plenum window outer opening is also an effective option for noise reduction. Longer hood produces higher sound insulation, which is more obvious at lower frequencies. All of the studied cases in this research meet the ventilation requirement.

Tong and Tang conducted a systematic study on the plenum window. First, Tong and Tang (2013) conducted a 1/4 scale down model experiment to investigate the acoustical performance of the plenum window. It is notable that a line source is used to mimic the traffic line. Two kinds of insertion losses based on the relative orientation between line source and model were presented in these experiments. Increasing the angle results in a lower noise reduction. For a plenum window, a “favorable” orientation was found. This refers to the case where the sound waves can enter into the model indoor space without much resistance. The existence of the “favorable” orientation, resulting from the configuration of plenum window design, will reduce the noise reduction rapidly. It is worth noting that the incidence angle should avoid such

“favorable” orientation for better noise attenuation. Reducing the window opening or the width of the air gap can also help ease the effect of “favorable” orientation.

For the first kind of insertion loss in Tong and Tang (2013), the best noise reduction is about 14 dB and the minimum insertion loss is between 4 and 6 dB. For the second examination, due to the selected reference case, both effects of the plenum window and incidence angle are taken into consideration. The maximum and minimum insertion losses obtained are 18 dB and ~8 dB respectively. The same “favorable” phenomenon occurs in this circumstance. Besides, the results show that the lower order acoustic modes have a significant effect on the noise reduction at low frequency that the insertion loss around 300 Hz is more than 15 dB suggested by the narrowband data.

With two mock-up test rooms built beside a busy traffic line, Tong et al. (2015) conducted a full scale field experiment to describe the benefit of the replacement of conventional window with a plenum window and the effect of indoor settings. These two test rooms were of the same configurations but installed with different windows. One room was installed with conventional windows and the other with plenum windows. Research results indicate that not only the acoustic modes in the chamber cavity of the plenum window but also the modes in the room space will affect the insertion losses at frequencies below the 400 Hz 1/3 octave band. The existence of a partition can strengthen the effect of room modes. Compared to the case with a conventional window, the case installed with a plenum window provides extra ~6 dB sound attenuation. At higher frequencies, the plenum window offer around 10 dB noise reduction. The placement of furniture has slightly affected the insertion losses in this

study. Results illustrate that a plenum window can provide better acoustical performance than the conventional window and the weighted noise reduction is from 7.1 dBA to 9.5 dBA. When both rooms were with furniture, the acoustical benefit difference was between 1 and 1.5 dBA. For the unfurnished cases, the acoustical benefit difference was smaller at between 0.6 dBA and 1 dBA.

Fiberglass is also a commonly used sound absorption material for the improvement of noise reduction. In Tang's on-site measurement (Tang, 2015), MPA and fiberglass were both adopted in the vertical type plenum window. In this research, plenum windows were installed on the façade of a student dormitory building in Hong Kong. When there was no absorption treatment, the obtained average transmission loss is 19 dB. When an indoor window glass panel was treated with fiberglass and micro-perforated absorbers, the highest insertion loss was 23 dB.

Except for the method of adding absorption material inside plenum window (Tang, 2015), Tang investigated the acoustical effect of the slant glass pane of a vertical plenum window (Tang, 2016). In this study, a 1/4 scale down model was adopted and the outdoor glass panel was fixed, the indoor glass panel was inclined. The acoustical performance of the plenum window with an incline angle of -5° and 5° was tested. Measurements results show that the inclined glass panes cannot enhance the noise reduction of the plenum window.

The effect of the active noise control system on the noise reduction of a horizontal plenum window was examined by Tang et al. (2016). In this test, a full-scale model with a plenum window was used to test the active noise cancellation system in the

laboratory. To gain the highest noise reduction, two secondary sources should be symmetrically mounted on the centreline directly facing the incoming noise inside the plenum chamber.

Then, another study about the introduction of add-in structure inside the plenum window was carried out by Tang (2018). A numerical simulation study was conducted to investigate the transmission loss of the plenum window after the installation of a rigid circular cylinder array. A series of two-dimensional FEM simulations were adopted to observe the acoustical benefit of the installation of different types of rigid cylinder array. The wave propagation in the window cavity was also discussed. By the installation of the rigid circular cylinder array, broadband improvement of sound insulation is achieved. Though more cylinders in the array produce higher noise reduction, the number of rows is advised to be less than 3 for acceptable natural ventilation. The nodal and anti-nodal positions are important locations for placement of cylinders, where the acoustic modes are affected greatly by the rigid cylinder array. Compared to a regular cylinder arrangement, an array with staggered rigid cylinder rows provide better noise attenuation performance. In this study, the maximum noise reduction is around 5 dBA. Compared to the improvement resulting from the addition of sound absorption linings, the obtained results are significant and comparable.

Huang et al. (2011) examined the use of active control in improving the low frequency acoustical performance of a plenum window using both analytical and experimental methods. They developed an analytical model for the sound field at low frequency in the plenum window cavity and room space. Through simulation validation,

the proposed model was proved to be effective. Results show that when the secondary loudspeaker is located at the center point of the plenum window bottom, this window system can provide the best acoustical performance. The effective frequency cap for single and multiple channel active noise control systems are 390 Hz and 420 Hz respectively. With the active noise control system, the plenum window could offer extra noise reduction as large as 20 dB. However, the sound in this study was assumed to be a plane wave and incident perpendicularly onto the plenum window outer opening, the case of oblique incidence was not considered.

By laboratory test and field measurements S øndergaard and Legarth (2014) investigated the noise reduction of a vertical plenum window. In the laboratory test, the effects of configurations, opening size and absorption material on the noise reduction were examined. Then the application effectiveness of the vertical plenum window in 14 flats of a building was presented. Results show that the sound attenuation was between 16 and 24 dB.

The double-facade system presented in the study of Bajraktari et al. (2015) could provide noise attenuation range from 18 to 26 dB.

Yu et al. (2017) proposed a simulation model to predict the noise reduction of the plenum window within the mid-to-high frequency range. They studied the effects of the window sizes, opening area and absorption material on the transmission loss.

Recently, Lee et al. (2019) carried out experimental study to explore the effect of sonic crystals and flap with jagged shape on the noise reduction of a plenum window. It is found that after the incorporation of the rectangular sonic crystals, plenum window

can provide a noise attenuation as high as 9.5 dBA in the white noise environment. Noise reduction resulted from the installation of flat flaps is not significant and is no more than 1.7 dBA in test cases. Between 900Hz and 1000 Hz, extra 2.3 dBA or more noise reduction is provided by the plenum window with rectangular sonic crystals.

Lee et al. (2020) investigated the acoustic performance of the plenum window by incorporation of sonic crystals. For the normal incident noise, plenum window installed with 3 sonic crystals give the best noise reduction, 4.2 dBA and 2.1 dBA at frequency around 1000 Hz for traffic noise and construction noise, respectively. Maximum noise attenuation is ~5.5 dBA at 630 Hz.

2.4 Summary

In this section, commonly used noise control devices are reviewed. These devices can provide noise reduction while maintaining natural ventilation. The noise control device, such as barrier, extended podia, balconies can provide acceptable noise reduction in required conditions. However, the construction of these structures needs space and land sources, rendering them not suitable for congested urban areas.

The research on plenum windows has been reviewed in detail. In more of the cases, noise reduction performance is the focus. In order to improve the acoustical performance of plenum windows, several methods have been implemented. These include add-in structures and absorption materials, active noise control method, numerical study of the propagation of the waves inside the structures, modification of the configuration of plenum windows, parametric study on the configuration of plenum window both on-site and in laboratory.

In consideration of the popularity of the plenum window, an engineering formulation for the prediction of the window sound insulation performance is needed in practice. One may do the prediction on a case-by-case basis using finite-element methods (Yu, 2017), but a 3D simulation that covers the whole traffic noise frequency range is too computer-resource demanding to implement. In addition, the acoustical performance of installation of rigid cylinder array inside the plenum window has not been validated in experiments. Meanwhile, the acoustical performance of the plenum window installed with rigid cylinder array at lower frequencies is not so significant such that an improvement method is required too.

Chapter 3 Prediction of Traffic Noise Transmission Loss across Single Plenum Window

In this chapter, a parametric study on the traffic noise transmission loss across plenum windows was carried out experimentally in an attempt to establish a simple empirical model for predicting this transmission loss.

3.1 Introduction

Despite the growing popularity of the plenum window, the prediction of its sound transmission loss is not straight-forward. The discontinuous boundary structure of a plenum window is not amendable to analytical solution. One can try mode matching approximation as in Cummings (1978) and Huang et al. (2011), but the oblique sound incidence condition in practice complicates the matching procedure. One will also need to take into account of a lot of acoustic modes if the analysis is to cover the practical traffic noise frequency range (Lau & Tang, 2000; Li & Hansen, 2005). The numerical procedure of Yu et al. (2017) can produce results in reasonable agreement with experimental data in general, but it is not easy for practitioners to use. One can always use finite-element computation, but it is impractically computing resources demanding for simulation above 500 Hz.

In this study, attempt is made to develop a simplified method to predict the traffic noise transmission loss across plenum windows. Laboratory experiments are conducted to calibrate the proposed method. Frontal sound incidence is considered in

this study as the effect of source orientation is basically known from the results of Tong and Tang (2013). Results of the field measurement of Tong et al. (2015) are used for validation.

3.2 Sound Transmission Loss Prediction Model

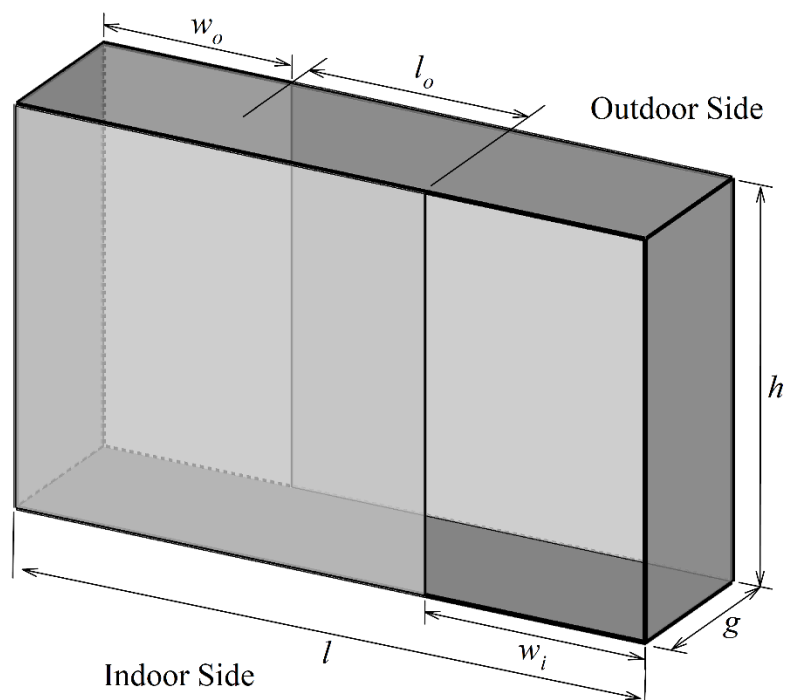


Figure 3. 1 Schematics of a plenum window and the nomenclatures adopted.

Figure 3.1 shows the schematics of a plenum window and the nomenclature adopted in this study. For simplicity, the plenum window is treated as a plenum chamber in the prediction model to be proposed. The sound field inside the window therefore consists of two components. One is the diffracted field and the other the reverberant field. Wells (1958) made use of room acoustics equations and approximated the sound transmission loss across a plenum chamber, TL , as :

$$TL = -10\log_{10} \left[w_o h \left(\frac{\cos \phi}{2\pi d^2} + \frac{1}{R} \right) \right], \quad Eq. 3.1$$

where R is the plenum cavity room constant, d the slanted distance between the centres of the two openings and ϕ the diffraction angle (thus, $\cos \phi = g/d$, where g is the gap distance between the two glass panes). Though the aspect ratio of the plenum window cavity is large compared to that of a regular plenum chamber (Ih, 1992) such that the assumption of a uniform reverberation field may not be so valid, the simplicity of the above approach suffices. Cummings (1978) proposed a hybrid model in which mode matching is used to obtain the low frequency TL , while the high frequency TL is estimated by a modified version of Eq. (3.1) :

$$TL = -10\log_{10} \left[w_o h \left(\frac{\cos^2 \phi}{\pi d^2} + \frac{1}{R} \right) \right]. \quad Eq. 3.2$$

For simplicity, it is proposed to estimate the plenum window cavity room constant using conventional method in building acoustics (Kinsler et al., 2000):

$$R = \frac{w_i h \alpha_i + g(2h + l)\bar{\alpha} + w_o h \alpha_o}{1 - \frac{w_i h \alpha_i + g(2h + l)\bar{\alpha} + w_o h \alpha_o}{2(gl + gh + lh)}}, \quad Eq. 3.3$$

where $\bar{\alpha}$ is the average sound absorption coefficient of the internal plenum surfaces excluding the window openings and the window cavity bottom. The latter location is not installed with any sound absorption in practice (Tong, 2015). α_o and α_i are the sound absorption coefficients of the window exit and entrance respectively.

It should be noted that α_o and α_i are not equal to unity in general because of the non-vanishing acoustic impedance at the window openings. For simplicity, it is assumed that the window exit is a thin rectangular air piston having an acoustic impedance, z_o , given by (Morse & Ingard, 1968):

$$z_o = \rho c \frac{w_o^2 \theta(kw_o) - h^2 \theta(kh) - jw_o^2 \chi(kw_o) + jh^2 \chi(kh)}{w_o^2 - h^2}, \quad Eq. 3.4$$

where

$$\theta(z) = 1 - 4 \frac{1 - J_0(z)}{z^2}, \quad \chi(z) = \frac{8}{\pi z} \left[1 - \frac{\pi}{2z} M_0(z) \right] \quad Eq. 3.5$$

and J_0 and M_0 are the zero order Bessel function of the first kind and the Struve function of zero order respectively. By considering a thin rectangular cavity at the window exit as in Huang et al. (2011) and similar phenomenon takes place at the window inlet, one can then approximate

$$\alpha_o \sim 1 - |G_o|^2 \quad \text{and} \quad \alpha_i \sim 1 - |G_i|^2, \quad Eq. 3.6$$

where $G_o = (z_o - \rho c)/(z_o + \rho c)$ and G_i is the inlet counterpart of G_o .

3.3 Experimental Validation

Full scale plenum window sound transmission loss experiments were carried out inside the building acoustic testing facility of the Department of Building Services Engineering, The Hong Kong Polytechnic University. This facility consisted of two isolated chambers with a common wall on which the test windows were installed. It was also structurally isolated from the institution building. The source room was made semi-anechoic to mimic an approximately free field condition, while the receiver room was reverberant.

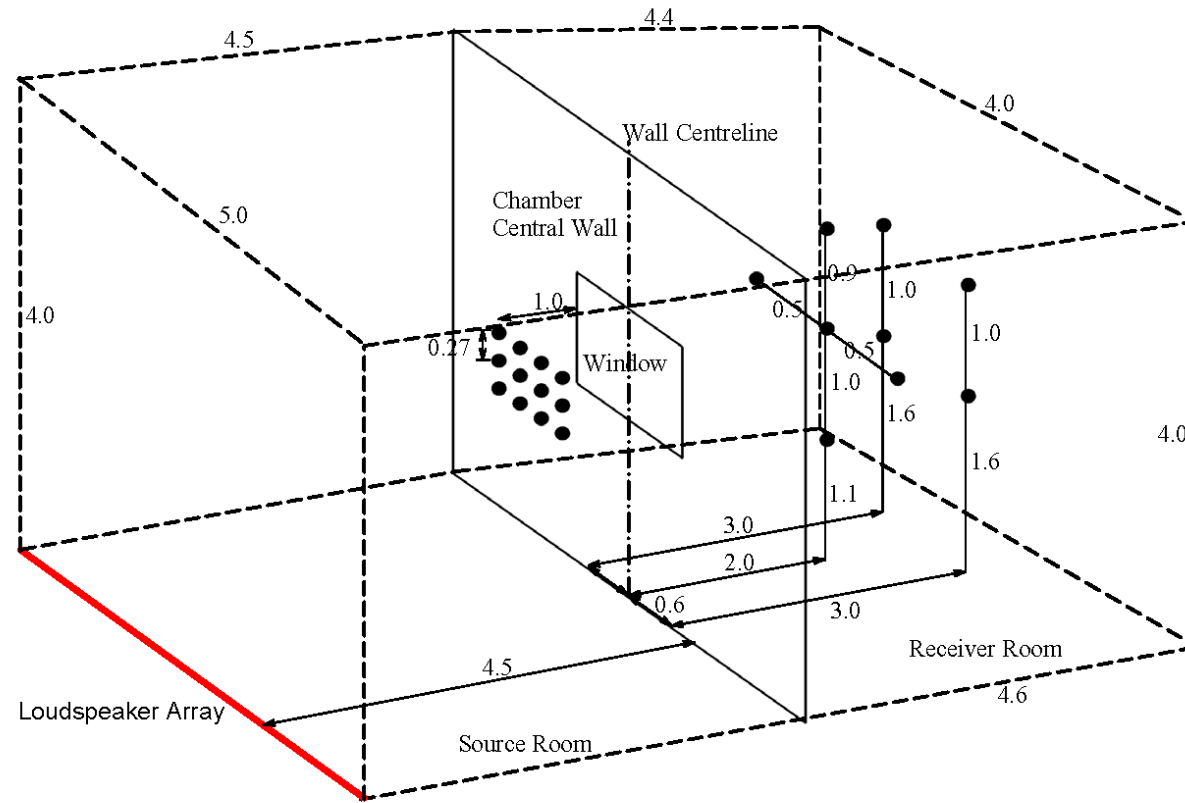


Figure 3. 2 Experimental setup and dimension of testing volume.

●: *Microphone*



(a)



(b)



(c)

Figure 3. 3 Examples of plenum windows tested.

(a) W01o; (b) W07a; (c) W11o.

Figure 3.2 shows the schematics of the measurement setup. Pictures of some plenum windows tested are presented in Figure 3.3. Twenty one Brüel & Kjær Type 4937 ¼” microphones were used in this study. In general, twelve of them were located inside the source room at 1m away from the window to record the average incident sound pressure levels, but only 9 microphones were used for small windows. The nine microphones which spanned over the receiver room volume measured the transmitted sound power. The sound source was made up of twenty five 600aperture loud-speakers arranged in the form of a linear array. Though this sourcedid not mimic fully the traffic noise source, the variations of one-third octave band sound levels measured by the

source-side micro-phones conformed to the requirements stipulated in ISO 16283-3(BS EN ISO 16283-3,2016).

The window outlets were small compared to the common wall area and the source room is not reverberant, making the sound transmission loss formula adopted in the standard BS EN ISO 10140 (BS EN ISO 10140-2, 2011) not useful. The classical room acoustics equation should be adopted instead, and the level of the transmitted power SWL_t and the average sound level in the receiver room SPL_{rec} are related to the room constant of the receiver room R_{rec} as (Peters, 2013)

$$SWL_t = SPL_{rec} - 10\log_{10}\left(\frac{4}{R_{rec}}\right). \quad Eq. 3.7$$

The source side microphones measured the incident and reflected sound simultaneously.

The measured sound pressure level, SPL , is thus

$$SPL = 10\log_{10}(10^{SPL_{inc}/10} + 10^{SPL_{refl}/10}), \quad Eq. 3.8$$

where the suffices *inc* and *refl* denote quantity associated with the incident sound and reflected sound respectively. The sound power that propagates into the plenum window via the window inlet, W should be equal to the sum of the transmitted power and the rate of acoustical energy dissipation within the plenum window. The related SWL can be approximated as (Peters, 2013)

$$SWL = 10\log_{10}(10^{SPL_{inc}/10} - 10^{SPL_{refl}/10}) + 10\log_{10}(w_i h) \quad Eq. 3.9$$

The formula of Wells (1958) suggests that the rate of acoustical energy dissipation within the plenum window due to the artificial sound absorption is $g(2h + l)\bar{\alpha}W/R$, thus the transmitted power is $W[1 - g(2h + l)\bar{\alpha}/R]$. One can then obtain the following approximation :

$$\begin{aligned}
SWL_t &\sim 10\log_{10}(10^{SPL_{inc}/10} - 10^{SPL_{refl}/10}) + 10\log_{10}(w_i h) \\
&+ 10\log_{10}\left(1 - \frac{g(2h+l)\bar{\alpha}}{R}\right) \\
&= 10\log_{10}(2 \times 10^{SPL_{inc}/10} - 10^{SPL/10}) + 10\log_{10}(w_i h) \\
&+ 10\log_{10}\left(1 - \frac{g(2h+l)\bar{\alpha}}{R}\right). \tag{Eq. 3.10}
\end{aligned}$$

Then, one can obtain the incident sound pressure level SPL_{inc} via window inlet opening from Eq.3.10, combine $L_W = L_I + \log_{10} S$ (Peters, 2013), the incident sound power level SWL_{inc} can be obtained . Then the sound transmission loss across the window is

$$\begin{aligned}
TL &= SWL_{inc} - SWL_t \\
&= 10\log_{10}\left\{\frac{1}{2}\left[\frac{10^{SWL_t/10}}{w_i h(1 - g(2h+l)\bar{\alpha}/R)} + 10^{SPL/10}\right]w_i h\right\} \\
&- SWL_t. \tag{Eq. 3.11}
\end{aligned}$$

However, though the fibreglass used in this study is a good sound absorber, its surface area is small compared to that of the whole internal window cavity surface. Its effect on the reverberation is also small compared to those of the two window openings. A rough estimation is that the contribution of such absorption in R is less than ~30% over the traffic noise frequency range. It will be shown later that the reverberant field inside the plenum window is much weaker than that assumed in the formulations of Wells (1958), such that the omission of this absorption term in Eq. (3.11) will only result in an approximately maximum 0.2 dB underestimation of SWL_t in some frequency bands. Its effect on TL is even smaller and thus practically insignificant. For simplicity, the term $g(2h+l)\bar{\alpha}/R$ is not considered hereinafter in the analysis. This parameter is also hard to measure reliably in practice. Thus,

$$\begin{aligned}
TL &= SWL_{inc} - SWL_t \\
&= 10\log_{10} \left[\frac{1}{2} \left(\frac{10^{SWL_t/10}}{w_i h} + 10^{SPL/10} \right) w_i h \right] \\
&\quad - SWL_t.
\end{aligned}
\tag{Eq. 3.12}$$

Experiments with five opened side-hung casement windows were done in the first place in order to check the validity of Eq. (3.12). Details of the results of two of these casement windows are tabulated in Table 3.1. The larger window was a double side-hung window, while the smaller one a single side-hung window. The normalized traffic noise spectrum (BS EN 1793-3, 1998) was adopted to convert the spectral TL s into a single A-weighted sound transmission loss rating, TL_{EN1793} , which is relevant to traffic noise reduction. Details of the conversion steps can be found in Garai and Guidorzi (2000) and Tong and Tang (2013) and thus are not repeated here. The TL s are small as expected, though there are some low frequency TL s which reach 6 dB probably because of the acoustic modes of the window openings (Tong et al., 2011). The TL_{EN1793} for all the five opened casement windows tested are all about 2 dBA. However, many of the one-third octave band TL_{ISO} s so calculated using the traditional ISO standard formula are negative as shown in table 3.1, showing that the above proposed approach is valid and should be used.

Fourteen plenum windows of the dimensions shown in Table 3.2 were tested in the present study. The last letter “o” and “a” in the window codes represent the cases without and with artificial sound absorption in the windows respectively. The last two windows, namely W13 and W14, are similar to those of Tong et al. (2015). The choice of window dimensions is based on the practical situation in Hong Kong. Though a

window opening of 320 mm (W09 to W12) is not so commonly found here, the corresponding windows have been included in this study as the lower bound of the window opening width range. The sound absorption used in this study was 25 mm thick fiberglass sheet of density 32 kg/m^3 .

Table 3. 1 Sound transmission across two sample casement windows ($h = 1.35$ m)

| Window Width, w (mm) | Acoustical Parameter | One-third Octave Band Centre Frequency (Hz) | | | | | | | | | | | | | | | | | EN1793 | |
|------------------------|-----------------------------|---|------|------|------|------|------|------|------|------|------|------|------|------|------|------|-------|-------|--------|-------|
| | | 100 | 125 | 160 | 200 | 250 | 315 | 400 | 500 | 630 | 1000 | 1250 | 1600 | 2000 | 2500 | 3150 | 4000 | 5000 | | |
| 1320 | SPL (dB) | 46.2 | 56.2 | 63.1 | 66.4 | 66.6 | 68.2 | 71.8 | 73.9 | 74.4 | 77.9 | 80.4 | 84.5 | 78.4 | 79.0 | 79.3 | 79.9 | 75.6 | | |
| | SPL_{rec} (dB) | 41.3 | 48.2 | 57.4 | 59.6 | 64.1 | 65.2 | 67.2 | 70.5 | 70.0 | 73.5 | 75.9 | 81.0 | 76.0 | 74.4 | 72.6 | 73.8 | 70.5 | | |
| | R_{rec} (m ²) | 7.80 | 5.42 | 5.84 | 6.10 | 6.19 | 6.27 | 6.46 | 7.66 | 8.59 | 9.29 | 9.00 | 8.40 | 8.54 | 8.78 | 9.44 | 10.98 | 10.70 | | |
| | SWL_t (dB) | 44.2 | 49.5 | 59.1 | 61.5 | 66.0 | 67.2 | 69.3 | 73.3 | 73.3 | 77.1 | 79.5 | 84.3 | 79.3 | 77.8 | 76.3 | 78.1 | 74.8 | | |
| | TL , Eq.3.12 | 2.82 | 6.70 | 4.41 | 5.20 | 1.86 | 2.11 | 3.21 | 1.85 | 2.18 | 1.91 | 2.06 | 1.61 | 0.88 | 2.26 | 3.53 | 2.66 | 1.94 | | |
| | TL_{EN1793} (dB) | | | | | | | | | | | | | | | | | | | 2.09 |
| | TL_{ISO} (dB) | | | | | | | | | | | | | | | | | | | |
| 660 | SPL (dB) | 46.2 | 56.6 | 63.4 | 66.4 | 66.4 | 67.2 | 70.4 | 74.7 | 74.7 | 77.3 | 83.5 | 84.6 | 77.7 | 79.4 | 78.0 | 78.3 | 74.5 | | |
| | SPL_{rec} (dB) | 39.2 | 45.9 | 54.3 | 58.6 | 61.5 | 61.8 | 65.8 | 68.3 | 68.7 | 71.7 | 75.4 | 79.7 | 72.9 | 70.7 | 69.1 | 70.9 | 68.9 | | |
| | R_{rec} (m ²) | 7.46 | 5.17 | 5.42 | 5.72 | 5.60 | 6.42 | 5.40 | 6.63 | 7.25 | 8.00 | 8.10 | 8.15 | 7.59 | 7.70 | 8.71 | 10.60 | 10.27 | | |
| | SWL_t (dB) | 41.9 | 47.0 | 55.6 | 60.2 | 62.9 | 63.8 | 67.1 | 70.5 | 71.3 | 74.7 | 78.5 | 82.8 | 75.7 | 73.6 | 72.5 | 75.2 | 73.0 | | |
| | TL , Eq.3.12 | 2.31 | 6.65 | 5.03 | 3.73 | 1.75 | 1.65 | 1.60 | 2.18 | 1.70 | 1.18 | 2.80 | 0.66 | 0.84 | 3.42 | 3.14 | 1.51 | 0.49 | | |
| | TL_{EN1793} (dB) | | | | | | | | | | | | | | | | | | | 1.77 |
| | TL_{ISO} (dB) | | | | | | | | | | | | | | | | | | | |
| 1130 | TL_{EN1793} (dB) | | | | | | | | | | | | | | | | | | | 2.22 |
| | TL_{ISO} (dB) | | | | | | | | | | | | | | | | | | | -2.18 |
| 585 | TL_{EN1793} (dB) | | | | | | | | | | | | | | | | | | | 1.78 |
| | TL_{ISO} (dB) | | | | | | | | | | | | | | | | | | | -2.86 |
| 430 | TL_{EN1793} (dB) | | | | | | | | | | | | | | | | | | | 2.00 |
| | TL_{ISO} (dB) | | | | | | | | | | | | | | | | | | | -2.56 |

Table 3. 2 Dimensions of the plenum windows included in the present study.

| Plenum window | Plenum Window Dimensions (mm) | | | | Absorption |
|---------------|-------------------------------|-------|------|-----|------------|
| | w_i | w_o | l | G | |
| W01o | | | | 205 | ✗ |
| W01a | | | 2600 | | ✓ |
| W02o | | | | 145 | ✗ |
| W02a | 950 | 950 | | | ✓ |
| W03o | | | | 205 | ✗ |
| W03a | | | 2000 | | ✓ |
| W04o | | | | 145 | ✗ |
| W04a | | | | | ✓ |
| W05o | | | | 205 | ✗ |
| W05a | | | 1900 | | ✓ |
| W06o | | | | 145 | ✗ |
| W06a | 600 | 600 | | | ✓ |
| W07o | | | | 205 | ✗ |
| W07a | | | 1300 | | ✓ |
| W08o | | | | 145 | ✗ |
| W08a | | | | | ✓ |
| W09o | | | | 205 | ✗ |
| W09a | | | 1340 | | ✓ |
| W10o | | | | 145 | ✗ |
| W10a | 320 | 320 | | | ✓ |
| W11o | | | | 205 | ✗ |
| W11a | | | 740 | | ✓ |
| W12o | | | | 145 | ✗ |
| W12a | | | | | ✓ |
| W13o | | | | 560 | ✗ |
| W13a | 560 | 560 | 1680 | | ✓ |
| W14o | | | | 340 | ✗ |
| W14a | 1050 | 1050 | 2440 | | ✓ |

Table 3. 3 Sound transmission loss of the plenum windows tested.

| Window | <i>TL</i> (dB) | | | | | | | | | | | | | | | | | | EN1793 |
|--------|---|------|------|------|------|------|------|------|------|------|------|------|------|------|------|------|------|------|--------|
| | One-third octave band centre frequency (Hz) | | | | | | | | | | | | | | | | | | |
| | 100 | 125 | 160 | 200 | 250 | 315 | 400 | 500 | 630 | 800 | 1000 | 1250 | 1600 | 2000 | 2500 | 3150 | 4000 | 5000 | |
| W01o | 4.6 | 8.8 | 10.1 | 14.8 | 10.7 | 7.2 | 10.4 | 11.6 | 14.6 | 12.7 | 12.1 | 9.6 | 9.3 | 13.0 | 11.3 | 15.2 | 13.9 | 12.8 | 11.0 |
| W01a | 6.0 | 9.0 | 10.7 | 14.9 | 11.2 | 7.7 | 12.0 | 13.3 | 17.7 | 15.0 | 15.7 | 11.7 | 11.7 | 16.1 | 13.7 | 18.6 | 16.7 | 14.6 | 13.0 |
| W02o | 4.6 | 10.6 | 10.4 | 13.4 | 10.6 | 7.3 | 10.0 | 12.0 | 13.2 | 10.4 | 12.0 | 13.0 | 14.4 | 12.9 | 13.3 | 16.2 | 15.1 | 12.6 | 11.7 |
| W02a | 5.3 | 11.0 | 10.6 | 13.7 | 11.0 | 7.6 | 11.2 | 13.3 | 15.4 | 12.1 | 14.2 | 16.1 | 16.7 | 15.2 | 16.7 | 19.9 | 18.1 | 16.2 | 13.2 |
| W03o | 4.8 | 11.0 | 13.0 | 12.8 | 8.0 | 9.6 | 12.2 | 10.2 | 8.7 | 10.4 | 8.6 | 7.6 | 12.0 | 12.3 | 12.3 | 11.6 | 11.0 | 12.1 | 9.7 |
| W03a | 2.9 | 10.6 | 13.3 | 13.0 | 8.2 | 9.4 | 13.4 | 11.9 | 10.2 | 12.1 | 10.1 | 9.8 | 14.4 | 15.6 | 14.6 | 13.8 | 12.8 | 14.0 | 11.2 |
| W04o | 5.8 | 12.3 | 13.6 | 13.7 | 8.2 | 9.3 | 12.3 | 8.8 | 7.5 | 8.2 | 9.7 | 12.4 | 16.2 | 13.4 | 12.3 | 13.1 | 12.2 | 12.3 | 10.3 |
| W04a | 5.4 | 12.2 | 13.9 | 14.0 | 8.6 | 9.8 | 13.2 | 9.9 | 8.4 | 9.4 | 11.8 | 15.4 | 18.9 | 17.0 | 14.8 | 15.0 | 13.6 | 14.0 | 11.7 |
| W05o | 0.9 | 5.5 | 6.4 | 10.5 | 9.7 | 9.3 | 13.2 | 11.4 | 16.1 | 12.3 | 9.6 | 7.7 | 9.4 | 9.4 | 9.4 | 11.2 | 12.4 | 9.7 | 9.7 |
| W05a | 0.7 | 5.3 | 6.7 | 11.2 | 11.3 | 11.5 | 15.7 | 15.2 | 19.4 | 16.3 | 13.5 | 11.6 | 12.2 | 12.3 | 11.8 | 14.9 | 15.7 | 11.6 | 12.3 |
| W06o | -2.0 | 7.6 | 6.9 | 9.9 | 9.2 | 8.1 | 11.7 | 10.9 | 14.5 | 9.9 | 12.1 | 12.4 | 9.8 | 9.8 | 12.3 | 12.6 | 14.7 | 12.2 | 10.2 |
| W06a | 1.4 | 7.3 | 7.4 | 10.5 | 10.0 | 9.3 | 13.1 | 13.4 | 18.0 | 12.7 | 14.5 | 14.9 | 11.8 | 13.0 | 14.9 | 14.9 | 16.2 | 12.5 | 12.4 |
| W07o | 2.4 | 4.6 | 6.0 | 7.4 | 3.5 | 3.0 | 10.5 | 12.7 | 15.2 | 10.7 | 11.3 | 7.8 | 7.4 | 9.1 | 7.9 | 12.3 | 13.7 | 12.8 | 9.3 |
| W07a | 1.5 | 4.2 | 6.2 | 7.8 | 4.6 | 4.2 | 13.4 | 16.8 | 17.8 | 14.7 | 16.9 | 11.0 | 10.5 | 14.3 | 11.2 | 18.4 | 17.9 | 16.1 | 10.9 |
| W08o | 8.3 | 7.1 | 5.2 | 7.5 | 3.6 | 2.8 | 8.8 | 11.5 | 12.7 | 7.3 | 9.1 | 14.1 | 10.9 | 7.5 | 10.2 | 14.5 | 14.8 | 14.5 | 10.2 |
| W08a | 4.3 | 7.1 | 5.5 | 7.9 | 4.7 | 3.7 | 11.1 | 14.3 | 15.3 | 9.7 | 13.0 | 17.9 | 14.6 | 11.8 | 16.1 | 19.0 | 17.7 | 16.6 | 11.3 |
| W09o | 3.7 | 8.6 | 8.0 | 8.4 | 6.4 | 10.8 | 11.1 | 8.9 | 10.7 | 11.9 | 8.9 | 7.1 | 10.2 | 9.7 | 9.6 | 11.8 | 11.8 | 13.4 | 8.5 |
| W09a | 3.3 | 8.7 | 8.2 | 8.7 | 7.7 | 11.9 | 11.6 | 10.5 | 12.9 | 13.5 | 10.0 | 9.2 | 12.4 | 13.5 | 11.6 | 14.0 | 13.9 | 14.9 | 10.9 |
| W10o | 5.2 | 9.9 | 9.0 | 9.8 | 8.1 | 9.0 | 10.8 | 8.8 | 8.5 | 9.0 | 10.8 | 13.1 | 12.1 | 10.0 | 10.5 | 12.4 | 12.9 | 13.8 | 8.7 |
| W10a | 4.8 | 10.2 | 9.3 | 10.1 | 8.2 | 9.7 | 11.3 | 9.7 | 9.8 | 10.6 | 12.3 | 15.4 | 13.6 | 11.5 | 12.3 | 13.8 | 14.7 | 15.5 | 10.9 |
| W11o | 4.4 | 8.0 | 6.0 | 3.2 | 2.2 | 3.3 | 11.1 | 13.9 | 13.0 | 12.7 | 9.2 | 4.6 | 6.2 | 8.6 | 7.6 | 9.8 | 7.7 | 8.0 | 7.3 |
| W11a | 4.4 | 8.0 | 6.0 | 3.2 | 2.7 | 4.6 | 13.9 | 16.4 | 14.9 | 14.9 | 10.8 | 6.3 | 8.6 | 12.0 | 11.2 | 14.2 | 10.3 | 10.2 | 8.9 |
| W12o | 4.5 | 9.5 | 7.9 | 5.6 | 3.3 | 4.0 | 9.9 | 11.5 | 9.2 | 9.8 | 7.0 | 12.0 | 13.0 | 7.2 | 8.4 | 11.5 | 9.7 | 9.0 | 8.4 |
| W12a | 3.1 | 9.6 | 7.7 | 5.6 | 3.3 | 5.0 | 11.3 | 13.2 | 10.8 | 10.5 | 10.0 | 14.7 | 15.1 | 11.3 | 13.2 | 14.9 | 11.4 | 10.4 | 10.0 |
| W13o | 5.3 | 7.6 | 7.2 | 7.5 | 5.3 | 8.0 | 13.2 | 10.8 | 11.1 | 10.4 | 10.8 | 12.0 | 9.1 | 9.2 | 6.9 | 11.8 | 12.3 | 8.9 | 9.3 |
| W13a | 5.1 | 7.8 | 7.4 | 8.1 | 6.4 | 10.3 | 16.0 | 13.7 | 13.8 | 13.7 | 14.7 | 14.5 | 11.8 | 11.8 | 8.6 | 14.4 | 14.7 | 11.0 | 11.7 |
| W14o | 4.1 | 11.2 | 13.0 | 10.4 | 7.5 | 8.3 | 13.3 | 12.2 | 10.4 | 11.0 | 8.2 | 9.6 | 13.0 | 14.7 | 11.6 | 13.1 | 12.6 | 12.9 | 10.1 |
| W14a | 4.1 | 11.4 | 13.5 | 11.0 | 8.0 | 9.2 | 14.9 | 13.0 | 13.0 | 13.0 | 9.9 | 13.2 | 15.2 | 17.7 | 13.8 | 16.4 | 14.6 | 14.6 | 11.9 |

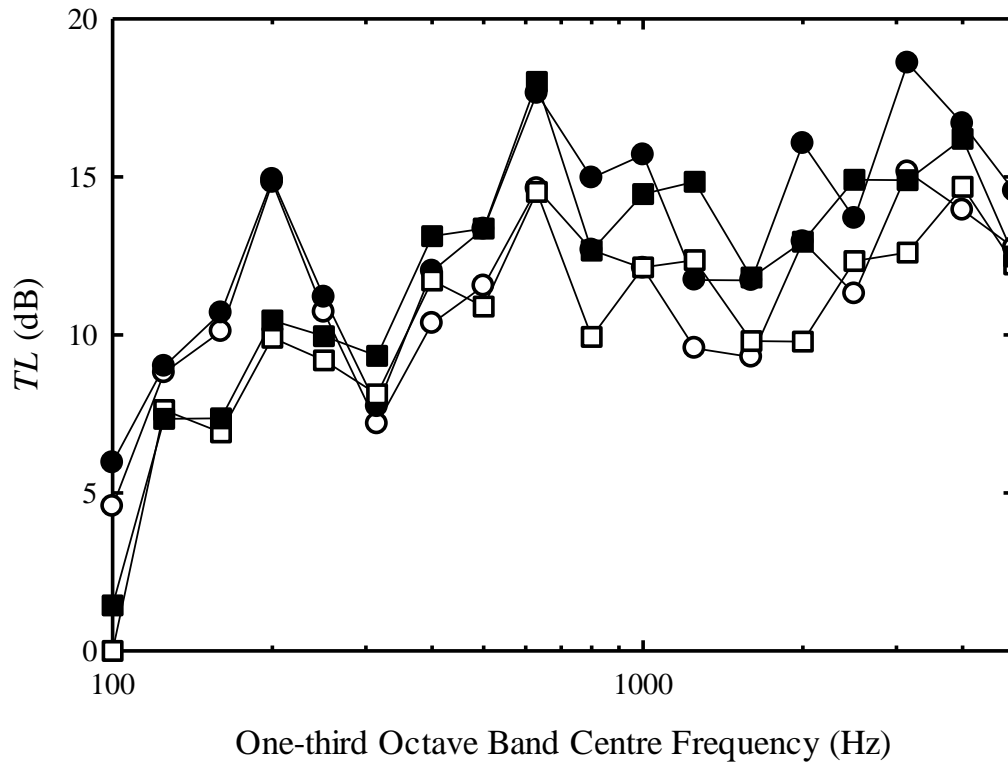


Figure 3. 4 Examples of the spectral variations of TL across plenum windows.

○ : W01o; □ : W06o; ● : W01a; ■ : W06a.

The one-third octave band TL s of the plenum windows estimated using Eq. (3.12) are summarized in Table 3.3. In general, TL increases with increasing overlapping length ($= l - w_o - w_i$) and/or decreasing g . It is not surprising that the plenum windows installed with sound absorption have higher TL s than those without the sound absorption in general, but the effect of sound absorption is only obvious at frequencies above the 315 Hz frequency band as shown in Figure 3.4. For the larger windows (W01, $w = 0.96\text{m}$), the TL peak within the 200 Hz band is believed to be due to a resonance between the two openings whose centrelines are separated by a distance

of 1.65 m. It is believed that longitudinal resonance within the windows also give rise to the TL peaks at the 630 Hz frequency band. It should be noted that the overall length of W01 is 2.6 m while the distance between the centrelines of the two openings of W03 is 1.3 m. A longitudinal mode across the horizontal spans of these windows can result in a nodal plane near to the window exit, resulting in the relatively larger TL . Similar resonances could result in weaker transmission loss, depending on where the anti-nodal planes are located.

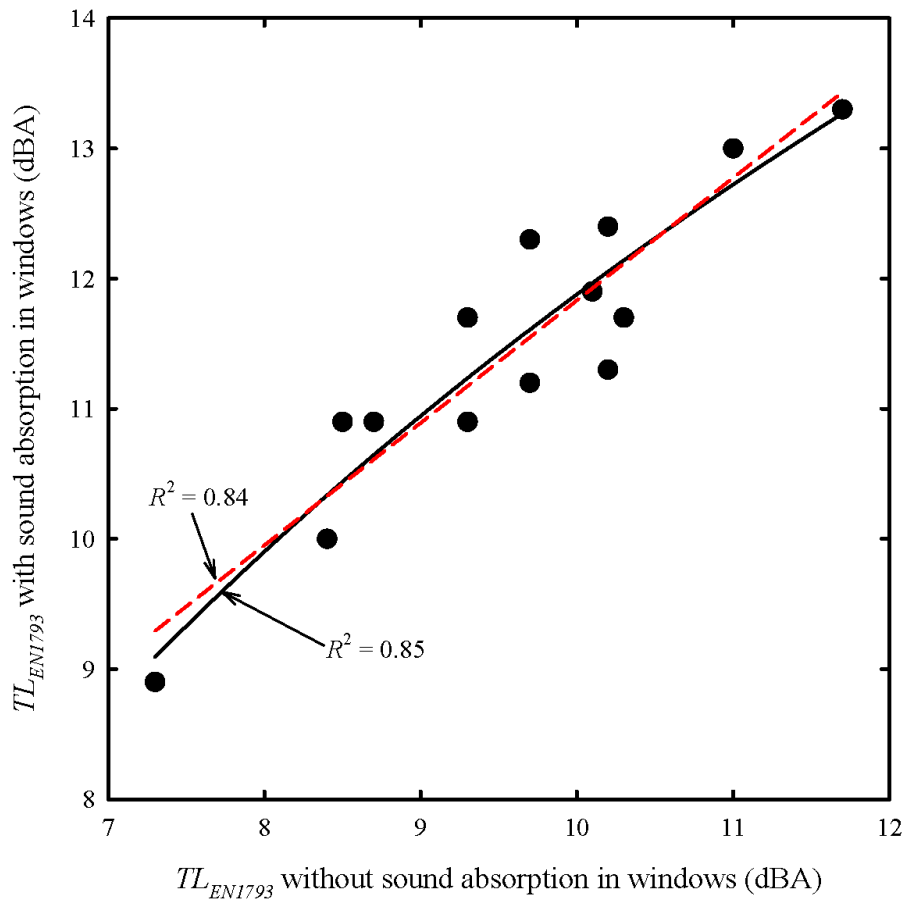


Figure 3. 5 Improvement of traffic noise reduction across plenum windows by artificial sound absorption.

———— : Logarithmic regression line; - - - - : linear regression line.

Figure 3.5 shows the strong relationship between the TL_{ENI793} (traffic noise transmission loss) of the plenum windows with and without the sound absorption lining. The increase in TL_{ENI793} ranges from 1.2 to 2.6 dBA and the root-mean-square increase is 1.9 dBA. However, such increase does not show any simple relationship with a single plenum window configuration dimension (that is, l , g , d or w). It is also found through regression analysis that a logarithmic curve represents better the observed relationship than a linear line, suggesting that sound absorption will become slightly less effective when the TL_{ENI793} of the original plenum window is relatively large.

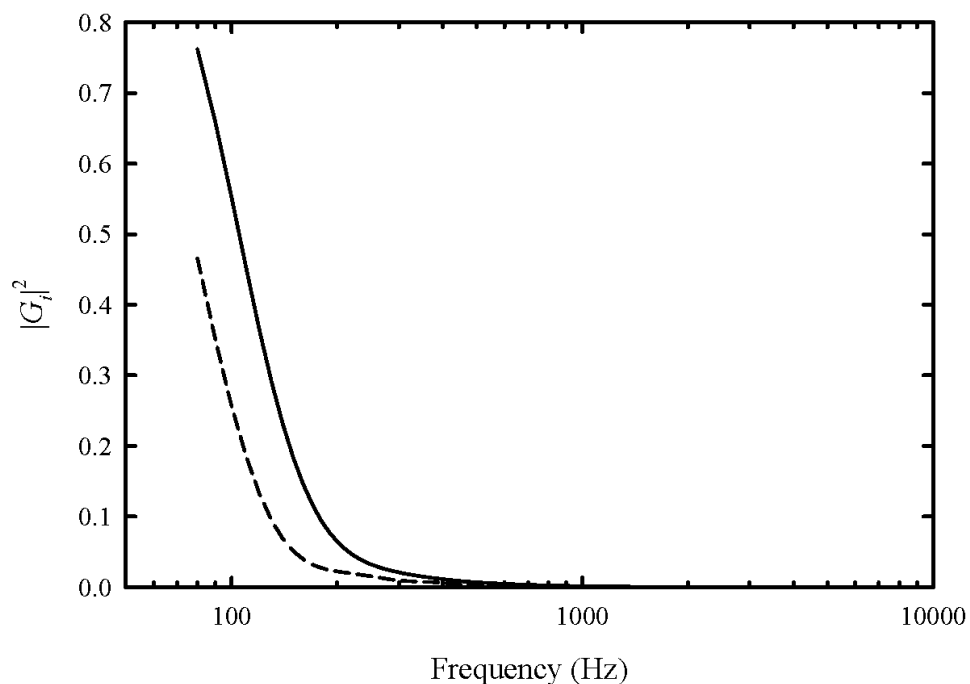


Figure 3. 6 Spectral variations of $|G_i|^2$.

———— : W14; - - - - : W09/W10/W11/W12.

The frequency variations of the magnitudes of G_i of W14 and W09 (same as

those of W10, W11 and W12) are presented in Figure 3.6. The window opening sizes of W14 and W09 are the largest and smallest in this study respectively, such that the corresponding results of other plenum windows should fall between theirs. It is noticed that the contributions of G_i and G_o are insignificant once the excitation frequency exceeds 200 Hz. The corresponding sound absorption coefficient $\alpha_i \sim \alpha_o \rightarrow 1$.

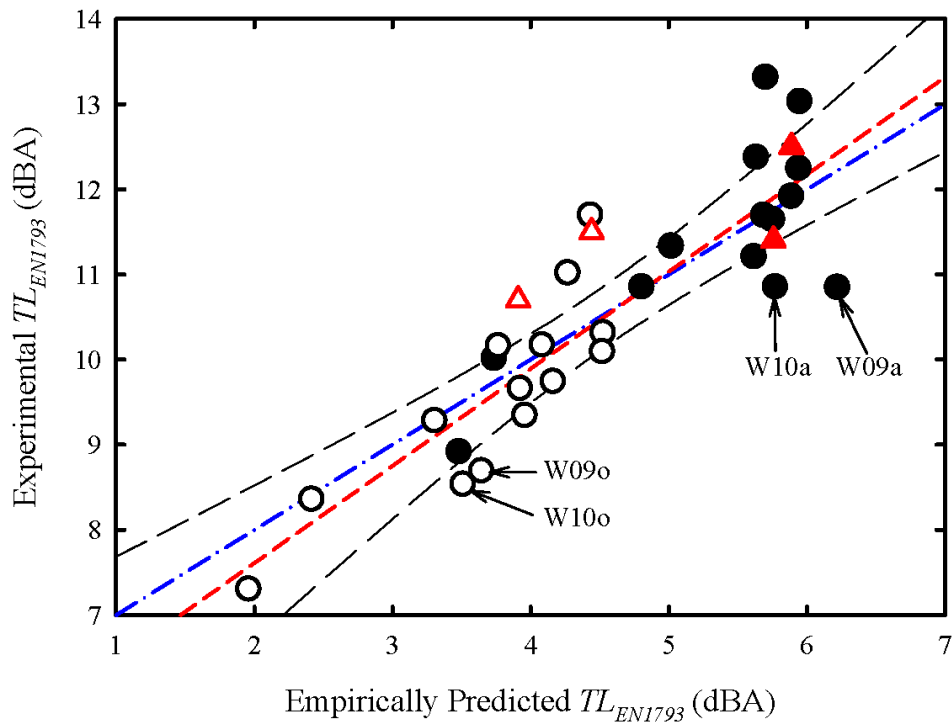


Figure 3. 7 Comparison between predicted and measured TL_{ENI793} (Eq. (3.13)).

- : Measurements; ▲ : Tong et al. [7].
- Opened symbol : windows without artificial sound absorption;
- Closed symbol : windows installed with artificial sound absorption;
- — — — : line of “prediction equals measurement”;
- . - . - : linear regression;
- — — — : 99% confidence level of regression.

In the foregoing analysis, the laboratory results will be used to calibrate the proposed empirical model. As plenum windows are often used for protection against traffic noise (Tong et al., 2015; Søndergaard & Legarth, 2014), the prediction of TL_{EN1793} is more important. TL_{EN1793} is thus adopted in this study as the main descriptor of prediction performance. Q is taken to be 4 initially as the two openings are located at the extreme ends of a plenum window. A comparison between Eq. (3.1) predictions and the experimental results are presented in Figure 3.7. One can notice that the correlation between the present empirical predictions and laboratory measurements is strong ($R^2 \sim 0.7842$). Standard deviation of prediction from measurement is ~ 6 dB.

The following model for TL prediction is thus a logical proposal :

$$TL = -10\log_{10} \left[w_0 h \left(\frac{g}{\pi d^3} + \frac{1}{R} \right) \right] + 6 . \quad Eq. 3.13$$

Eq. (3.13) is also close to the linear regression line. The mean square difference between Eq. (3.13) predictions and measurements is 0.7 dB, but with a maximum deviation of more than 2 dB. The corresponding results obtained with $Q = 4\cos\phi$ are not satisfactory (Figure 3.8) and thus are not further considered in this study. There are quite a number of outliers which are outside the 99% confidence boundaries of the regression model as shown in Figure 3.7. Also, the 6 dB underestimation of Eq. (3.6) cannot be explained. Eq. (3.13) is definitely not in its optimal form though it predicts satisfactorily the TL_{EN1793} s of Tong et al. (2015) with maximum deviation of ~ 1.1 dB.

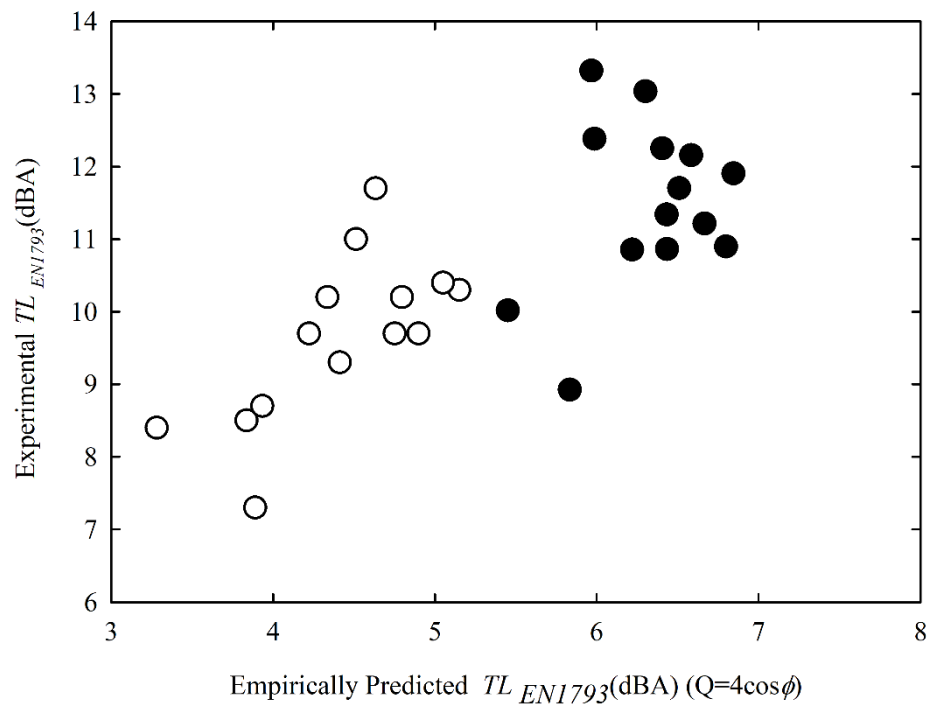


Figure 3. 8 Comparison between predicted and measured TL_{ENI793} ($Q = 4\cos\phi$).

Legends: same as those of Figure 3.7.

It can also be observed from Figure 3.7 that the measured TL_{ENI793} s of W09 and W10 are exceptionally low if one includes all the present data and the results of Tong et al. (2015) into consideration together. The reason is not clear and is left to further investigation. However, the width of these window openings is 320 mm and the separating distance between the two openings is 700 mm (large). Such plenum window dimension is not practically common and thus the corresponding results are not considered in foregoing data analysis.

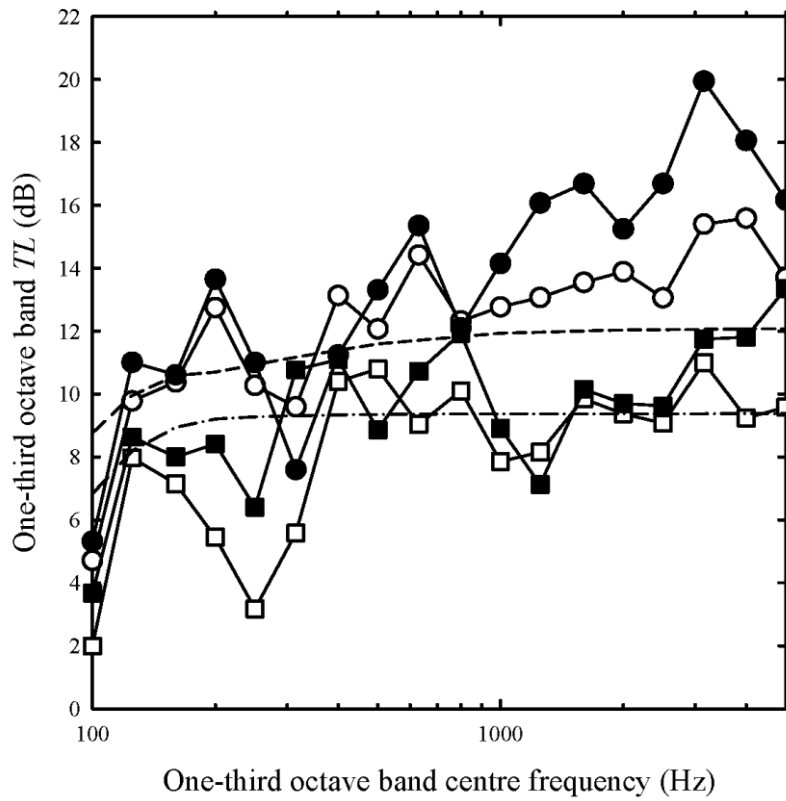


Figure 3. 9 Comparison between predicted and measured TL spectra.

- : W02a (measured); ■ : W07o (measured);
- : W02a (Eq. (3.14) with frequency dependent Q_{op} and K_{op});
- : W07o (Eq. (3.14) with frequency dependent Q_{op} and K_{op});
- : W02a (Eq. (3.13))
- · - · - : W07o (Eq. (3.13))

Though traffic noise reduction is the main theme of this study, it is also worthwhile to have an understanding on how the empirical model predicts the TL spectra. Figure 3.9 shows some comparisons between the predictions of Eq. (3.13) and the experimental TL data. The results of W02a and W07o are chosen as they represent the largest and the least deviations in this study respectively. One can

observe that the prediction is roughly around the averaged spectral TL values for the case of W07o, while Eq. (3.13) fails to give predictions which can follow the shape of the TL spectrum in the presence of artificial sound absorption inside the windows (W02a). These observations apply in general to all the windows tested. However, it is not too surprising as the acoustics within the elongated window cavity is not likely to be modelled so well by Wells' approach, which is developed for use in plenums with much more regular aspect ratios. For traffic noise application, it is the TL values between 500 Hz to 2000 Hz that are practically important (BS EN 1793-3, 1998). In this sense, Eq. (3.13) is still acceptable.

3.4 Optimization of Empirical Model

Since the transmission loss across a plenum window depends on the diffraction loss and the reverberation gain within the window, it is conjectured that the 6 dB TL underestimation of Eq. (3.1) observed in Section 3.3 is due to a less significant reverberation inside the plenum window and/or a larger diffraction loss than those assumed in the model of Wells (1958). It is therefore proposed to optimize the empirical model of Eq. (3.13) by absorbing the 6 dB constant back in the two main physical energy transmission processes. It is proposed that

$$TL = -10\log_{10} \left[w_o h \left(Q \frac{g}{4\pi d^3} + \frac{K}{R} \right) \right], \quad Eq. 3.14$$

where Q is the directivity factor and K is a newly introduced parameter which describes the reduction of reverberant intensity due to the largely elongated plenums. It will be

referred to as the reverberant field attenuation factor hereinafter in the discussion. The optimal values of Q and K , denoted by Q_{op} and K_{op} respectively, can be determined by minimizing the root-mean-square difference between predictions and experiments, Δ :

$$\Delta = \sqrt{\overline{\sum (TL_{Eq.(14)} - TL_{experiment})^2}}, \quad Eq. 3.15$$

where the overbar represents mean value.

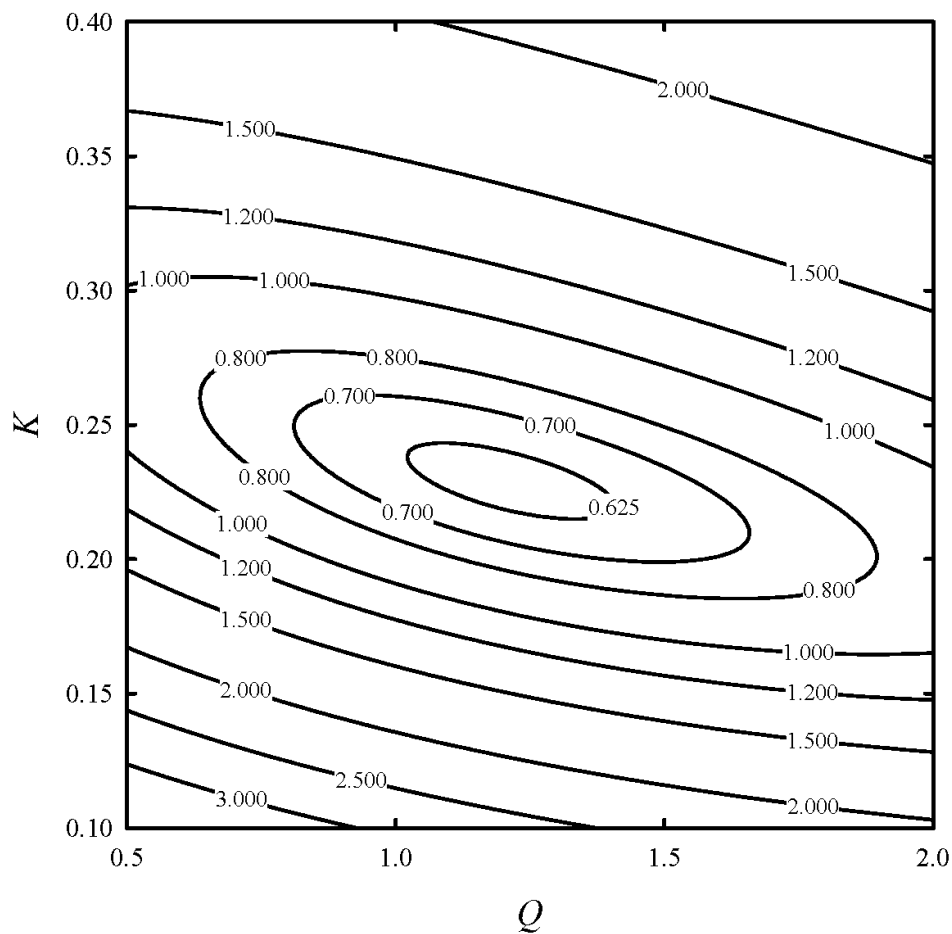


Figure 3. 10 Variation of Δ with Q and K (Eq. (3.14) with constant Q_{op} and K_{op}).

The prediction of TL_{EN1793} is considered in the first place by assuming that Q_{op} and K_{op} are not frequency dependent for simplicity. Figure 3.10 confirms that Δ is a smooth function of Q and K and has a well-defined minimum value. Q_{op} and K_{op} can be found

by solving the simultaneous equations

$$\frac{\partial \Delta}{\partial Q} = \frac{\partial \Delta}{\partial K} = 0 \quad \text{Eq. 3.16}$$

using Newton's method. It is found that $Q_{op} = 1.2088$ and $K_{op} = 0.2288$. The correlation between Eq. (3.14) predictions under this optimal condition and measurements is illustrated in Figure 3.11. Though the results of W09 and W10 are not used in the calculation, they are included in the figure for the sake of completeness. Δ is equal to 0.5 dB and the maximum deviation from experimental results is only 1.3 dB, which is well within engineering tolerance. The optimized Eq. (3.14) predicts very well the $TL_{EN1793S}$ of Tong et al. (2015). The corresponding standard deviation is 0.6 dB, with a maximum deviation of 0.8 dB.

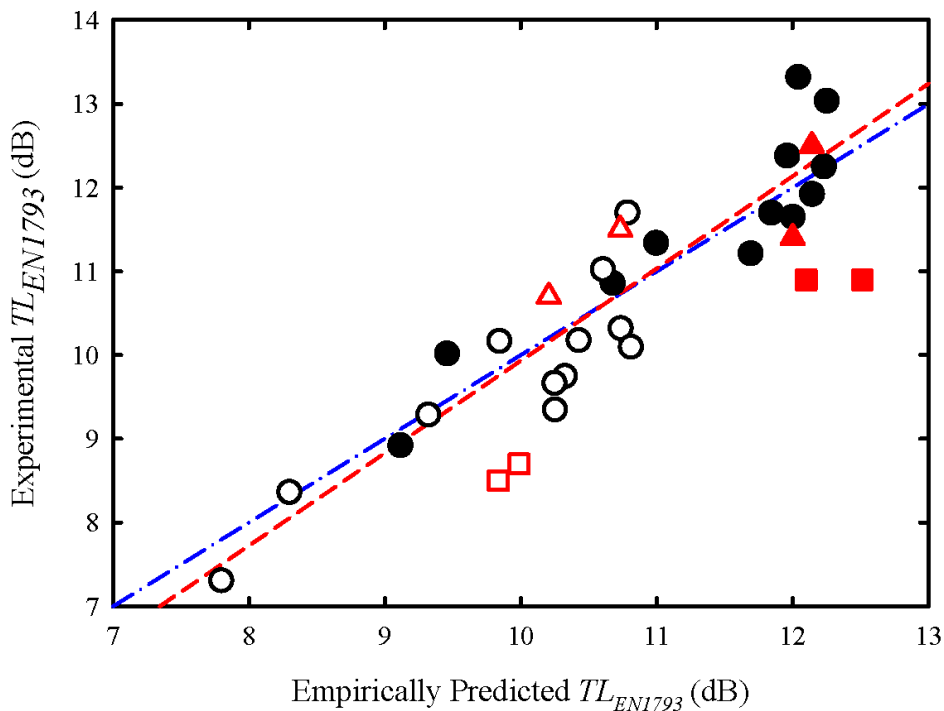


Figure 3. 11 Comparison between predicted and measured TL_{EN1793} (Eq. (3.14) with constant Q_{op} and K_{op}).

■ : W09 and W10; Other legends : same as those of Figure 3.7.

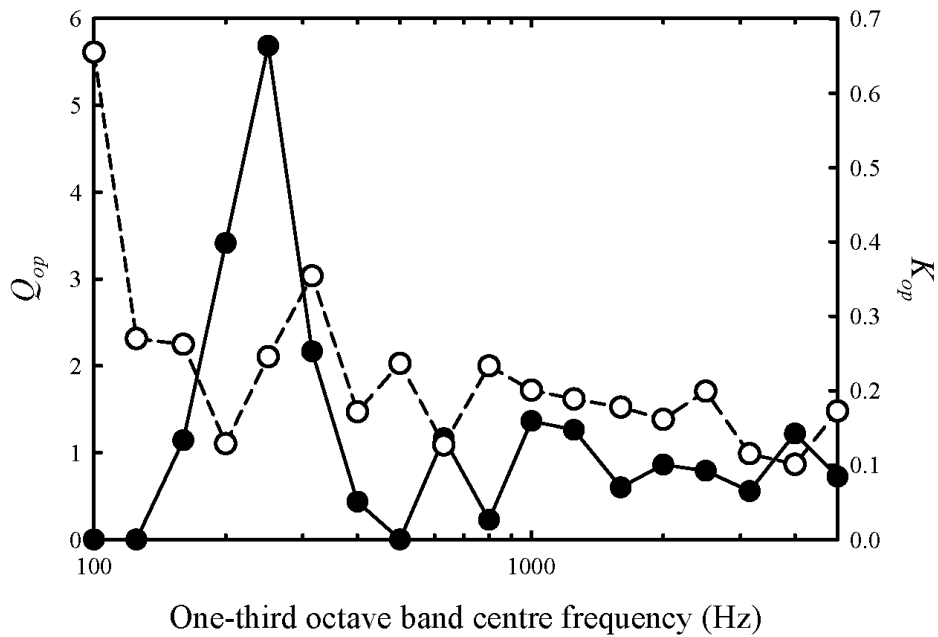


Figure 3. 12 Spectral variations of Q_{op} and K_{op} .

● : Q_{op} ; ○ : K_{op} .

The above procedure can be applied to individual frequency bands in order to understand how Q_{op} and K_{op} may vary with frequency. The corresponding band Δs are understandably larger as the discrepancies are not smoothed out by the weighted averaging in the estimation of TL_{EN1793} . Also, the errors at low frequencies are likely to be large as the acoustics inside the window cavity could be strongly affected by individual acoustic modes.

Figure 3.12 shows the frequency variations of Q_{op} and K_{op} . K_{op} is relatively large (but not as large as that assumed in Well (1958)) at low frequencies and there is a tendency of K_{op} to decrease with increasing frequencies, indicating that the reverberant field within the window cavity will become weaker as frequency increases. This

appears in-line with general room acoustics theory. The spectral variation of Q_{op} is less straight-forward. Q_{op} is large at 250 Hz and this is also the frequency band where the TL s of the plenum windows are relatively low in general (c.f. Figure 3.9). Though room acoustics model does not include any resonance of acoustic modes, the large Q_{op} estimated is likely to be the result of the strong sound resonant pressure within the cavity, which has apparently been translated into a strong diffraction towards the window exit in the present model. At higher frequencies, Q_{op} is fluctuating about unity, indicating a roughly monopole-like radiation at the window inlet in the presence of a weak reverberant field within the window cavity.

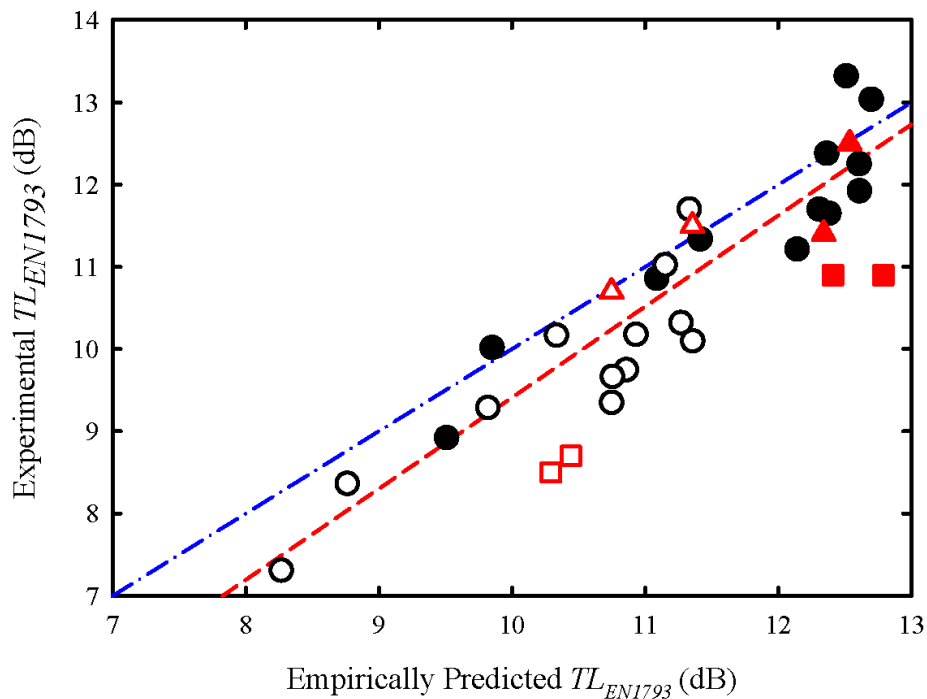


Figure 3. 13 Comparison between predicted and measured TL_{ENI793} (Eq. (3.14) with frequency dependent Q_{op} and K_{op}).

Legends : same as those of Figure 3.11.

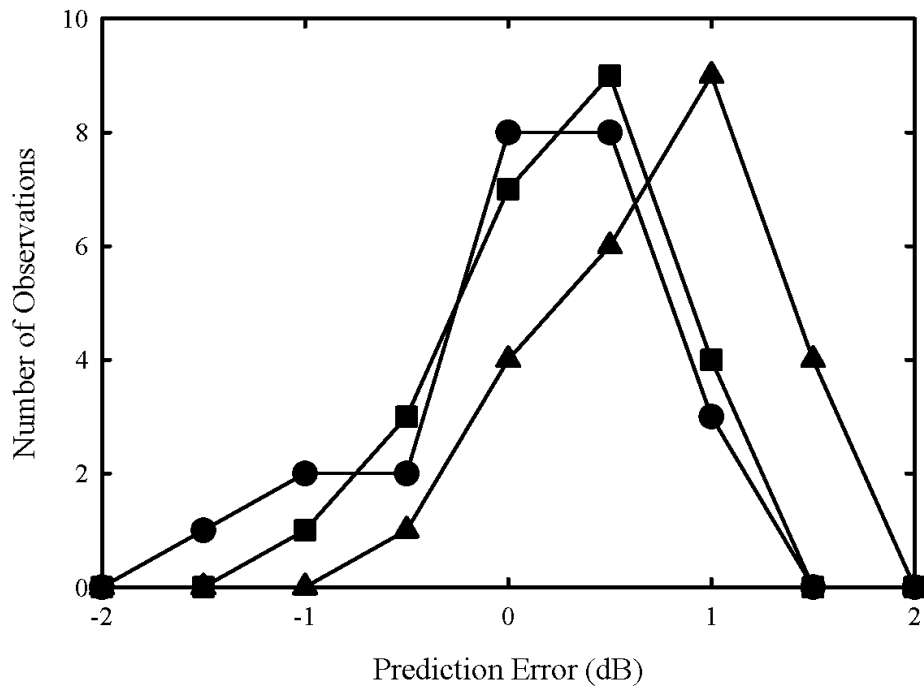


Figure 3. 14 Prediction error distributions.

- : Eq. (3.13); ■ : Eq. (3.14) with frequency independent Q_{op} and K_{op} ;
- ▲ : Eq. (3.14) with frequency dependent Q_{op} and K_{op} ;

One can use the Q_{op} and K_{op} of each frequency band to estimate the band TLs , and then apply the traffic noise weighting to these band TLs to obtain the TL_{EN1793} of each plenum window. Though, it is expected that the TL spectra predicted using band Q_{op} and K_{op} should be closer to the measured ones in general, the corresponding TL_{EN1793} predictions are not necessarily better than those presented above since the prediction accuracy depends strongly on those within the dominant traffic noise frequency range. The comparison between the new predictions and experiment is shown in Figure 3.13. In this case, the standard deviation is 0.7 dB and the prediction

scheme tends to overestimate the traffic noise transmission loss TL_{ENI793} for most of the plenum window configurations. The regression line in Figure 3.13 deviates obviously from the line of equality. The observed good agreement between predictions and the “without artificial sound absorption” cases of Tong et al. (2015) is believed to be just a coincidence.

In Figure 3.14 is presented a comparison between the prediction errors of the three TL_{ENI793} prediction models investigated in this study with a bin width of 0.5 dB. The prediction of Eq. (3.14) using frequency-independent Q_{op} and K_{op} results in the most Gaussian-like error distribution with mean error at 0 dB. The one using Eq. (3.14) together with band Q_{op} and K_{op} gives rise to a positively skewed error distribution and its performance is the worst among the three models tested in this study. A 1 dB downward adjustment to the prediction should be adopted in practice if this relatively complicated method is used.

3.5 Conclusions

A parametric study was carried out in the present investigation inside the building acoustics testing chambers of the Hong Kong Polytechnic University in an attempt to establish a simple empirical prediction model for the traffic noise transmission loss across plenum windows. The sound source adopted was a linear array made up of twenty five 6” aperture loudspeakers. Owing to practical reasons, the source chamber was converted into a semi-anechoic facility for the present study. The results of an

independent site measurement of the Tong et al. (2015) were included in the analysis for prediction model validation. The normalized traffic noise spectrum was used to convert the one-third octave band sound transmission loss into a single A-weighting traffic noise reduction rating as in existing literature and previous studies of Tong et al.(2011, 2013,2015). This rating is adopted in this study as the traffic noise transmission loss.

The simplified traffic noise transmission loss prediction scheme proposed in this study was developed based on the plenum theory in existing literature, in which the sound field inside the window cavity was assumed to make up of a diffracted and a reverberant field. Results in the present study suggest that the reverberant field inside the plenum windows is very much weaker than those assumed inside normal plenum chambers studied in existing literature. The diffracted field also has a directivity factor lower than those adopted in plenum chamber theory except at low frequencies.

Three models are investigated and their traffic noise transmission loss prediction performances are compared. The first one is simply the plenum chamber model in existing literature augmented with a constant. A regression analysis using the present experimental data suggests that this constant is approximately 6 dB. The second one assumes frequency-independent diffracted field directivity and reverberant field attenuation in the plenum chamber model without any artificial constant. The last one is basically the same as the second model, except that the diffracted field directivity and reverberation field attenuation are obtained in one-third octave bands. The second

model gives the best prediction with a standard error of 0.5 dB. Similar error is observed when the independent field mockup data of the Tong (2015) are compared with predictions. The third model performs the worst with standard error of 0.7 dB and an overestimation of nearly 1 dB is observed for most of the plenum windows tested.

It should be noted that the diffracted field directivity and the reverberant field attenuation in the newly proposed models are likely to change with the spectral characteristics of the sound source. However, the experimental data and the present proposed model development protocol should be useful for handling source of different spectral content.

Chapter 4 Sound Reductions Prediction of Multiple Plenum Windows

Extensive traffic noise transmission loss measurements were carried out inside the residential units of a standalone 30-storey housing block located in an opened environment next to a very busy and noisy main trunk road in this chapter. A total of 35 units, which were all equipped with plenum windows, was surveyed. The results further validate in-situ the prediction model established in Chapter 3 using laboratory and site mockup data. Generalized models for the estimation of the traffic noise transmission loss across a residential flat unit façade installed with multiple plenum windows are developed. The differences between their estimations are discussed.

4.1 Introduction

The use of plenum window has been more and more popular recently (Yu et al., 2017; Cheung et al., 2019), but the sound transmission loss across a practical plenum window remains hard to predict. An empirical model for predicting the traffic noise transmission loss across a plenum window based on parametric laboratory tests and site mockup data (Tong et al., 2015) is developed in Chapter 3. However, the acoustical performance of plenum windows has not been studied on site so far. Also, the effects of receiver elevation from and the window orientation relative to the ground traffic line on the window performances are unclear.

In this chapter, the results of an extensive measurement of sound transmission losses of plenum windows carried out in a public housing estate, which is the first housing block in Hong Kong installed with this window type, are presented. This housing block is located at the mockup site of Tong et al. (2015) and was completed in

2018. Details of the building layout and the dimensions of the residential units tested are given later in Section 4.2. Apart from the acoustical performance of plenum windows, the results will also be used to further validate the prediction model established in Chapter 3 and more importantly to develop a new prediction model to cover cases where multiple plenum windows are installed on the same flat unit façade.

4.2 Site Measurement

4.2.1 Building orientation, floor layout and test unit dimensions

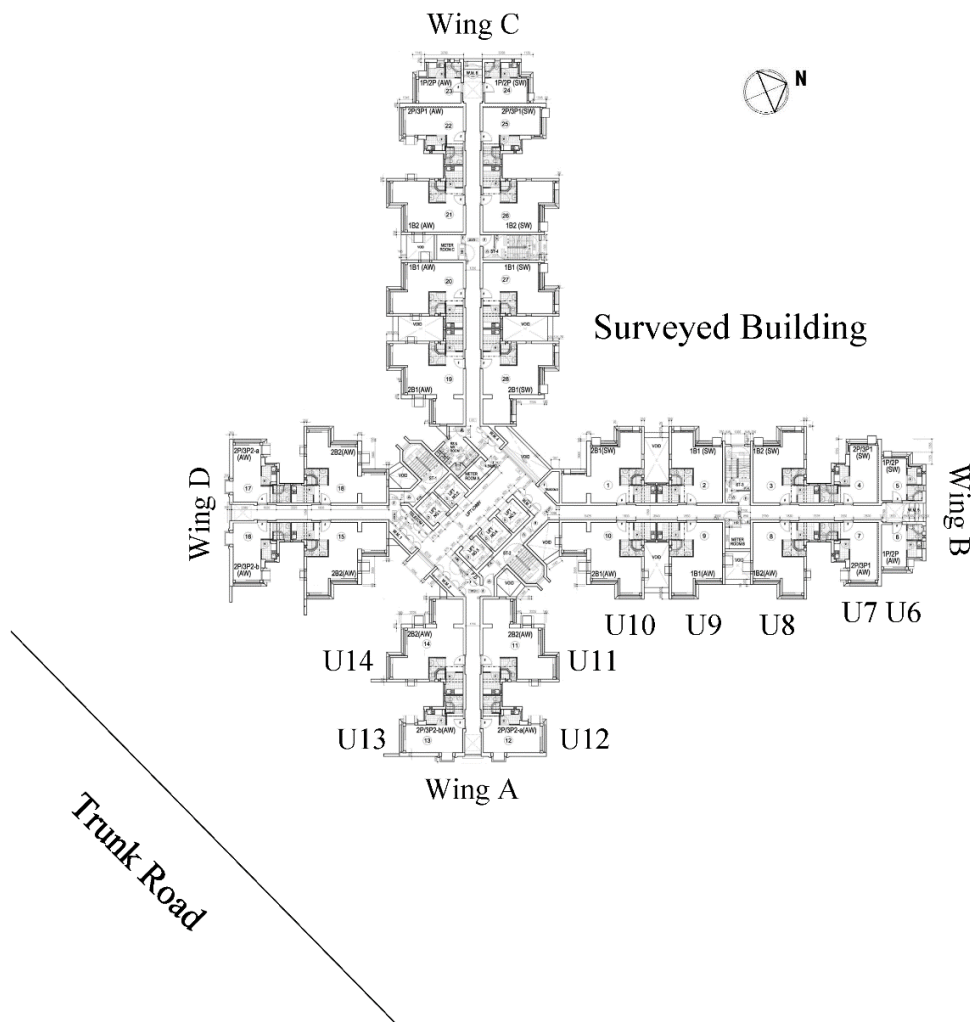


Figure 4. 1 Typical floor layout of the surveyed building and its orientation relative to the noise source.



Figure 4. 2 The surveyed building and its surrounding.

- (a) Façade of the surveyed building facing the main trunk road (Wings A and D in the front);
- (b) the trunk road, left of the surveyed building;
- (c) the trunk road, right of the surveyed building;
- (d) view of U8 at high floor level.

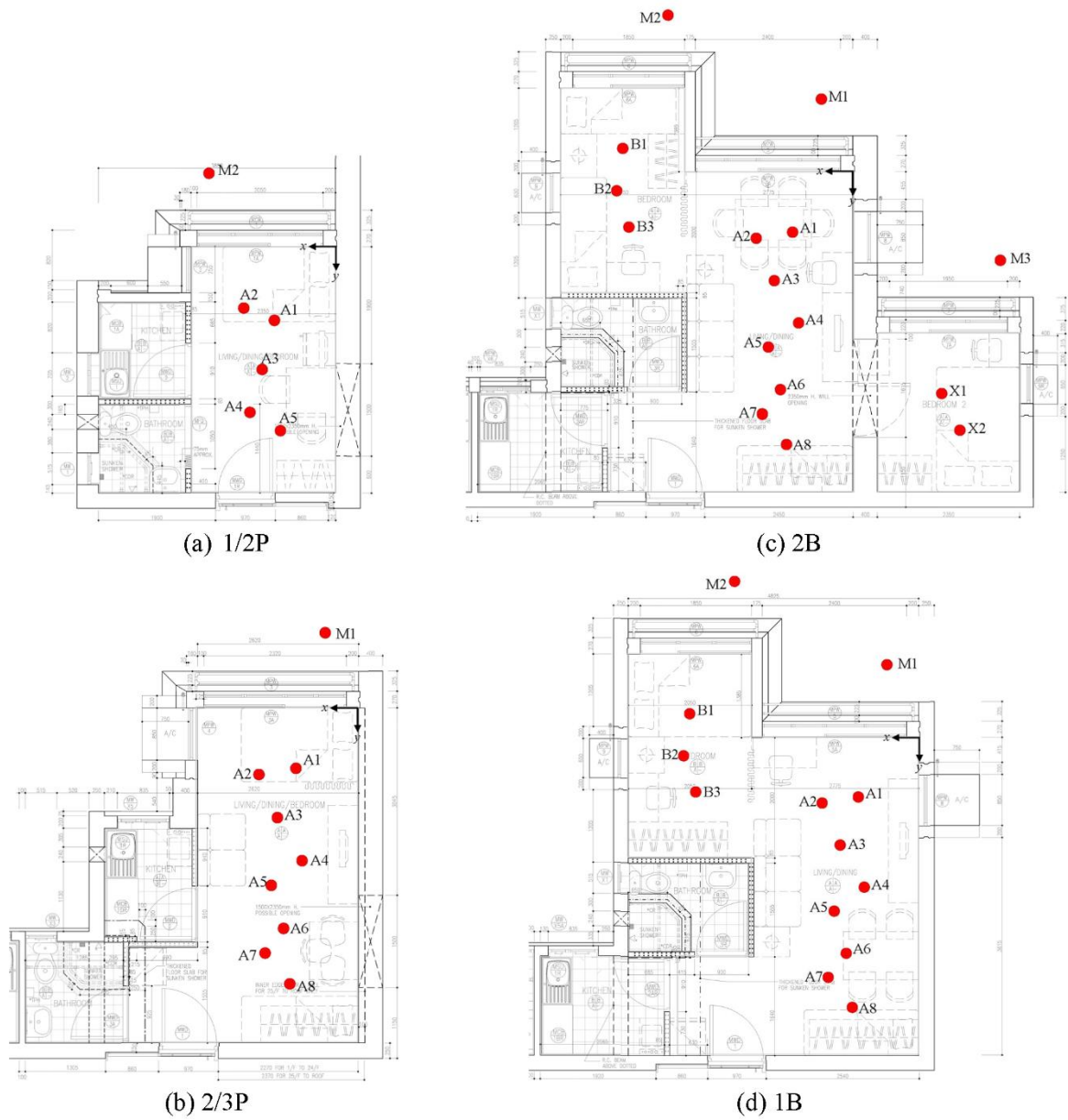


Figure 4. 3 The four flat layouts and the microphone locations.

(a) 1/2P; (b) 2/3P; (c) 2B; (d) 1B.

● : microphone.

The building surveyed in the present study is a 32-storey single housing block. Figure 4.1 shows the building layout and its orientation relative to the major trunk road. Unlike the case of Tong et al. (2015), the present building façade is not parallel to the trunk road. It should be noted that only the flat units facing the trunk road are equipped

with plenum windows. Figure 4.2 illustrates the outlook of the surveyed building and its surrounding environment. There are buildings on the opposite side of the trunk road, but they are not less than 200 m away from the surveyed building. This environment can be regarded as “opened” according to the categorization of Ko (1978).

Table 4. 1 Flat layout parameters for acoustical calculations.*

| Layout | Test flat unit | Room space | Floor area (m ²) | Floor perimeter (m) |
|--------|----------------|-----------------|------------------------------|---------------------|
| 1/2P | U6 | Living/bedroom | 9.4 | 127 |
| 2/3P | U7, U13 | Living/bedroom | 16.0 | 183.7 |
| 1B | U8 | Living room | 16.6 | 186.7 |
| | | Bedroom | 7.0 | 109.4 |
| 2B | U10, U14 | Living room | 16.8 | 188.4 |
| | | Bedroom (outer) | 7.0 | 109.4 |
| | | Bedroom (inner) | 7.2 | 107.3 |

*Floor-to-ceiling height : 2.75 m.

There are 14 flat units on each floor equipped with plenum windows and units U6, U7, U8, U10, U13 and U14 are selected for measurement (Figure 4.1). These flat units altogether cover all the four different flat layouts found in the surveyed building (namely 1/2P, 2/3P, 1B and 2B). Table 4.1 summarizes the flat unit dimensions necessary for later acoustic calculation. The floor-to-ceiling height is 2.75 m. The detailed layout drawings of the four layout types are presented in Figure 4.3. Unit U9 is excluded from the survey as it is just a mirror image of U8. Units U11 and U12 are not facing the trunk road directly, and thus are also not included in the measurement. There were no partition inside these flat units and the doors of the bathrooms and kitchens were kept closed during measurement. All windows, except the plenum windows, were all closed throughout the site measurement.

Measurements were carried out every 5 floors starting from the fifth floor. Corridor windows and staircase doors were all closed to further minimize flanking transmission of noise into the test units. The noise levels inside the test units with all the windows closed were in general more than 15 dB below those when the plenum windows were opened. Flanking transmission can thus be neglected. The site measurement was carried out before the formal release of the building to the residents and thus the walls, floors and ceilings were just with the basic finishing (plastered walls and ceilings, and plain concrete floors). There was no building services in operation during that period of time.

4.2.2 Measurement setup

The number of microphones adopted for the indoor noise measurement varies with the size of the test unit. The positioning of these microphones is schematically showed in Figure 4.3 and the exact co-ordinates of the microphones relative to the lower right hand façade corner of each test flat unit are given in Table 4.2. The indoor microphone positions are determined based on the requirement stipulated in ISO 16283-1 (BS EN ISO 16283-1, 2014) as far as possible.

Table 4. 2 Positions of microphones relative to lower right hand corner of test unit living room.*

| Microphone | 1/2P | | | 2/3P | | | 1B | | | 2B | | |
|------------|-------|-------|-------|-------|-------|-------|-------|-------|-------|-------|-------|-------|
| | x (m) | y (m) | z (m) | x (m) | y (m) | z (m) | x (m) | y (m) | z (m) | x (m) | y (m) | z (m) |
| M1 | -- | -- | -- | 0.53 | -1.20 | 1.15 | 0.53 | -1.20 | 1.15 | 0.53 | -1.20 | 1.15 |
| M2 | 2.07 | -1.20 | 1.15 | -- | -- | -- | 3.06 | -2.59 | 1.15 | 3.06 | -2.59 | 1.15 |
| M3 | -- | -- | -- | -- | -- | -- | -- | -- | -- | -2.42 | 1.47 | 1.15 |
| A1 | 1.00 | 1.20 | 1.65 | 1.00 | 1.00 | 1.20 | 1.00 | 1.00 | 1.20 | 1.00 | 1.00 | 1.20 |
| A2 | 1.50 | 1.00 | 1.20 | 1.60 | 1.10 | 1.70 | 1.60 | 1.10 | 1.70 | 1.60 | 1.10 | 1.70 |
| A3 | 1.20 | 2.00 | 1.40 | 1.30 | 1.80 | 1.40 | 1.30 | 1.80 | 1.40 | 1.30 | 1.80 | 1.40 |
| A4 | 1.40 | 2.70 | 1.50 | 0.90 | 2.50 | 1.60 | 0.90 | 2.50 | 1.60 | 0.90 | 2.50 | 1.60 |
| A5 | 0.90 | 3.00 | 1.10 | 1.40 | 2.90 | 1.30 | 1.40 | 2.90 | 1.30 | 1.40 | 2.90 | 1.30 |
| A6 | -- | -- | -- | 1.20 | 3.60 | 1.50 | 1.20 | 3.60 | 1.50 | 1.20 | 3.60 | 1.50 |
| A7 | -- | -- | -- | 1.50 | 4.00 | 1.25 | 1.50 | 4.00 | 1.25 | 1.50 | 4.00 | 1.25 |
| A8 | -- | -- | -- | 1.10 | 4.80 | 1.60 | 1.10 | 4.80 | 1.60 | 1.10 | 4.80 | 1.60 |
| B1 | -- | -- | -- | -- | -- | -- | 3.80 | -0.39 | 1.15 | 3.80 | -0.39 | 1.15 |
| B2 | -- | -- | -- | -- | -- | -- | 3.90 | 0.32 | 1.65 | 3.90 | 0.32 | 1.65 |
| B3 | -- | -- | -- | -- | -- | -- | 3.70 | 0.92 | 1.35 | 3.70 | 0.92 | 1.35 |
| X1 | -- | -- | -- | -- | -- | -- | -- | -- | -- | -1.45 | 3.67 | 1.10 |
| X2 | -- | -- | -- | -- | -- | -- | -- | -- | -- | -1.75 | 4.27 | 1.55 |

*Origin : lower right corner of living room façade, z : height from floor, see Figure 4.3 for the definitions of x and y

Table 4. 3 Plenum window configurations.

| Unit | Space | Plenum Window Configuration (mm) | | | | |
|-----------|-----------------|----------------------------------|-------|-------|-----|------|
| | | w_i | w_o | l_o | g | h |
| U6 | | 850 | 870 | 340 | 175 | 1352 |
| U7 | | 980 | 1010 | 340 | 175 | 1352 |
| U8 | Living room | 1020 | 1050 | 340 | 175 | 1352 |
| | Bedroom | 550 | 560 | 525 | 175 | 1352 |
| U10 & U14 | Living room | 1020 | 1050 | 340 | 175 | 1352 |
| | Bedroom (outer) | 550 | 560 | 525 | 175 | 1352 |
| | Bedroom (inner) | 658 | 668 | 634 | 175 | 1352 |
| U13 | | 980 | 1010 | 340 | 175 | 1352 |

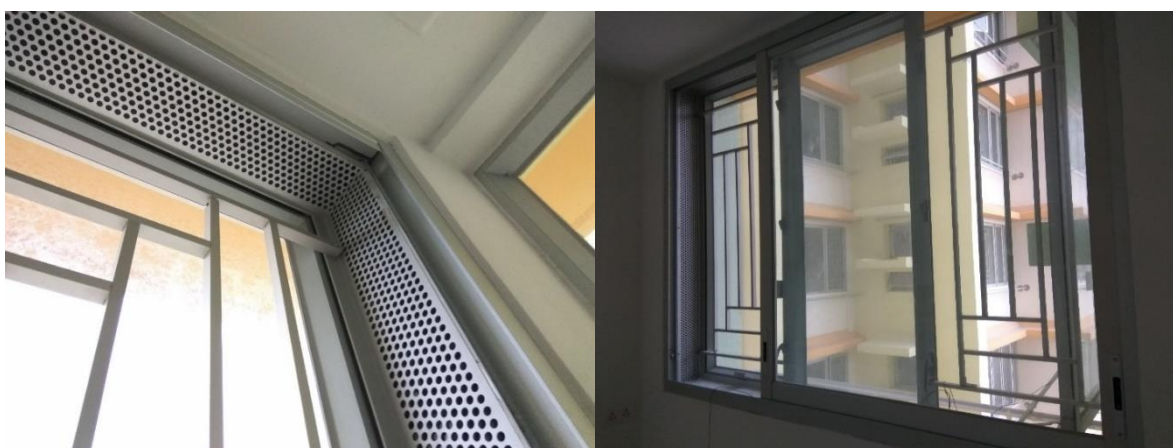


Figure 4. 4 The locations with treatment of sound absorption.

Each of the test unit is installed with one to three plenum windows. The sound reduction capacity of a plenum window is characterized by five basic parameters, namely the outer and inner window opening widths (w_o and w_i respectively), the window height (h), the gap distance (g) and the overlapping length (l_o) (see Chapter 3). The schematic of a plenum window is shown in Figure 3.1. Table 4.3 summarizes the configurations of the plenum windows tested and the test flat units where these windows are installed. In this housing project, sound absorption of NRC 0.7 is installed

on the two vertical side walls and ceiling of every plenum window, shown in figure 4.4 .

Noise measurements at the façade and the interior of each test unit were done simultaneously using the Brüel & Kjær Type 3560D PULSE system with Brüel & Kjær Type 4935 ¼” microphones. The sampling rate was set at 64000 samples per second per channel. Each measurement lasted for at least 30 minutes. The reverberation times (RT) were measured in the test flat units in accordance with ISO 3382 (BS EN ISO 3382-2, 2008). The Brüel & Kjær Type 4296 omni-directional sound source and the software DIRAC were adopted for the RT measurement.

4.3 Results and Discussions

The major objectives of the present study are first, to validate, using data from extensive site measurement, the empirical plenum window traffic noise transmission loss ($TL_{traffic}$) prediction scheme developed in Chapter 3 and second, to develop a generalized scheme to cover façades with multiple plenum windows.

Before the validation, the overall acoustical properties of the flat units, which can be revealed collectively using reverberation times, will be discussed. Also, since traffic noise is the main concern in this study, the normalized traffic noise spectrum (BS EN1793-3, 1998) is used as a weighting to estimate the A-weighted traffic noise transmission losses of the plenum windows as in existing literature (for instance, Garai and Guidorzi (2000), Buretti (2002) and Tong and Tang (2013)).

4.3.1 Reverberation times

The reverberation time represents the time taken for the indoor sound pressure level to decay by 60 dB after the sound source is switched off. For the reverberant surveyed flat units in the present study, it is related simply to the total sound absorption (in m^2

Sabine) and the unit room volume by the Sabine's formula (Sabine, 1964). The total sound absorption is an important parameter for the estimation of the sound transmission loss across a plenum window (Fry, 1988).

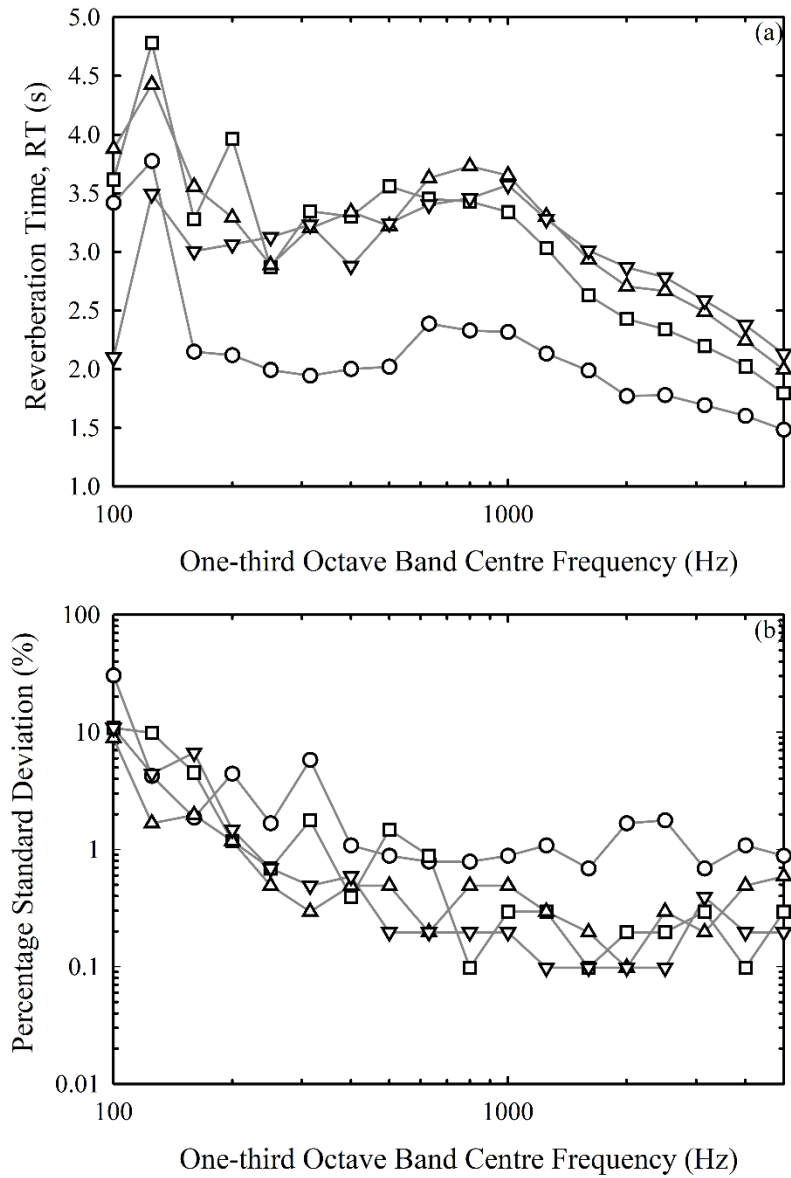


Figure 4. 5 One-third octave band reverberation times.
 (a) Mean reverberation times; (b) percentage standard deviations.
 ○ : U6; □ : U7; △ : U8; ▽ : U10.

Figure 4.5 a shows the one-third octave band RTs measured in U6, U7, U8 and U10. Since the conditions of U13 and U14 are basically the same as those of U7 and U10 respectively (Table 4.3), RT measurements were not done in U13 and U14. As measurements were carried out every 5 floors, the data in Figure. 4.4a are the averages over flat units of the same layout. The corresponding standard deviations are presented in Figure. 4.4b. The RTs are in general long and comparable to those of the churches (Öhrström et al., 2006), confirming that the surveyed flat units are very reverberant. One can notice that the RTs of U6 are relatively shorter, but with larger percentage standard deviations. The measurements at low frequency for U6 and U7 are less reliable probably because of the lower order acoustic modes. However, the RTs at frequencies higher than 200 Hz for individual flat layouts are almost constant. The corresponding standard deviations are in general less than 2%, except for those of U6. Also, the larger the flat unit, the smaller the percentage standard deviation. As one is focused on the A-weighted traffic noise transmission losses, the small problem at low frequencies does not really matter.

4.3.2 Traffic noise transmission loss across a plenum window

The sound transmission loss of a plenum window is calculated from the façade noise spectra together with the indoor average sound levels after correction for reverberation effect. In this sub-section, the data of U6, U7 and U13 will be discussed. It should be noted that U13 is very close to the main noise source (Figure 4.1) such that there is no U13 flat below the ninth floor of the surveyed building. There are a total of six U6 flats, six U7 flats and five U13 flats included in this analysis.

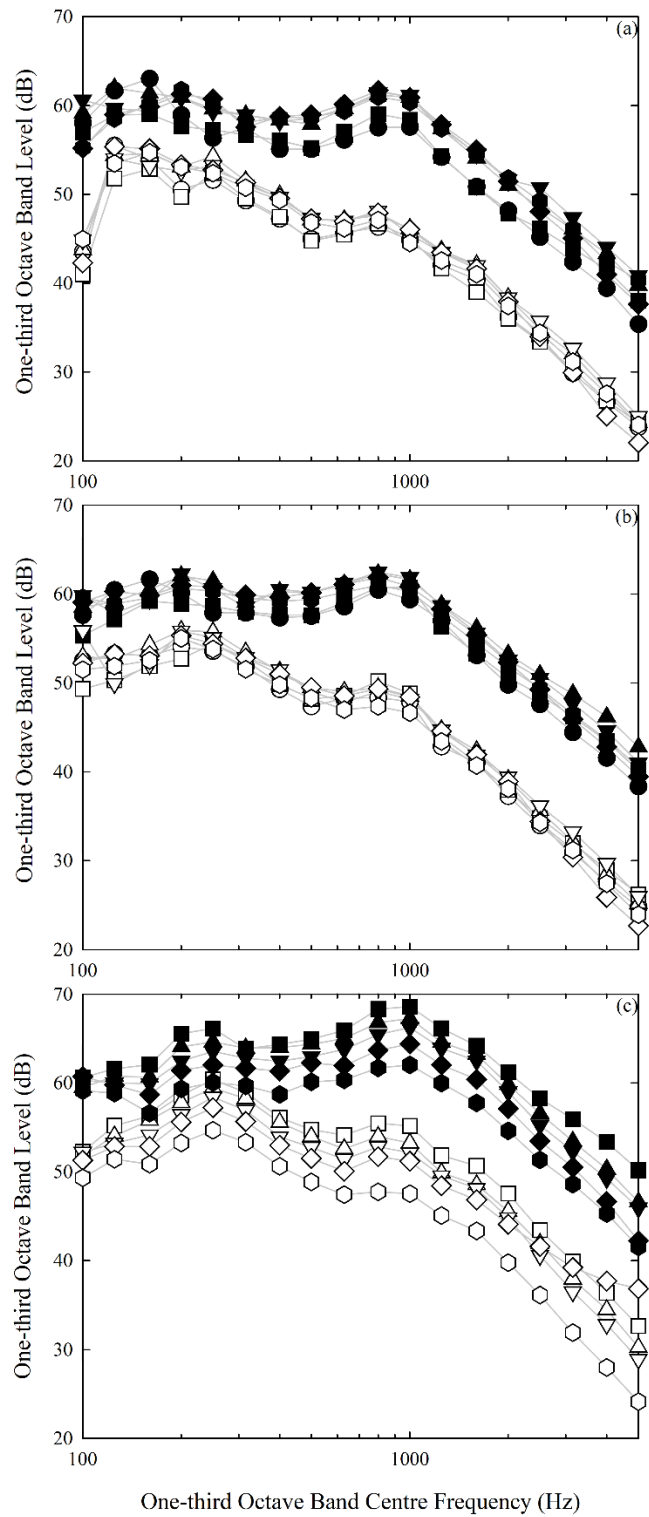


Figure 4. 6 One-third octave band sound levels.
 (a) U6; (b) U7; (c) U13.
 ● : 5/F; ■ : 10/F; ▲ : 15/F; ▼ : 20/F; ◆ : 25/F; ⬢ : 30/F.
 Opened symbols : indoor averages; closed symbols : façade.

Figure 4.6 illustrates the one-third octave band spectra of the façade noise and average indoor noise. Owing to the limited number of microphones available, only the measurements associated with a particular flat unit was done simultaneously. However, though the measurements at different floors were not carried out simultaneously, one can still observe in general a decrease of façade noise level with increasing floor level for U6, U7 and U13. This tends to suggest that the traffic volume along the major road was also fairly steady during the measurement periods. Also, the spectral shapes of the noise spectra recorded are very similar, indicating that the traffic composition along the nearby major trunk road was also fairly constant within busy hours during which the measurements were carried out.

For U6 and U7, the average indoor noise levels appear relatively independent of floor level though the measurements at different floors were not done at the same time. There is slightly higher variation of façade noise levels with floor level. One can also notice that the noise level difference is in general higher as frequency increases, which is a commonly observed phenomenon in building acoustics. U13 is very near to the main noise source and the façade traffic noise levels are understandably higher than those at U6 and U7. The variations of sound levels with floor level are also larger than those of U6 and U7. This is due to the fact that U13 is the closest flat unit to the major traffic line, such that the distance effect on the sound level decay is the strongest among the three flat types considered here.

Figure 4.7 illustrates the $TL_{traffic}$ of U6, U7 and U13 calculated using the measured data as in Chapter 3 and a comparison between these measured $TL_{traffic}$ with the predictions obtained using Eq. (3.14). It is noticed that, under the current opened environment and with various scattered reflections from the surveyed building façade,

the $TL_{traffic}$ s of the plenum windows in U6, U7 and U13 actually do not vary much with floor level (i.e. elevation angle of the window from the trunk road). The maximum variation is that of U6, which is only about 2 dB for a vertical height difference of 75 m (25 floors). Though the $TL_{traffic}$ s of U6 and U7 show a trend of slow increase with floor level, the small variation suggests that the $TL_{traffic}$ s of the plenum windows can practically be assumed to be constant. For U13, there is a dip of $TL_{traffic}$ at the 25/F, but the corresponding variation of $TL_{traffic}$ is still practically small.

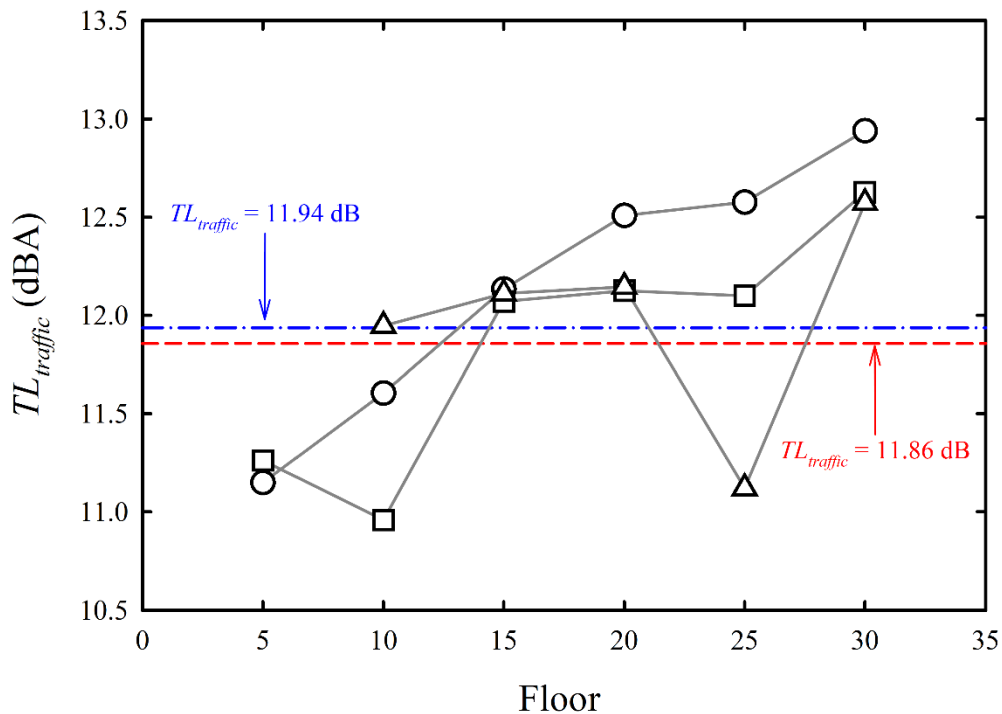


Figure 4. 7 The measured and predicted $TL_{traffic}$ s of U6, U7 and U13.

○ : U6; □ : U7; △ : U13;

--- : Prediction for U6; - · - : predictions for U7 and U13.

The formula proposed in Chapter 3 gives very good prediction with a discrepancy of within ± 1 dB. The mean measured $TL_{traffic}$ s of U6, U7 and U13 are 12.2 dB, 11.9 dB and 12.0 dB respectively, which compare very well with the predictions (11.86 dB for

U6, 11.94 dB for U7 and U13). It should be noted that Eq. (3.14) gives a single $TL_{traffic}$ for a plenum window with a fixed configuration.

4.3.3 Cases of multiple plenum windows

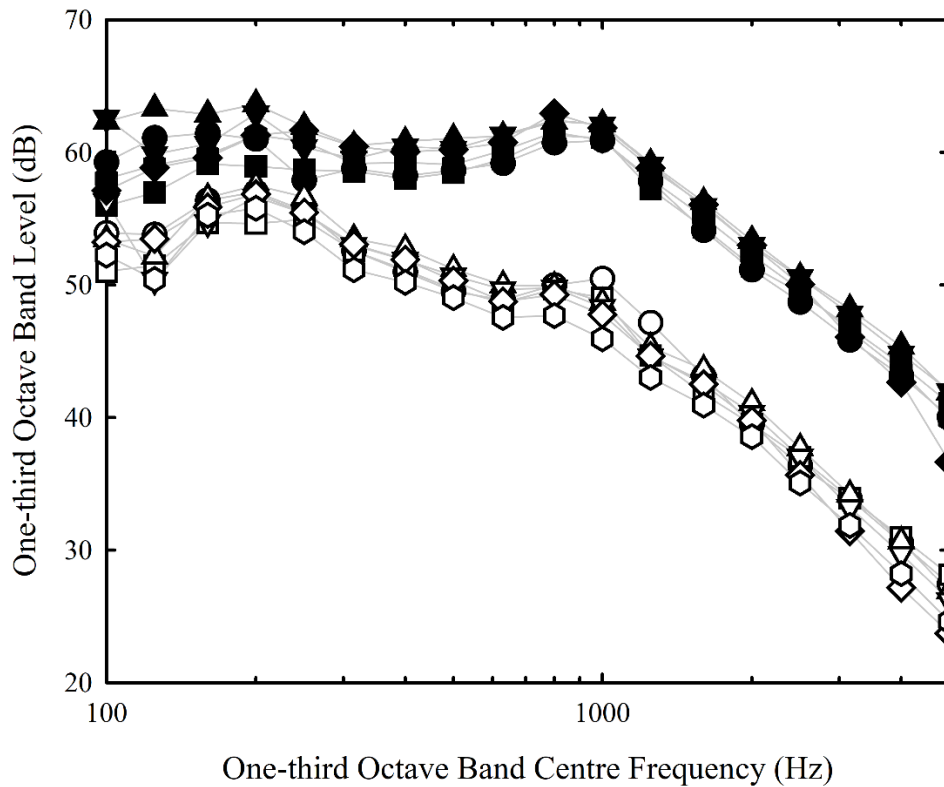


Figure 4. 8 One-third octave band sound levels for U8.

● : 5/F; ■ : 10/F; ▲ : 15/F; ▼ : 20/F; ◆ : 25/F; ● : 30/F.

Opened symbols : indoor averages; closed symbols : façade.

There are two plenum windows in U8 and three plenum windows in U10 and U14. Effort is made in this section to develop a traffic noise reduction prediction formula for these cases. Each of these windows are supposed to look after a particular area/space inside the flat units. The acoustical coupling between these spaces (Meissner, 2012) has not been taken into account in Chapter 3.

Unit U8 consists of a bedroom space and a living room space but there was no

partition between these spaces at the time the unit was tested (Figure 4.3). Figure 4.8 shows the average one-third octave band sound levels associated with the U8 unit. In fact, the differences between the average band levels of the bedroom and the living room are very small in general, except at frequencies below 200 Hz where a maximum difference of 2 dB can be observed in limited isolated cases. Same applies to the outdoor measurements at M1 and M2. However, as this study is focused on traffic noise reduction, which is an A-weighted index, low frequency transmission characteristics are not important. The variations of these sound levels with floor height basically follow those of U6, U7 and U13 and thus are not further discussed. The shapes of the spectra are very similar to those shown in Figure 4.6 though the measurements were taken at different times. The data further confirm the more-or-less steady traffic flow and traffic composition along the trunk road in concern. The same general phenomena apply also to corresponding results of U10 and U14 and thus they are not presented.

Before the development of a traffic noise transmission loss prediction model suitable for cases of multiple plenum windows, it is interesting to look at how Eq. (3.14) performs in the presence of coupled spaces. To do this, the bedroom and living room data of U8 are separately analyzed. The $TL_{traffic}$ s of the bedroom and living room plenum windows are 11.88 dB and 11.96 dB respectively (from Eq. 3.14). A comparison between the measured $TL_{traffic}$ and that estimated using Eq. (3.14) are given in Figure 4.9a. One can observe that the prediction model in Chapter 3, though is not developed for coupled spaces, can give reasonable agreement with the living room window measurements. For the bedroom window, the agreement is less satisfactory but the deviation is still within 2 dB with a standard deviation of 1.1 dB.

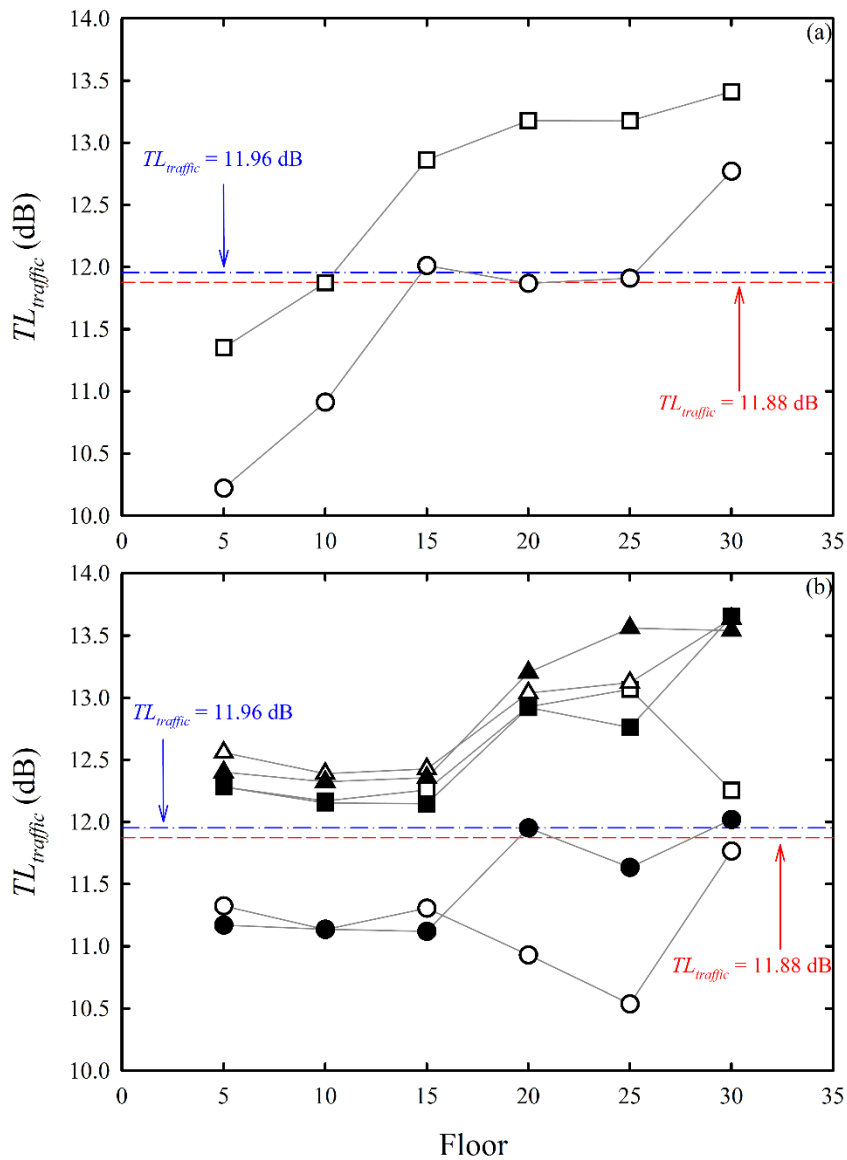


Figure 4. 9 Comparison between estimated $TL_{traffic}$ s of U8, U10 and U14 plenum windows.

(a) U8; (b) U10/U14 (closed symbols for U14, opened for U10).

Measurement (approach in Chapter 3) :

○ : living room; □ : outer bedroom; △ : inner bedroom.

- · - : living room/inner bedroom (Eq. 3.14); - - - : outer bedroom (Eq. 3.14).

In Figure 4.9b are presented the corresponding data of U10 and U14. Again, one can notice the large deviations between the predicted and measured bedroom window

$TL_{traffic}$. Such deviations in these triple plenum window cases are more serious than that in the dual plenum window case. On the contrary, the measured living room window $TL_{traffic}$ s are in general lower than the predictions.

However, one should note that the transmitted powers calculated above for the bedrooms using the approach of Chapter 3 and the measured data are likely to be overestimations. The larger living room, which has similar finishing as the bedroom, has longer reverberation sound decay than the bedroom in principle (Buratti, 2002), resulting in net acoustical power flow from the living room into the bedrooms. The fact that longer reverberation time for larger room is also illustrated in Figure 4.5. The reverberant field inside the each bedroom is thus resulted from the acoustical power transmitted across the bedroom plenum window as well as that comes from the living room reverberation, which is a condition not catered for in Chapter 3.

Once the dimensions of a plenum window are known, one can use Eq. (3.14) to estimate the traffic noise transmission loss across the window. It is then relatively straight-forward to estimate the overall traffic noise transmission loss of the multiple plenum windows. Since the sound pressure levels and their spectral characteristics at the outdoor window openings in the present study are very similar (Figure 4.8), one can write, by considering the total acoustical power incidents on the outer openings of the windows, the outer opening area weighted traffic noise transmission loss as :

$$TL_{overall} = 10 \log_{10} \left(\frac{\sum_{j=1}^N w_{o,j} h_j 10^{TL_{traffic,j}/10}}{\sum_{j=1}^N w_{o,j} h_j} \right), \quad Eq. 4.1$$

where N is the total number of plenum windows on the façade of a flat unit. The $TL_{traffic,j}$ of individual plenum window can be estimated using Eq. (3.14).

The estimation of $TL_{overall}$ from the measured sound pressure levels is less simple. Following the method presented in Chapter 3, one can write for the i th one-third octave

band and for the j th plenum window :

$$W_{i,j}^{inc} = W_{i,j}^{ref} + W_{i,j}^{tra} + W_{i,j}^{dis}, \quad Eq. 4.2$$

where W denotes sound power and the superscripts *inc*, *ref*, *tra* and *dis* denote incident, reflected, transmitted and dissipated respectively. Also, the sound intensity $I_{i,j}$ at each outdoor window opening, which was measured in this study, is the sum of the incident and reflected sound intensity :

$$\begin{aligned} I_{i,j} &= I_{i,j}^{inc} + I_{i,j}^{ref} \\ \Rightarrow I_{i,j}w_{o,j}h_j &= W_{i,j}^{inc} + W_{i,j}^{ref} \\ \Rightarrow W_{i,j}^{ref} &= I_{i,j}w_{o,j}h_j - W_{i,j}^{inc}, \end{aligned} \quad Eq. 4.3$$

where I denotes sound intensity. The sound power dissipated within the plenum window is limited such that the absorbed sound power in Eq. (4.2) can be ignored (Tong et al., 2015). Combining Eqs. (4.2) and (4.3) gives

$$2W_{i,j}^{inc} - I_{i,j}w_{o,j}h_j \approx W_{i,j}^{tra}, \quad Eq. 4.4$$

One then obtains by summing up the corresponding cases for all plenum windows :

$$\begin{aligned} 2 \sum_{j=1}^N W_{i,j}^{inc} - \sum_{j=1}^N I_{i,j}w_{o,j}h_j &\approx \sum_{j=1}^N W_{i,j}^{tra} \Rightarrow W_i^{inc} \\ &= \left(W_i^{tra} + \sum_{j=1}^N I_{i,j}w_{o,j}h_j \right) / 2. \end{aligned} \quad Eq. 4.5$$

The overall sound transmission loss in the i th one-third octave band is therefore

$$\begin{aligned} TL_i &= 10 \log_{10}(W_i^{inc} / W_i^{tra}) \\ &= 10 \log_{10} \left(1 + \frac{1}{W_i^{tra}} \sum_{j=1}^N I_{i,j}w_{o,j}h_j \right) - 3. \end{aligned} \quad Eq. 4.6$$

The overall transmitted power can be estimated using the average reverberation time and sound pressure level inside the flat unit by the classical room acoustics equation:

$$SWL^{tra} = 10\log_{10}\left(\frac{W^{tra}}{W_{reference}}\right) = SPL^{rec} - 10\log_{10}\left(\frac{4}{R_{rec}}\right), \quad Eq. 4.7$$

where $W_{reference}$ is the reference sound power (10^{-12} W). R_{rec} is the room constant of the flat unit, SWL^{tra} the transmitted sound power level and SPL^{rec} the average sound level in the flat unit. The room constant R_{rec} can be estimated using the measured reverberation time. The A-weighted traffic noise transmission loss for the case of multiple plenum windows, $TL_{overall}$, can then be obtained after the application of normalized traffic noise spectrum to the one-third octave band TL_i s as in existing literature (Tong & Tang, 2013; Garai & Guidorzi, 2000). For the case of single plenum window ($N = 1$), the above approach converges to that given in Chapter 3.

It can be observed from Figure 4.10 that the predictions of Eq. (4.1) agree very well with the measured $TL_{overall}$ s estimated using the above approach (Eq. 4.6), especially for the larger flat units U10 and U14, which are of the same layout. For U8, the agreement is slightly less, but the average measured $TL_{overall}$ is very close to that predicted by Eq. (4.1), which is 11.93 dBA, with a standard deviation of 0.81 dBA.

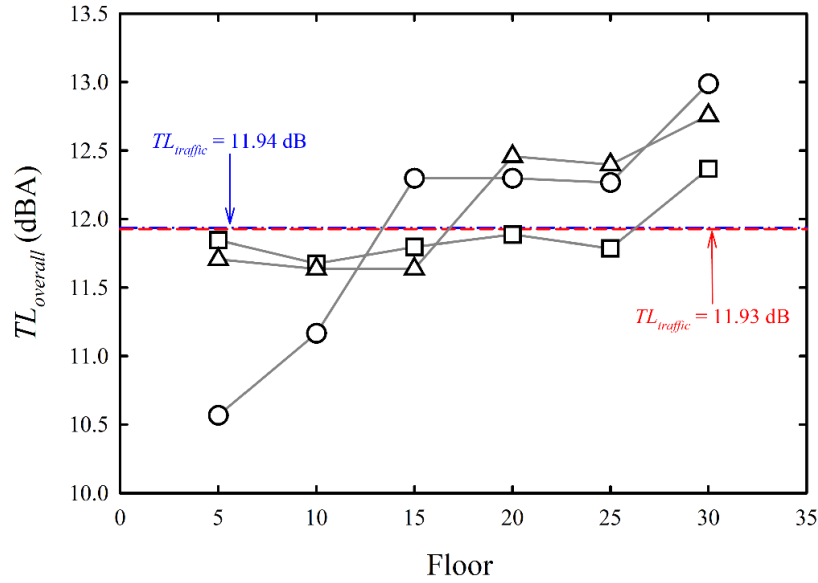


Figure 4. 10 Comparison between estimated $TL_{overall}$ s of U8, U10 and U14.

Measurement (Eq. 4.6) : \circ : U8; \square : U10; \triangle : U14.

Eq. (4.1) : - · - : U10 / U14; - - - : U8.

Table 4. 4 Comparison between predicted and measured $TL_{overall}$ (in dBA).

| Descriptor | Flat Unit | | | | | |
|--|-----------|-------|-------|-------|-------|-------|
| | U6 | U7 | U8 | U10 | U13 | U14 |
| Prediction | 11.86 | 11.94 | 11.93 | 11.94 | 11.94 | 11.94 |
| Average | 12.15 | 11.86 | 11.93 | 11.90 | 11.98 | 12.10 |
| Measurement | | | | | | |
| Maximum | 12.94 | 12.63 | 12.99 | 12.37 | 12.57 | 12.76 |
| Minimum | 11.15 | 10.96 | 10.57 | 11.68 | 11.12 | 11.64 |
| Average | 0.31 | 0.08 | 0.00 | 0.04 | 0.04 | 0.16 |
| Discrepancy between measurement and prediction | | | | | | |
| Standard deviation | 0.68 | 0.57 | 0.81 | 0.23 | 0.48 | 0.48 |
| Maximum | 1.08 | 0.98 | 1.35 | 0.43 | 0.82 | 0.83 |
| Minimum | 0.25 | 0.13 | 0.34 | 0.05 | 0.01 | 0.23 |

Table 4.4 summarizes the performance of the overall traffic noise transmission loss prediction model. One can find that the differences between predictions and measurements are very small and are within engineering tolerance. Such good

agreement, together with the weak dependency of the traffic noise transmission loss with floor level observed in the site survey, confirm the high practicality of the prediction model established in the present study for high-rise building plenum window applications in opened environment.

4.4 Conclusions

Extensive measurement of the noise transmission across plenum windows was carried out in the present study in a newly erected 30-storey single housing block located next to a busy trunk road in an opened environment. There were no significant reflection from nearby buildings at the time of measurement. The major noise source was the nearby trunk road. This building is the first residential public housing block equipped with plenum windows for the acoustical protection of the residents against the very strong traffic noise from the busy trunk road. A total of 35 flat units facing the trunk road, located between the fifth to the thirtieth floor and with four different layouts were surveyed. Measurements were done every 5 floors starting from fifth floor. Among these flat layouts, two of them consisted of a single plenum window, one of them had two windows and the last one had three.

It is observed that the measured sound levels at the building façades and the shapes of their one-third octave band spectra do not vary much with increasing elevation from the trunk road. The variation of equivalent sound pressure levels from the fifth to the thirtieth floor appears to be just around 2 dBA. For the flat units with a single plenum window, the results of the present site measurement further validate directly the empirical model developed earlier in Chapter 3. The corresponding discrepancy is within engineering tolerance.

The method developed in Chapter 3 for estimating the traffic noise transmission

loss of a standalone plenum window is generalized to deal with cases of multiple plenum window façades. Again, the corresponding predictions agree very well with site measurement results with a root-mean-square deviation of about 0.8 dBA for the dual plenum window cases and that for the triple plenum window cases is even smaller.

Owing to the dimensions of the plenum windows adopted, the traffic noise transmission losses of the flat unit façades measured in the present study varies over a very narrow range of 10.6 to 13.0 dBA. The predicted ones are all very close to 11.9 dBA. It is also observed that the variation of measured traffic noise transmission loss with elevation from the noisy trunk road (floor level) is small. The close agreement between predictions and measurements and the very weak variations of the major acoustical parameters with floor level manifest the practical significance of the present generalized prediction model for high-rise building applications at least in opened environments, where sound reflections from neighbouring buildings are not important.

Chapter 5 Sound Insulation of Plenum Windows Installed with Rigid Cylinder Array

In this chapter, a 1:4 scale down model was established to study the acoustic performance of the plenum window installed with different types of rigid cylinder array experimentally. Plenum windows with three different gaps, cylinders with three different diameters and the rigid cylinder array with three types of arrangement were included to explore the acoustic performance of the plenum window.

5.1 Introduction

Plenum window could provide an acoustical protection about 8 dB higher than an opened conventional window with minimum ventilation requirement (Tong et al., 2015). In order to improve the noise reduction further and maintain a reasonable degree of ventilation simultaneously, some methods with add-in noise attenuation materials, such as adding sound absorption combinations (Tang, 2015) and transparent micro-perforation absorbers (Kang & Brocklesby, 2005), inside the central cavity of the plenum window were studied. The use of active noise control has also been explored (Huang et al. 2011 and Tang, 2016). Though the noise reduction is acceptable, these methods are not practical in engineering. By a 2-D finite-element simulation, Tang (2018) found that the noise reduction improvement could be as large as 4-5 dB when a simple rigid cylinder array was installed inside the plenum window.

In the present study, experimental method was applied to test the acoustic performance of the plenum window installed with different types of rigid cylinder array in the central cavity. The typical rigid cylinder array arrangements in the simulation study of Tang (2018) are also included. Besides, some newly proposed rigid cylinder array arrangements, which are expected to be able to achieve more significant noise reduction, are tested.

5.2 Measurement Setup

5.2.1 Test Chamber

In this study, all tests were conducted in the semi-anechoic chamber, which is a prefabricated house made of color steel plate with a dimension of 4.5m (length) by 4m (width) by 5m (height), shown in Figure 5.1. The surfaces of the walls and ceiling inside this chamber were covered by fiberglass curtains (2 inch thick Owens Corning type 703). Floor of the test chamber was made of cement without sound-absorbing material, thus it was semi-anechoic and could simulate the actual acoustical environment of residential buildings. Reverberation time inside this chamber was tested. At frequencies above the 200 Hz one-third octave band, it was less than 0.2s one-third octave band.

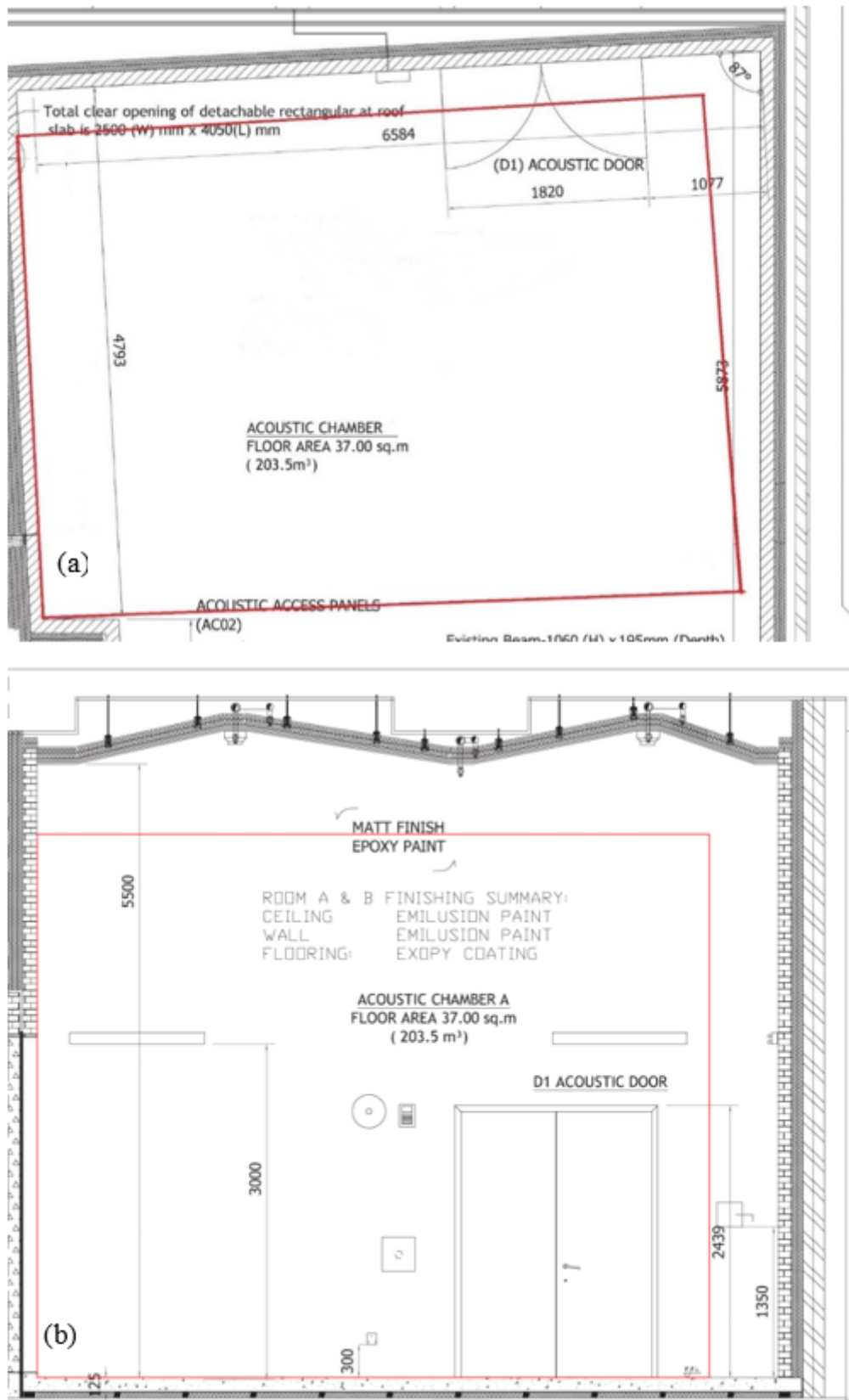


Figure 5. 1 2-D Layouts of the test chamber (in red)

(a). Top view; (b). Lateral view

5.2.2 Scale down model

In present measurements, a 1:4 scaled down reverberation model made of 18 mm-thick varnished plywood was adopted with no parallel internal surfaces. Same scaled down proportion plenum window with a dimension of 500 mm length (L), 260 mm height (H) was installed on the facade of this reverberation model, shown in Figure 5.2. There were two openings of plenum window, which are defined in the present study as the outer side opening ($w=167$ mm wide) and the inner side opening of the same size. Gap (G) of the scaled down plenum window was set as 98mm, 158mm and 218mm. Two 3 mm thick Perspex panes were inlaid crosswise on the inlet and outlet of the window to create an air passage across the plenum window. These Perspex panes acted as the glass panels of the full-size plenum window. For convenience, all data has been scaled back to 1:1 in the foregoing discussions in this chapter.

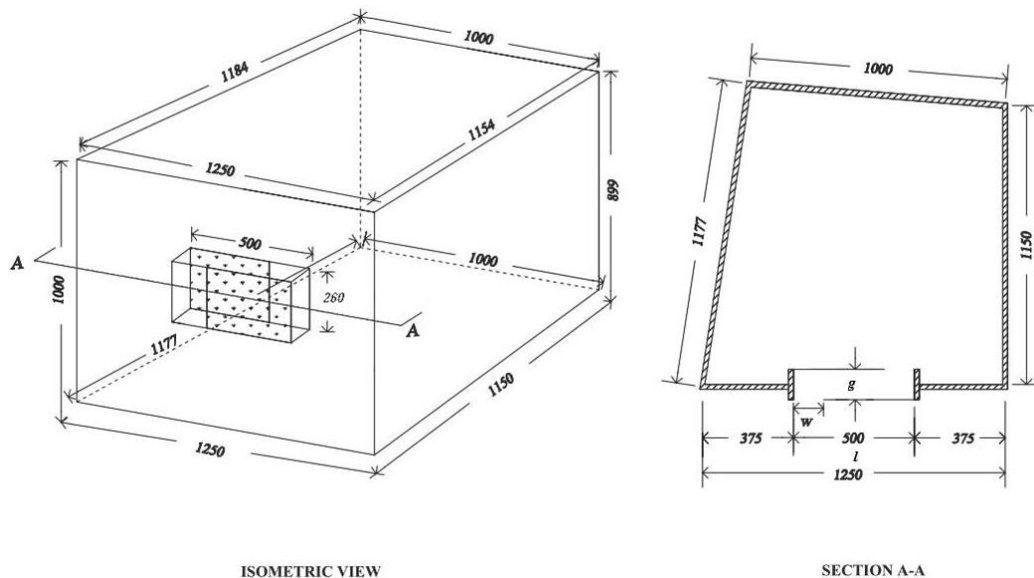


Figure 5. 2 Scale down model. (Dimension in mm)

5.2.3 Sound Source

A line source was used in this measurement, with a length of 3.2m. The line source consisted of 20 eight-inch loudspeakers, which could produce noise at frequencies between 100 Hz - 20 kHz, as shown in Figure 5.3. The traffic noise study of Tong and Tang (2013) adopted this type of line source. Thus, the adoption of such line source in present measurement is reasonable and acceptable.

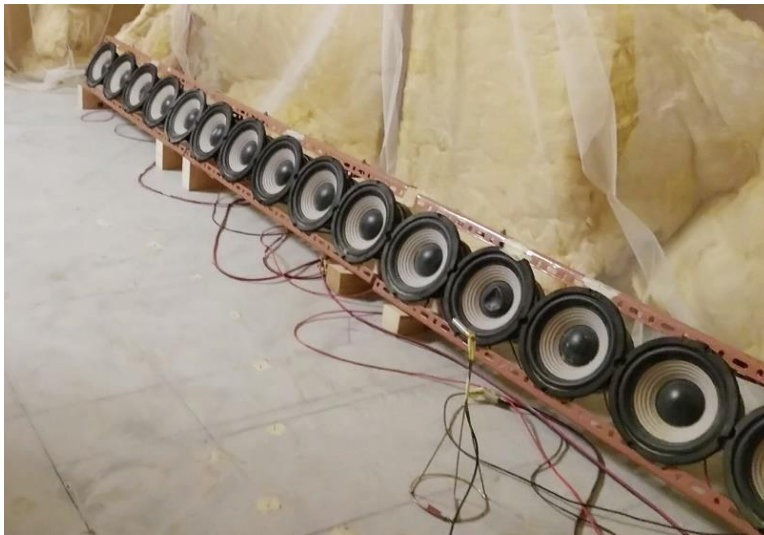


Figure 5. 3 Line source adopted in this measurements.

5.2.4 Reverberation Time

As the reverberation time (RT) inside the scaled down model box can affect the transmission loss of the plenum window. Test cases were conducted to certify that the RT difference before and after the installment of cylinder array have no significant effect on the transmission loss of the plenum window.

An 8 cm-aperture loudspeaker was placed at the corner of the model receiver chamber and a 1/4" Brüel & Kjær Type 4935 microphone was used to capture the data.

A total of 8 random points inside the receiver chamber were selected to measure the average reverberation time using DIRAC system with MLS signal. RTs inside the receiver room with and without rigid cylinder array were tested. For the case with rigid cylinder array inside the plenum widow, a (2,3) rigid cylinder array, which consisted of 6 rigid cylinders, was adopted for this test. The corresponding test results are shown in Figure 5.4. One can find that the RT difference between the cases with and without rigid cylinder array is so insignificant that it will have almost no effect on the transmission loss of the plenum window. In the subsequent discussion, RT correction will be neglected.

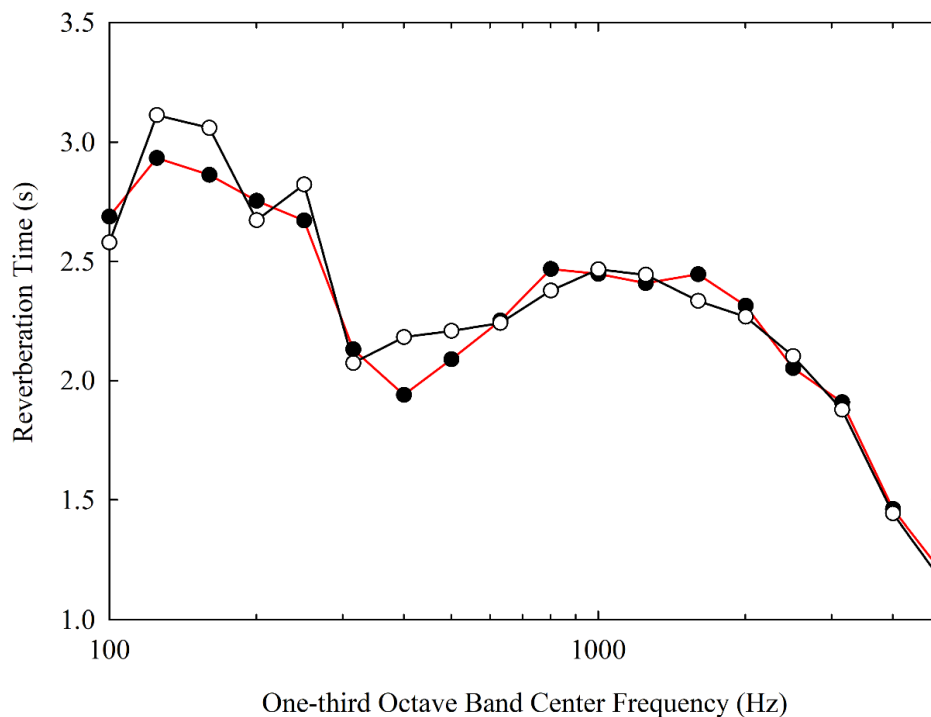


Figure 5. 4 Average reverberation times acquired inside scale down model.
 Open circle: Case of the plenum window installed with 2x3 rigid cylinder array;
 Closed circle: Plenum window without rigid cylinder array.
 (Gap of tested plenum window: 98mm; Diameter of the rigid cylinder: 19mm.)

5.3 Measurement procedure

The 3.2 m line source was placed at 1 m horizontally away from the facade of the plenum window. Three $\frac{1}{4}$ Brüel & Kjær Type 4935 microphones are placed at the inlet side of the plenum window uniformly and vertically to capture the average inlet sound pressure level. Six Brüel & Kjær Type 4935 microphones were scattered inside the scaled down model room space to record the receiver side sound pressure levels. Figure 5.6 illustrates the locations of microphones used in present measurement. All data were acquired by the Brüel & Kjær 3506D PULSE system. For each test setting, there were 3 measurements and each lasted for 20 seconds. The measurement devices are shown in Figure 5.5.

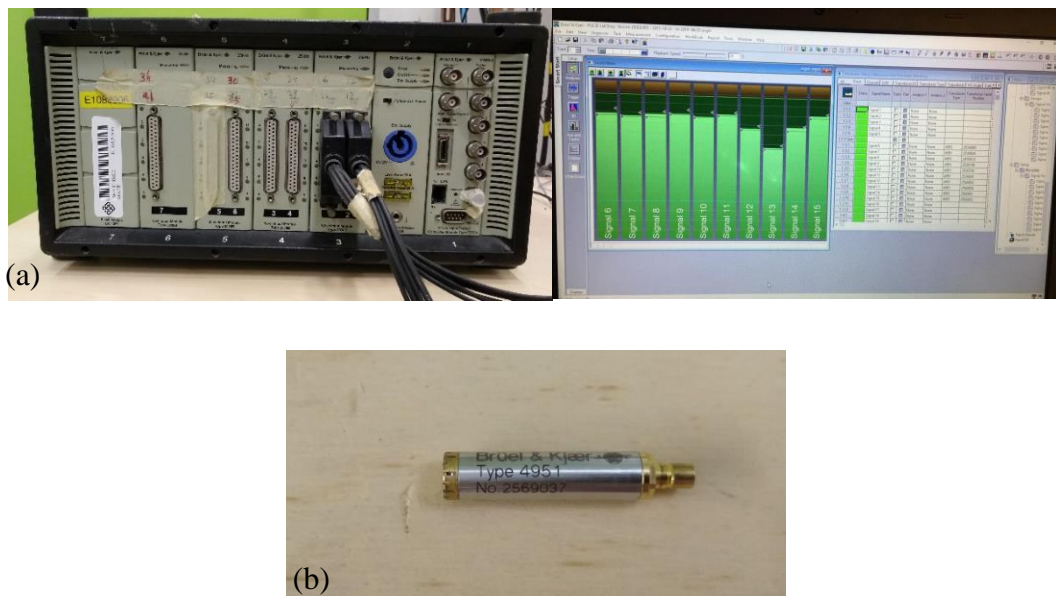


Figure 5. 5 Measurement devices used for data acquisition.

(a). Brüel & Kjær 3506D PULSE system;

(b) $\frac{1}{4}$ Brüel & Kjær Type 4935 microphone

As the RTs inside the receiver chamber did not change significantly before and

after the installation of rigid cylinder array, they were omitted from the calculation. The sound pressure level between cases with and without rigid cylinder array inside the plenum window is defined as change in transmission loss (ΔTL) as the incident power was kept constant throughout the experiment, as equation (5.1). In order to present the performance of both windows in front of traffic noise, the normalized traffic noise spectrum in the standard EN 1793-3 (BS EN1793-3. 1998) was adopted to obtain the single rating results as shown in equation (5.2):

$$\Delta TL = SPL_{i,cyl} - SPL_{i,ref} \quad Eq. 5.1$$

$$\Delta TL_{EN1793} = -10 \log_{10} \left(\frac{\sum_{i=1}^{18} 10^{0.1(N_i - \Delta TL_i)}}{\sum_{i=1}^{18} 10^{0.1N_i}} \right) \quad Eq. 5.2$$

where i represents the i th one-third octave band data, from 100 Hz to 5 kHz, N_i is the corresponding normalized noise band level (BS EN1793-3. 1998), the suffices *cyl* indicates the case with rigid cylinder array inside the plenum and *ref* indicates the case without rigid cylinder array inside the plenum window.

| Signals | Coordinates (x y z) |
|---------|------------------------|
| S1 | 500 625 500 |
| S2 | 540 280 300 |
| S3 | 580 875 400 |
| S4 | 650 580 450 |
| S5 | 800 250 550 |
| S6 | 950 750 600 |
| S7 | -50 792 600 |
| S8 | -50 792 500 |
| S9 | -50 792 400 |

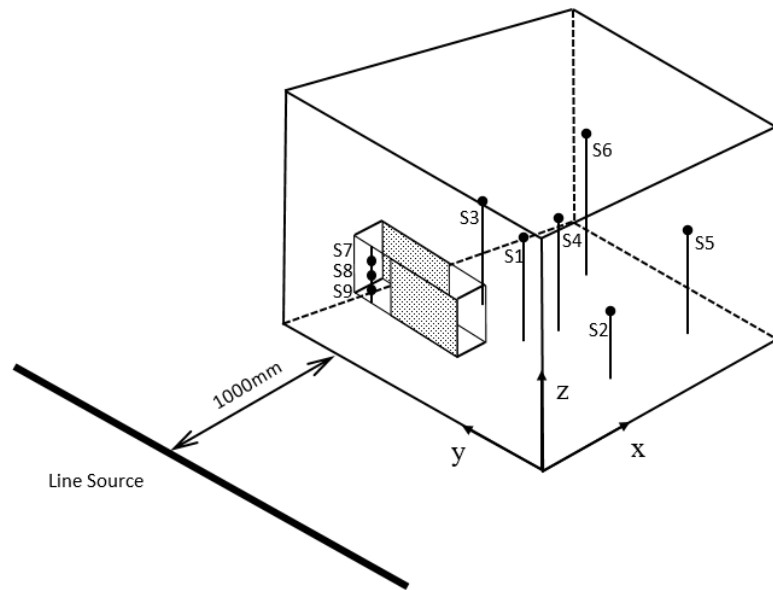


Figure 5. 6 Locations of microphones. (Dimension: mm)

5.4 Rigid cylinder array arrangements

Cylinders adopted in this study are made of aluminum. All cylinders were with the same length of 260mm. Three rigid cylinder diameters were used in the test (10mm, 19mm and 32mm) as shown in Figure 5.7(b).

A total of 13 rigid cylinder array arrangements are included in the present study and the adjacent dimensions are shown in Figure 5.8. These arrangements can be classified into 3 different types, regular type, single staggered row type and dual staggered rows type. The regular type is the same as that adopted in Tang (2018), shown in Figure 5.8 (a)-(e). The single staggered row type is similar to the staggered array in Tang (2018). But the difference is that the half-cylinder close to the glass panel in Tang's study was replaced with a complete cylinder, shown in Figure 5.8 (f)-(i). The dual staggered rows type is shown in Figure 5.8 (j)-(m). The array arrangement is

represented by the matrix form of $V(m, n)$, and the distance between any 2 adjacent cylinders is defined as G/n for regular and dual staggered rows type. $V(0,0)$ represents the case of plenum window without rigid cylinder array. For single staggered row type, due to the adding of a complete cylinder, the adjacent distance to the cylinders near the glass panel in staggered row is $G/n-d/2$. According to the simulation research of Tang (2018), the number of rows in the cylinder array should better be no more than 2. In present study, $m \leq 2$. All rigid cylinder arrays were placed near to the inlet side of the plenum window cavity.

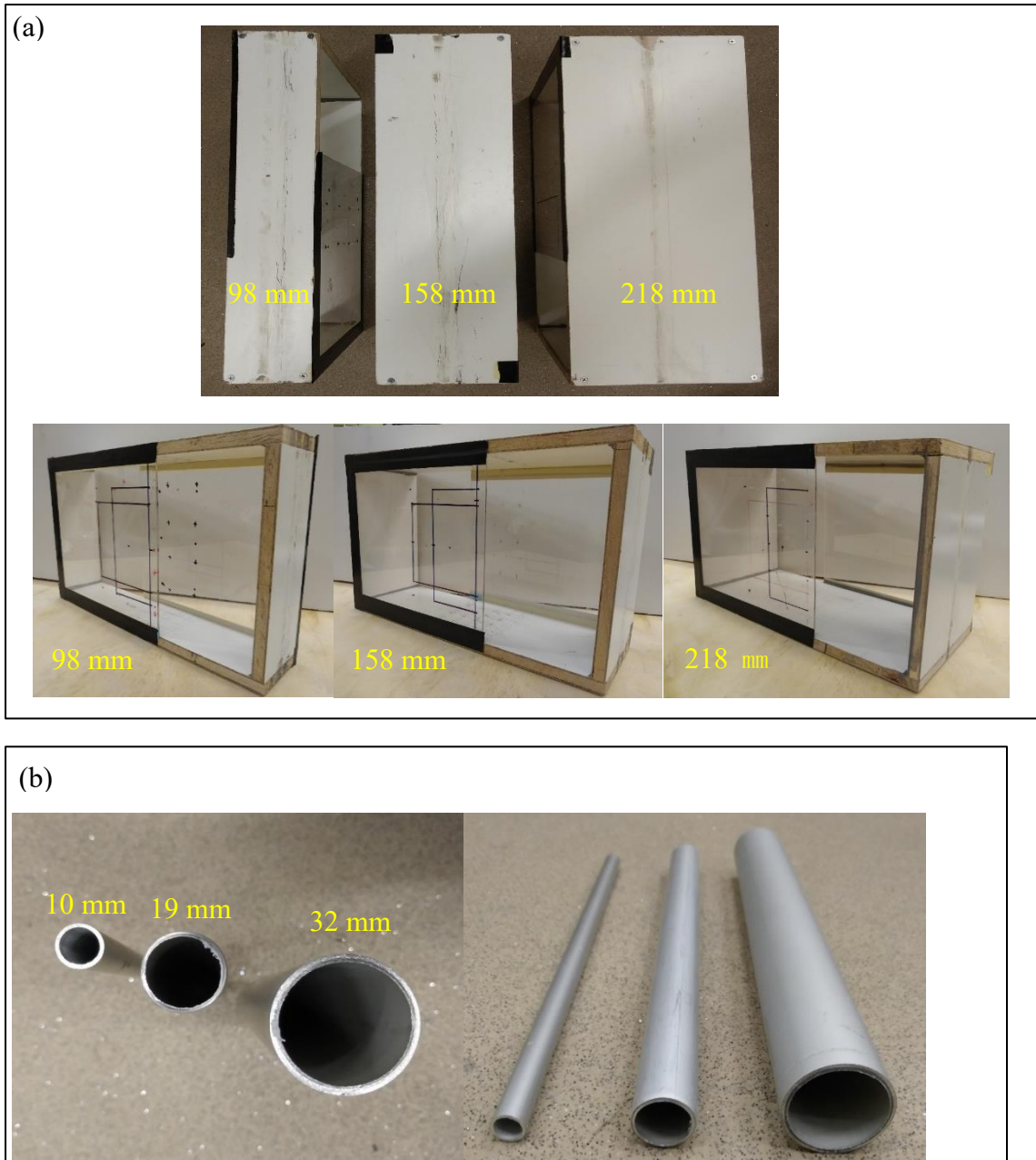


Figure 5. 7 Tested plenum windows and cylinders.

(a) Plenum windows with three different gaps.

(b) Rigid cylinder with different diameters.

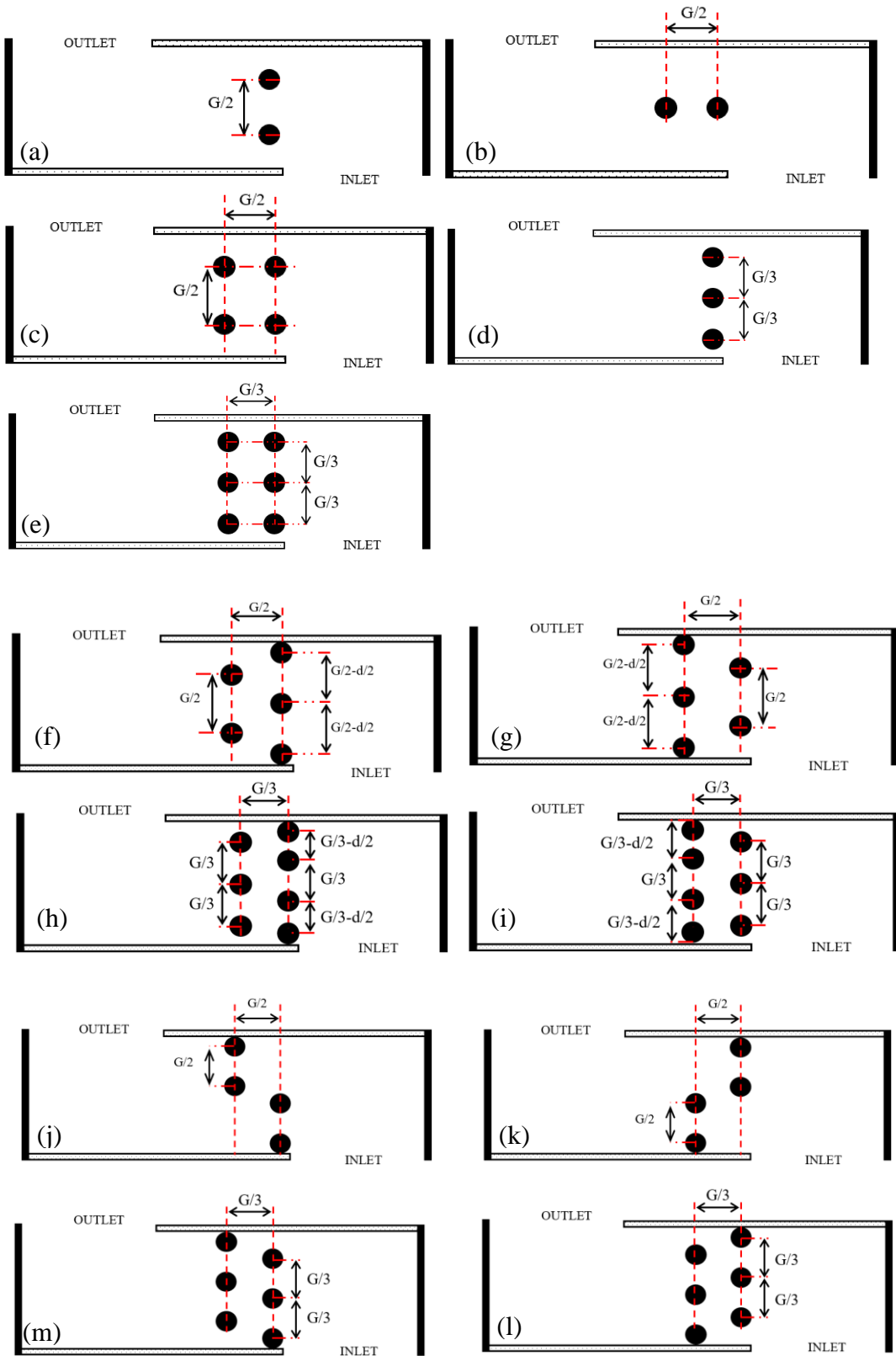


Figure 5. 8 Rigid cylinder array arrangement.

(G is the gap of plenum window; d is the diameter of the cylinder)

- (a): $V(1,2)$; (b): $V(2,1)$; (c): $V(2,2)$; (d): $V(1,3)$; (e): $V(2,3)$. (f). $V(2,2)^s$; (g). $V(2,2)_s$;
 (h). $V(2,3)^s$; (i). $V(2,3)_s$. (j). $V(2,2)^{ds}$; (k). $V(2,2)_{ds}$; (l). $V(2,3)^{ds}$; (m). $V(2,3)_{ds}$.

5.5 Numerical simulation

In present study, the simulation tests were implemented with the software COMSOL (version 5.3a). By the help of simulation results, one can better understand the interior sound field inside the plenum window space.

Owing to the limitation of the computational resources, the frequency range was set to be between 100 Hz and 1000 Hz. According to the experiment results, the acoustic performance of the plenum window installed with rigid cylinder array is not so significant at frequencies below 800 Hz, the simulation work could help to show the sound field at this frequency range and find the reasons of low performance.

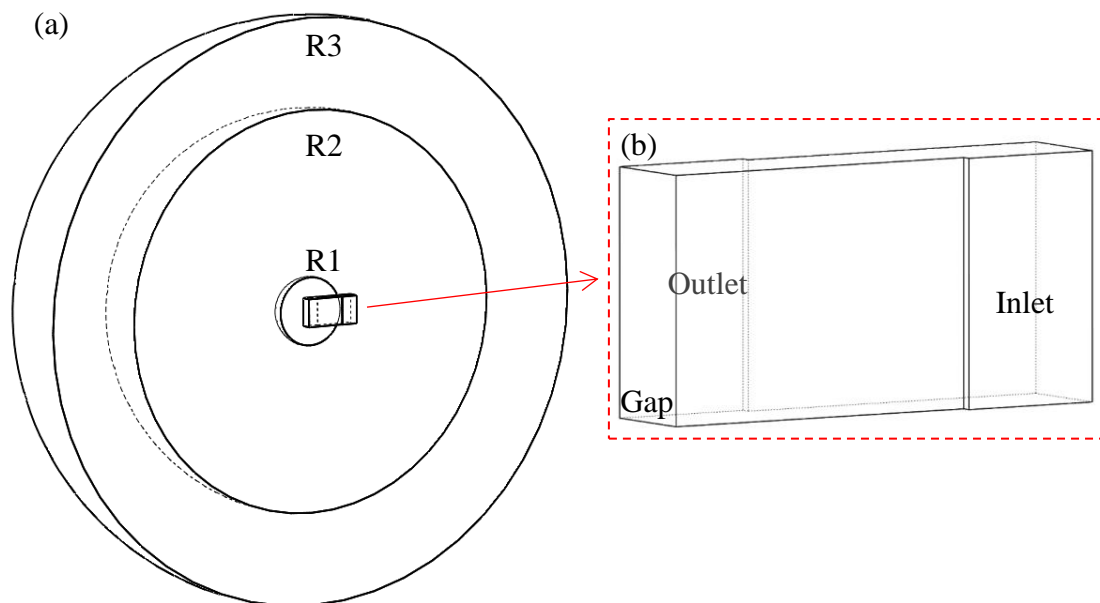


Figure 5. 9 Computational domain and plenum model.

The computational domain is shown in Figure 5.9 (a), which includes three hemispheres. The surface of the inner hemisphere (R1) is the reference layer where the SPL of receiver side is obtained. Radius of R1 is double times of the window gap, the same reference layer dimensions adopted in Tang (2018). The layer between R2 and R3 is set as the Perfect Match Layer (PML) to eliminate the effect from the sound

reflections inside the computational domain. The thickness of PML is set at no less than the wavelength of the lowest frequency of calculation. The radius of computational domain (R3) is set at no less than 4 times of the wavelength of the lowest frequency of calculation range. Sound source is from the inlet opening of the plenum window, which is set as plane wave with an amplitude of 1. Emitted from the inlet opening shown in Figure 5.9 (b), sound wave propagates through the plenum chamber then comes out from the plenum window outlet opening into the hemisphere computational domain.

The dimensions of plenum windows adopted in the computational simulation is the same as that adopted in the laboratory measurements. The thickness of the glass is set at 3mm. All frequencies presented in this thesis are scaled up to those of the 1:1 model. The maximum element size is no longer than 1/6 wavelength of the lowest frequency in the calculation frequency bandwidth and the computational step is 10 Hz, shown in Figure 5.10.

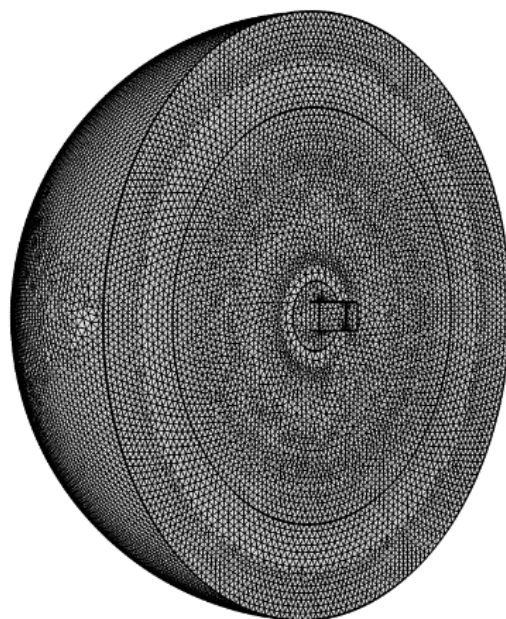


Figure 5. 10 Computational model with meshing.

5.6 Results and Discussions

5.6.1 TL of the reference plenum windows with different gaps

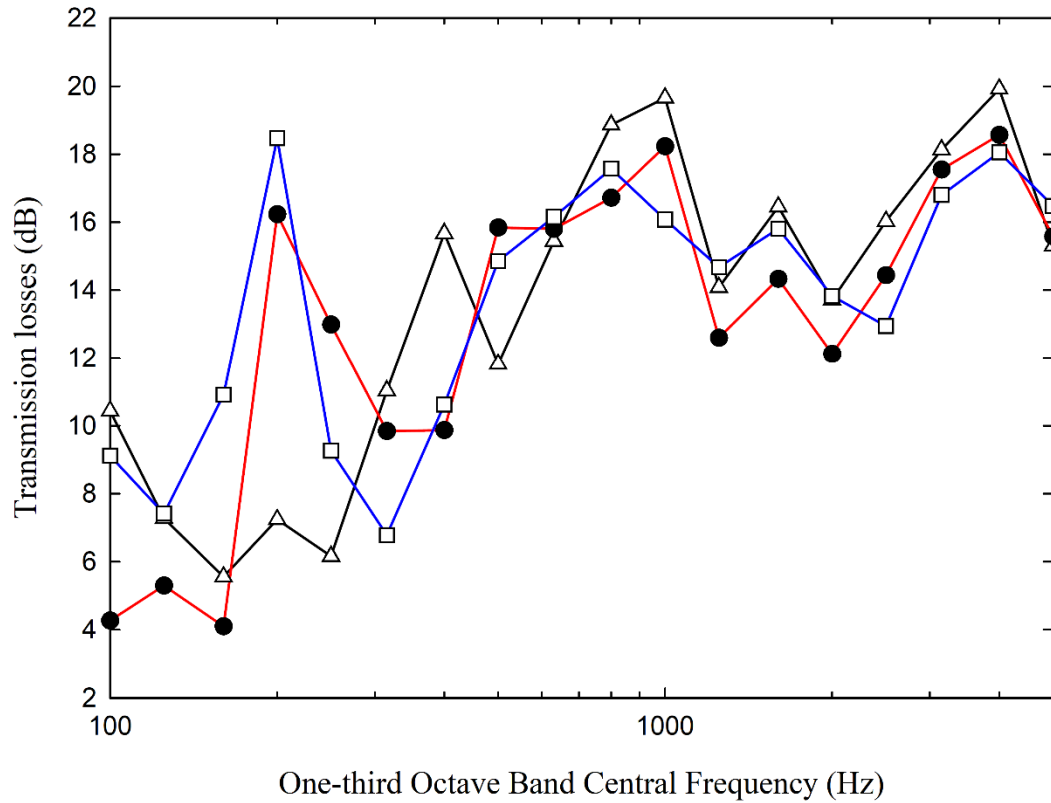


Figure 5. 11 Transmission losses of plenum window with different gaps.

△: Gap=98mm; ●: Gap=158mm; □: Gap=218mm.

Firstly, TLs of plenum windows with three different gaps were tested. It is obvious that the spectral variations of TLs can be divided into two regions in Figure 5.11. At frequencies lower than the 400Hz one-third octave band, there are extraordinary fluctuations, which are due to the effect of acoustic mode (Figure 5.12).

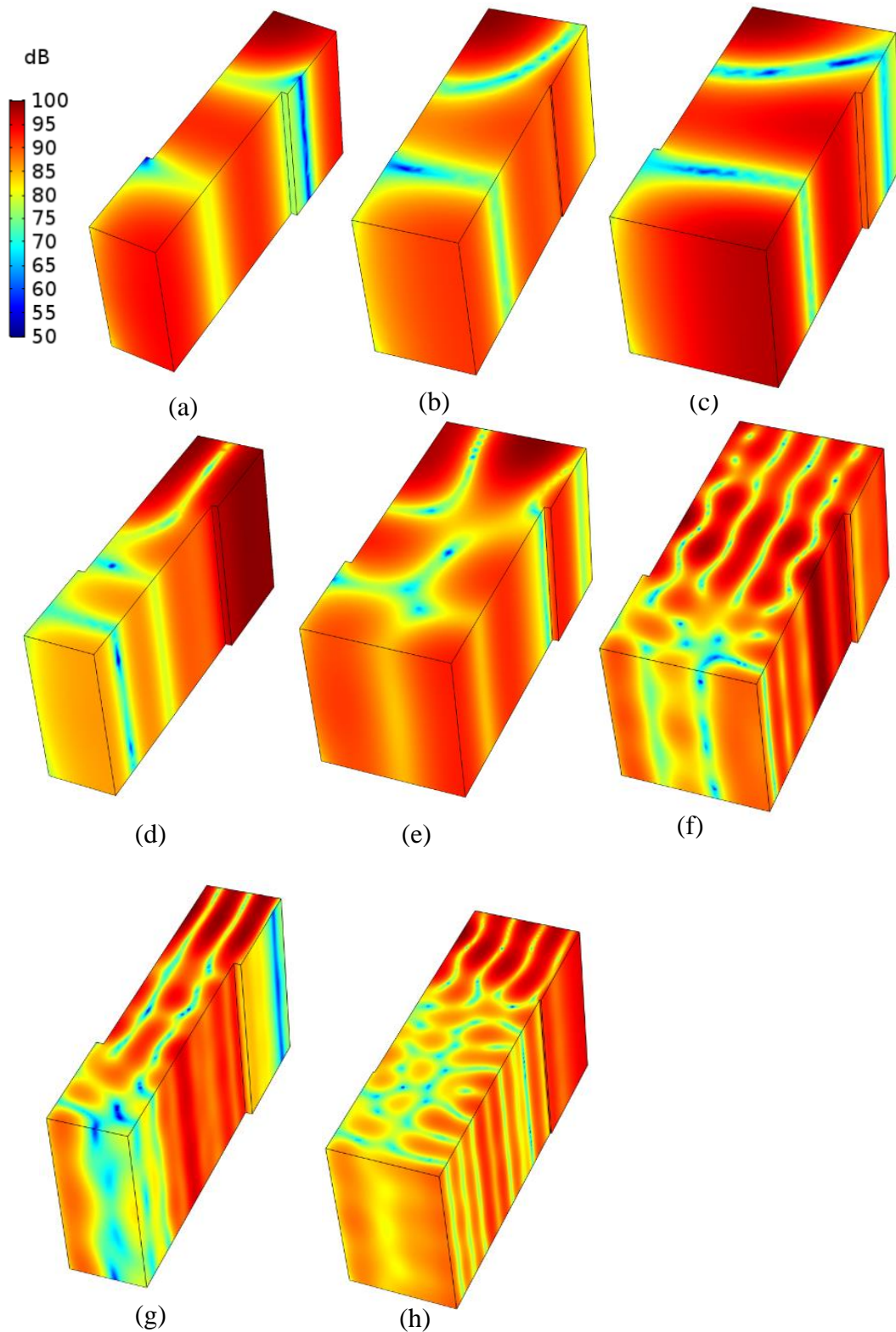


Figure 5. 12 Sound field of the plenum windows with different gaps.

- (a). Gap=98mm, frequency=200 Hz; (b). Gap=158mm, frequency =200Hz;
(c). Gap=218mm, frequency =190Hz; (d). Gap=98mm, frequency =400Hz;
(e). Gap=218mm, frequency =310Hz; (f). Gap=218mm, frequency =800Hz;
(g). Gap=98mm, frequency =990Hz; (h). Gap=158mm, frequency =1000Hz.

At frequencies around the 200Hz one-third octave band, there are very prominent peaks for plenum windows with gap of 158 mm and 218 mm, which are due to low frequency resonance inside the cavity of the plenum window. The length of plenum window is 500mm, which corresponds to a resonance frequency of 173 Hz. From the simulation results shown in Figures 5.12 (b) and (c), one can find that there are resonances along the length and the gap of the plenum windows in each case at frequency 200 Hz and 190 Hz respectively. These resonances play a key role here and help reduce the SPL near the window opening resulting in low SPL regions near the plenum window exit. As a result, less sound energy can go into the indoor space and high TL is obtained near 200 Hz. This circumstance occurred in the study of Kropp and B é rillon (1998), Jean (2009), Tong et al. (2015). For the plenum window with gap of 98mm, the peak at frequencies around 200 Hz one-third octave band is not so prominent in Figure 5.11. According to the simulation results, resonance of plenum window with gap of 98 mm is not so intensified compared to the other 2 cases around 200 Hz, shown as Figure 5.12(a).

Around 300 Hz, there is an obvious dip for plenum window with gap of 218mm. From Figure 5.12(e), one can find that there is a high SPL region at the outlet opening of the plenum window around 310 Hz, which can reduce the TL.

The peak appears around 400 Hz for plenum window with gap of 98 mm from Figure 5.11. Figure 5.12(d) shows the sound field inside this plenum window at 400 Hz. It is obvious that the SPL at the window outlet is much lower than that at the inlet region

where high sound energy is trapped, thus resulting in high TL.

One may find that the computational results are not always completely consistent with the actual measurements, which is due to the existence of air damping in actual measurements and the difference between the numerical model and the lab model.

Above the 600 Hz octave band, the TL gradually increases up to a high level of around 20 dB. Beyond 1000 Hz, TLs stay in a relatively high level at no less than 12 dB though there are some insignificant fluctuations.

Around 800Hz one-third octave band, the peak for the plenum window with gap of 218mm is due to the resonance along and perpendicular to the length of the plenum window as shown in Figure 5.12(f). Around this frequency range, sound energy is constrained in the central cavity of the plenum window and less sound energy goes to the exit opening.

Around 1000 Hz, there are extreme peaks for plenum window with gap of 98mm and 158 mm in Figure 5.11. As shown in Figure 5.12(g), the SPL near the outlet opening is much lower than the SPL at other frequency range inside the plenum window with a gap of 98mm. Most of the sound energy is blocked at the inlet opening of the plenum window, resulting in a large region with low sound pressure level at the corner near the outlet opening. It enhances the sound transmission loss across the window cavity, resulting in an extreme TL peak of this plenum window. Same phenomenon also appears in the plenum window with a gap of 158mm at 1000Hz as shown in Figure 5.12(h). The resonances caused by high frequency sound waves help reduce the sound

energy transmission across the plenum window cavity and provide an extreme TL.

It is noticed that there are TL peaks for all plenum windows at around 1600 Hz. Given the glass thickness is ~3 mm and the width of gap is 98 mm, 158mm, 218 mm in scale down model, which corresponds to possible resonance at 1683 Hz, 1583Hz and 1538 Hz, respectively. Resonances take place along the length of the plenum window gap near the inlet opening at around 1600Hz. Thus there are peaks for every plenum window around 1600 Hz as shown in Figure 5.11. Δ TL peaks around 4000 Hz is also led by the resonances along the plenum window gap.

Besides, one can find that when the window height is constant, increasing the gap may reduce the acoustic performance of the plenum window especially at high frequencies, which is obvious for plenum window with gap of 98 mm as shown in Figure 5.11. With the decrease of the plenum window gap, this phenomenon becomes more significant. This was also observed in Tong (2015).

According to the results in Tang (2018), array (3,3) could result in ~ 16 % reduction of the air flow rate across the plenum window. In present study, the maximum installed array is cylinder array (2,3), which could provide an acceptable air flow rate than cylinder array(3,3).

5.6.2 Effects of regular rigid cylinder array

In the present and subsequent sections, the plenum window with gap of 98 mm installed with rigid cylinder array with cylinder diameter of 19 mm are taken as example to illustrate the acoustical performance.

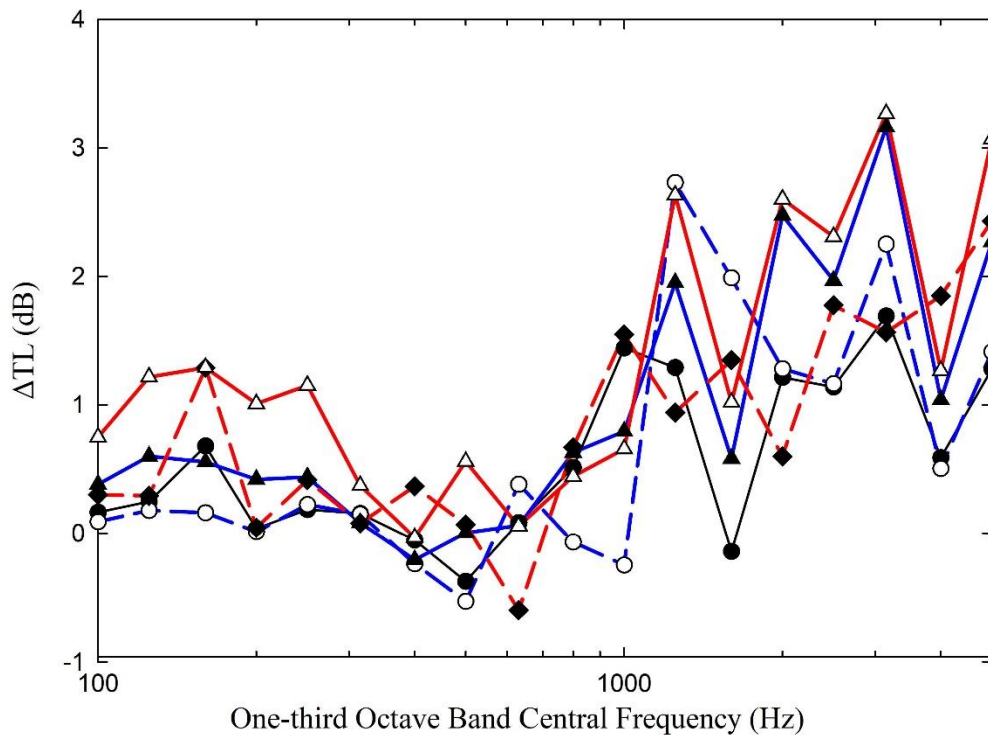


Figure 5. 13 ΔTL of the plenum window (gap: 98mm) installed with regular rigid cylinder arrays (cylinder diameter: 19mm) in one-third octave band.

●: V(1,2); ○: V(2,1); ▲: V(2,2); ◆: V(1,3); △: V(2,3).

It is obvious that increasing the number of cylinder results in higher ΔTL , which becomes more obvious at high frequency as shown in Figure 5.13. The presence of more cylinders increases the reflection and lead to trapped mode inside the plenum cavity resulting in higher ΔTL (Tang, 2018). Comparing the results of V(1,2) and V(2,2), one can find that more cylinder row will increase ΔTL . This also applies to the

pair $V(1,3)$ and $V(2,3)$. In the present study, the ΔTL of $V(2,3)$ can be as high as ~ 1.1 dBA. One more added row improves the effect of sound wave reflection and scattering out of the chamber from the plenum window.

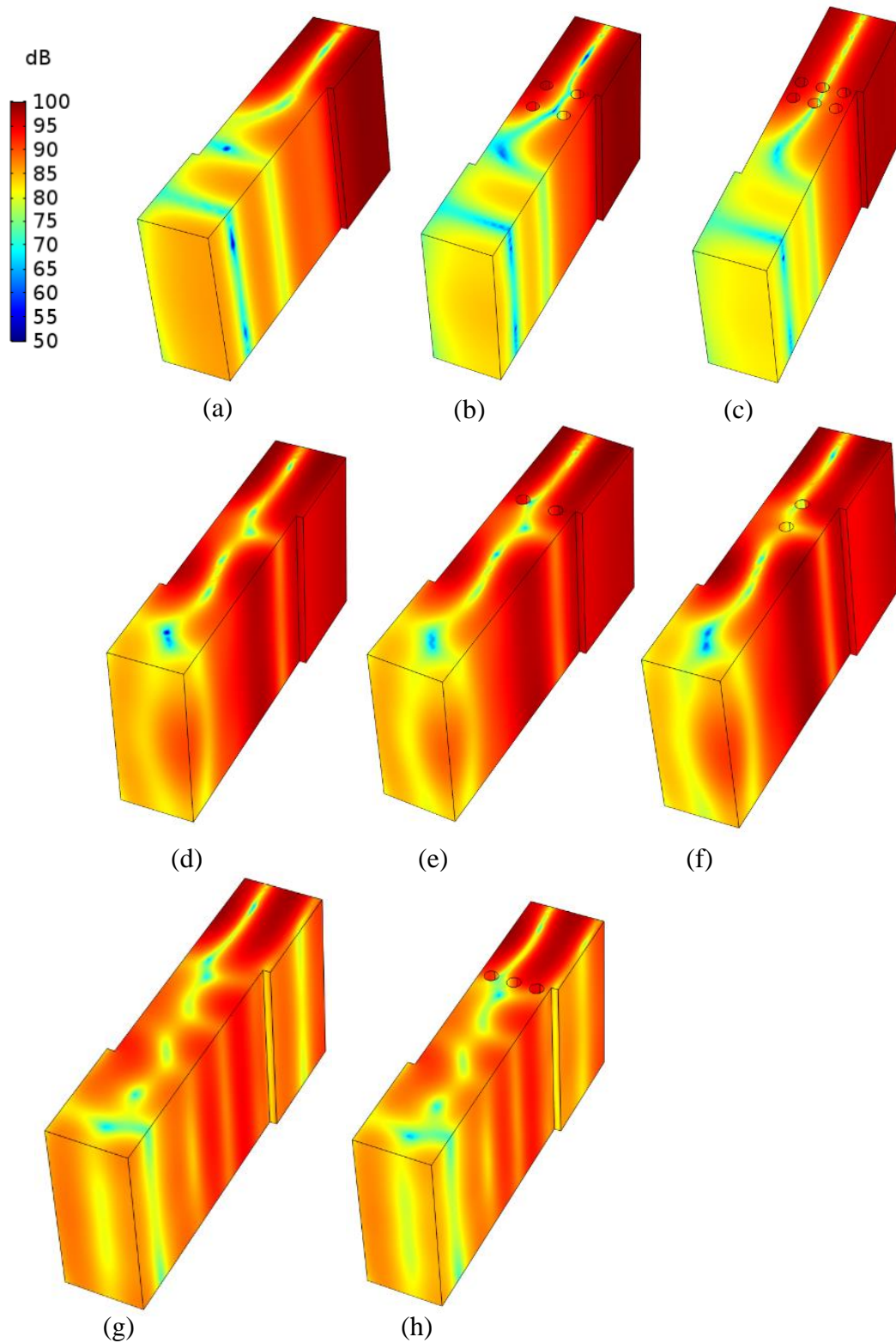


Figure 5.14 Sound field of the plenum windows with regular rigid cylinder array.
 (a). $V(0,0)$, frequency=400 Hz; (b). $V(2,2)$, frequency=400 Hz;
 (c). $V(2,3)$, frequency=400 Hz; (d). $V(0,0)$, frequency=500 Hz;
 (e). $V(1,2)$, frequency=500 Hz; (f). $V(2,1)$, frequency=500 Hz;
 (g). $V(0,0)$, frequency=630 Hz; (h). $V(1,3)$, frequency=630 Hz;

At frequencies around 400Hz, there are small dips for V(2,2) and V(2,3) (Figure 5.13). Sound fields of these two cases inside the plenum window at 400 Hz are shown in Figures 5.14(b) and 5.14 (c). Compared to the reference case without rigid cylinder array as shown in Figure 5.14(a), the placement of rigid cylinder array V(2,2) and V(2,3) almost has no significant effect on the sound field. Thus the TL has no change and ΔTL is near to 0 dB.

At frequencies around 500 Hz, the acoustic performance of the add-in rigid cylinder array fail to enhance the ΔTL of V(1,2) and V(2,1). Comparing to sound field of V(0,0) at 500 Hz shown in Figure 5.14 (d), the sound field of V(1,2) in Figure 5.14(e) and V(2,1) in Figure 5.14(f) has no change after the installment of rigid cylinder array, resulting in poor ΔTL . For V(2,1), the similar circumstances appear at frequency around 1000 Hz again.

For the add-in rigid cylinder array V(1,3), the dip occurs at frequencies around 630Hz one-third octave band as shown in Figure 5.13. Compared the sound field of the reference case V(0,0) in Figure 5.14(g) at 630 Hz, the sound field of case with V(1,3) barely changes as shown in Figure 5.14 (h).

For the cases abovementioned, the ΔTL is near to 0 dB, which means that the placement of rigid cylinder array fail to increase the sound transmission loss across the plenum window. This is due to the fact that the position of cylinder is not on the antinode position. When placed near the node positions where the sound energy is much lower than other positions, the cylinders barely change the sound field. Because at node

positions the sound pressure level is low, so that the placement of rigid cylinder array at the pressure node positions will have small effect on the sound wave energy propagation and contributes little to the noise reduction. On the contrary, placing the rigid cylinder array at the anti-node positions where the sound pressure level reaches maximum, can block the sound energy and increases the noise reduction.

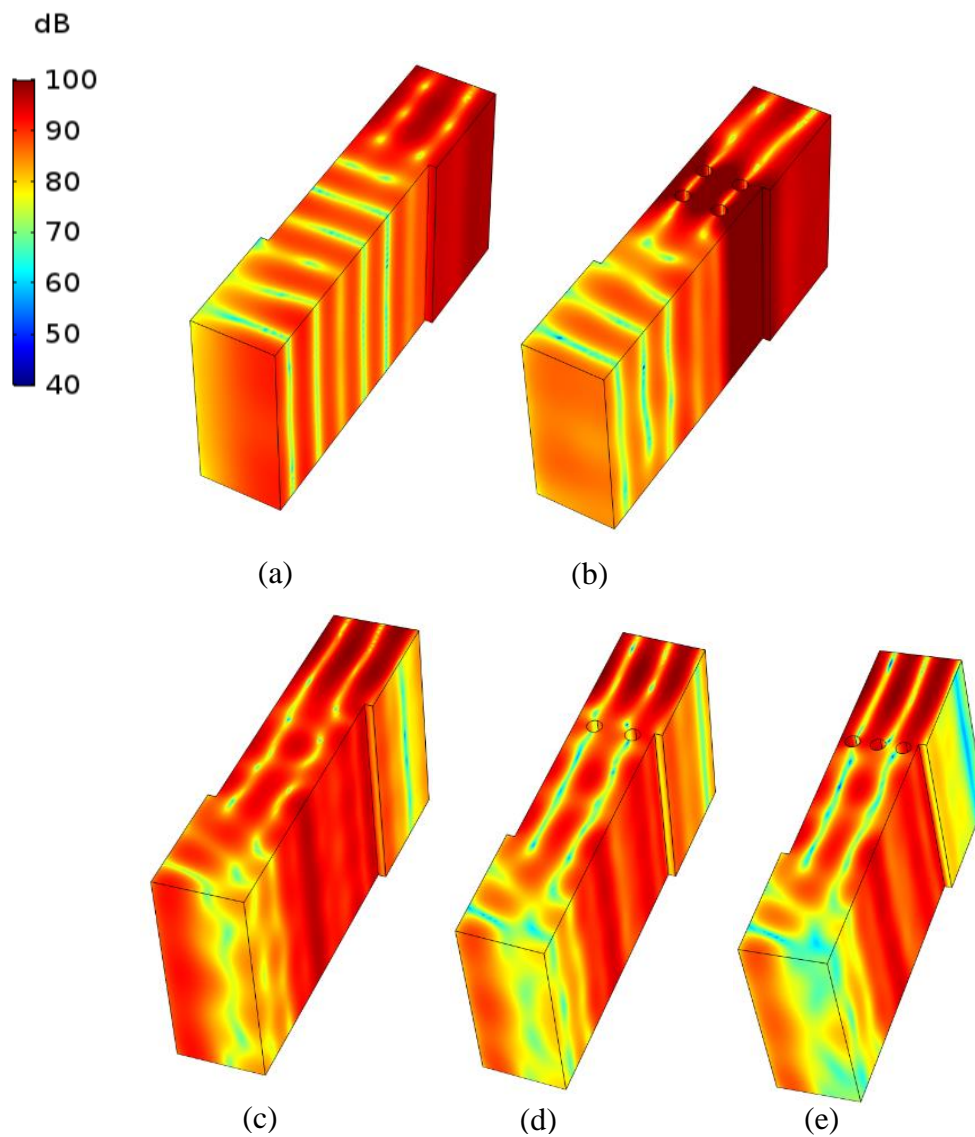


Figure 5. 15 Sound field of the plenum windows installed with staggered rigid cylinder array.

- (a). $V(0,0)$, frequency=720 Hz; (b). $V(2,2)$, frequency=720 Hz;
(c). $V(0,0)$, frequency=1000 Hz; (d). $V(1,2)$, frequency=1000 Hz;
(d). $V(1,3)$, frequency=1000 Hz.

At 780 Hz, trapped mode is observed in $V(2,2)$ in Figure 5.15(b), which is enforced by the rigid cylinder array. Figure 5.15(b) shows that the enforced second order mode has an effect on the sound field of the plenum window cavity compared to the sound field of $V(0,0)$ given in Figure 5.15(a), but contributes to weak improvement of the ΔTL as shown in Figure 5.13.

At frequency 1000 Hz one-third octave band, there are small peaks for $V(1,2)$ and $V(1,3)$. According to the simulation results in Figure 5.15(d) and 5.15(e), one can find that the placement of $V(1,2)$ and $V(1,3)$ has blocked the propagation of sound wave along the plenum chamber. The rigid cylinder array is placed at the antinode positions, thus it can reduce the sound energy effectively. However, the TL of $V(0,0)$ around 1000 Hz is significant enough as shown in Figure 5.15(c) and 5.12(g), resulting in small improvement of ΔTL at this frequency range.

Around 1250 Hz, there are ΔTL peaks, which is caused by the resonance along the total length for the plenum window gap and the glass thickness, which is 101mm with corresponding frequency ~ 1274 Hz. In the subsequent sections included the plenum window with gap of 98 mm, resonance always occurs around 1250 Hz.

ΔTL peaks also occur at around 3150 Hz (Figure 5.13), whose corresponding wavelength is ~ 27 mm in scale down model. Given the total length along the inlet opening is 101mm, which is about 3.75 times the wavelength of frequency 3150 Hz, resonances can take place along the gap. Besides, rigid cylinder array with 2 cylinder rows provide more sound wave reflections out of the window inlet opening, thus around

3150 Hz, the Δ TLs resulted from the rigid cylinder arrays V(2,1), V(2,2) and V(2,3) are higher than those due to V(1,2), V(1,3).

5.6.3 Effect of rigid cylinder array with single staggered row

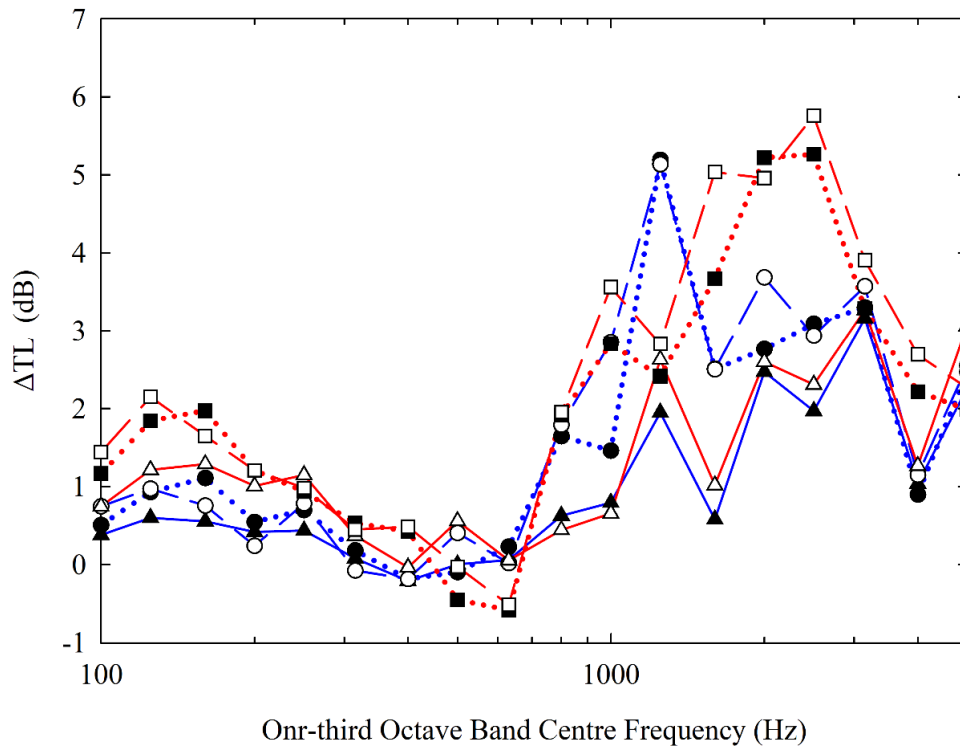


Figure 5. 16 Δ TL of the plenum window (gap: 98mm) installed with single staggered row rigid cylinder array (diameter: 19mm) in One-third octave band.

▲: V(2,2); ●: V(2,2)^S; ○: V(2,2)_S; △:V(2,3); ■:V(2,3)^S; □:V(2,3)_S.

For the cases included in Figure 5.8 (f)-(i), one can find that the acoustic performance of the rigid cylinder array with single staggered row is better than the corresponding regular array both in low and high frequency range from Figure 5.13 and 5.16 in general. Trapped mode exists between the cylinder row of regular rigid array V (2,2) can still be observed in the array V (2,2)_S as shown in Figure 5.17 (c). It excites a

second higher gap mode that reduces the sound wave radiation into the inlet opening and improve the ΔTL . The position of upper cylinder row of $V(2,2)_s$ is close to the antinode of the resonance, reducing the sound energy that propagates into plenum window cavity. On the contrary, the upper cylinder row of $V(2,2)^s$ is placed near to the node position thus resulting in lower ΔTL .

ΔTL dips have been observed around 400Hz for $V(2,2)^s$, $V(2,2)_s$ and at around 630 Hz for $V(2,3)^s$, $V(2,3)_s$ (Figure 5.16).

Around 400 Hz, there are dips for $V(2,2)^s$ and $V(2,2)_s$. The sound field of $V(0,0)$ at 400 Hz is shown in Figure 5.17(a). After the placement of rigid array $V(2,2)^s$ and $V(2,2)_s$, the sound field of $V(2,2)^s$ in Figure 5.17(b) and that of $V(2,2)_s$ in Figure 5.17(c) do not change much. So the ΔTL is small and near to 0 dB.

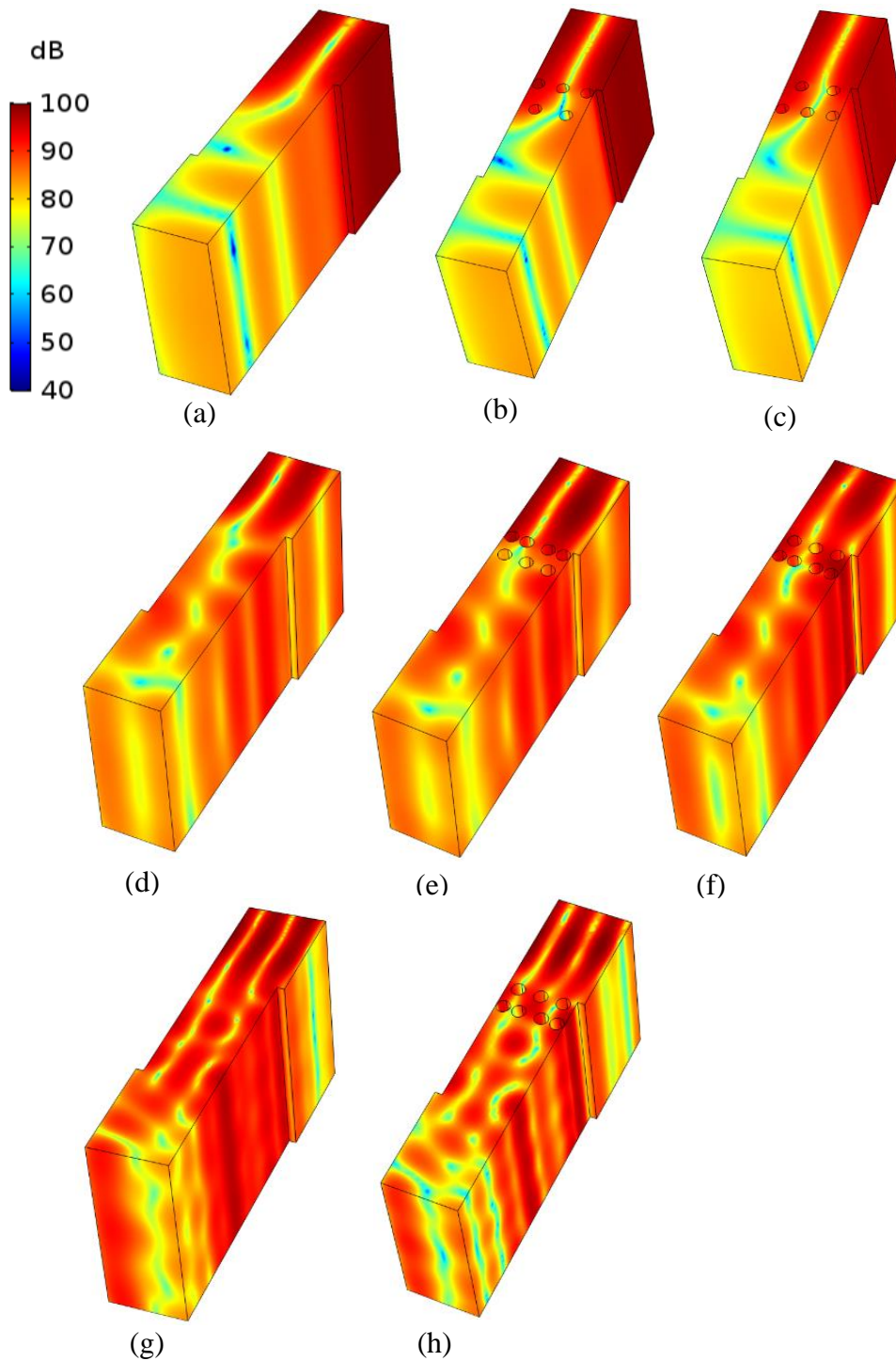


Figure 5. 17 Sound field of the plenum windows installed with staggered rigid cylinder array.

- (a). $V(0,0)$, frequency=400 Hz; (b). $V(2,2)^s$, frequency=400 Hz;
(c). $V(2,2)_s$, frequency=400 Hz; (d) $V(0,0)$, frequency=630 Hz;
(e). $V(2,3)^s$, frequency=630 Hz; (f) $V(2,3)_s$, frequency=630 Hz;
(g). $V(0,0)^s$, frequency=1000 Hz; (h) $V(2,3)_s$, frequency=1000 Hz.

For $V(2,3)^S$ and $V(2,3)_S$, the dips is around 630Hz one-third octave band. The sound field of $V(0,0)$ at 630 Hz is shown in Figure 5.17(d). Comparing the sound field of $V(2,3)^S$ shown in Figure 5.17(e) and that of $V(2,3)_S$ shown in Figure 5.17(f), it is obvious that the sound field does not change much after the placement of the rigid cylinder array $V(2,3)^S$ and $V(2,3)_S$, especially the SPL at the plenum window outlet is almost the same in Figure 5.17 (d) (e) and (f). As a result, the ΔTL dips of the rigid array $V(2,3)^S$ and $V(2,3)_S$ appears at 630 Hz.

At 1000Hz one-third octave band, there is a weak ΔTL peak for $V(2,3)_S$ in Figure 5.16. The sound field of $V(0,0)$ and $V(2,3)_S$ at 1000 Hz is shown in Figure 5.17(g) and (h) respectively. It is found that owing to the placement of rigid cylinder array $V(2,3)_S$, less sound energy can pass through the cylinder array and reach the outlet opening, resulting in lower SPL around the outlet opening of the plenum window as shown in Figure 5.17(h).

It is apparent that at 1250 Hz one-third octave band, there are ΔTL peaks. The reasons for these peaks have been explained in the above section, which is due to the resonance along the gap width.

Around the 2500 Hz one-third octave band, peaks and dips appear. The corresponding wave length is ~ 34 mm. In terms of the total length for the window gap and the thickness of glass is 101 mm, resonances can take place along the window gap. As the sound reflections out of the window opening due to the rigid cylinder array is different, there are difference between the ΔTL s shown in Figure 5.16.

5.6.4 Effect of rigid cylinder array with dual staggered rows

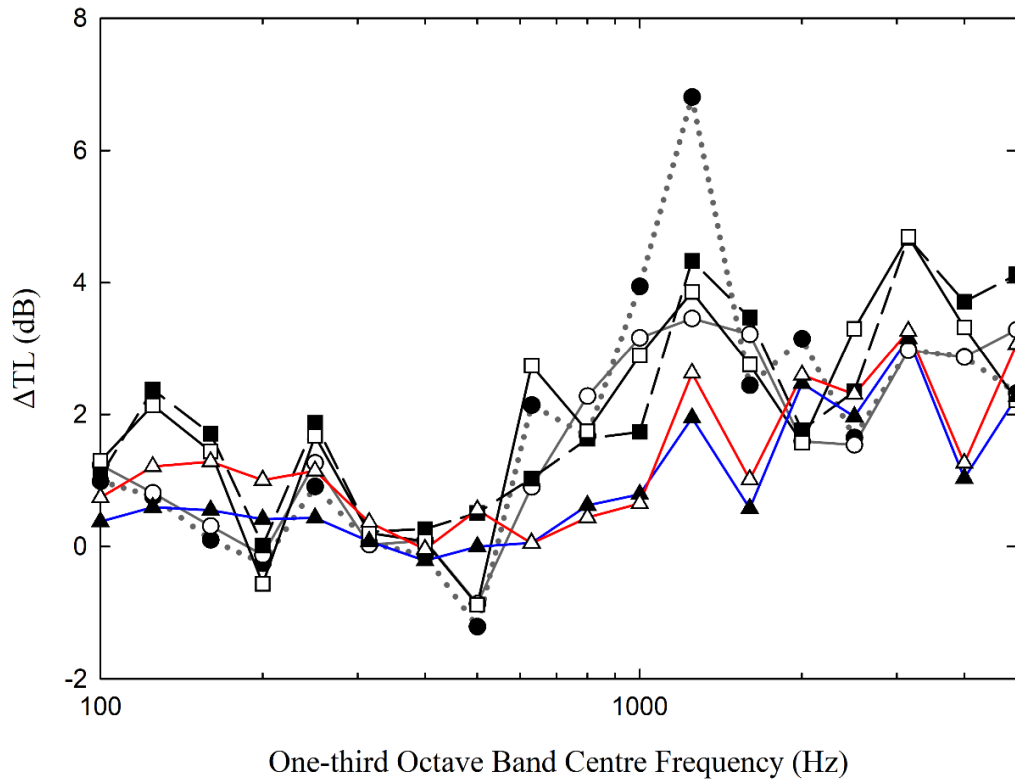


Figure 5. 18 ΔTL of the plenum window (gap: 98mm) installed with dual staggered rows rigid cylinder array (diameter: 19mm) in one-third octave band.

●: $V(2,2)^{ds}$; ○: $V(2,2)_{ds}$; ■: $V(2,3)^{ds}$; □: $V(2,3)_{ds}$. ▲: $V(2,2)$; △: $V(2,3)$;

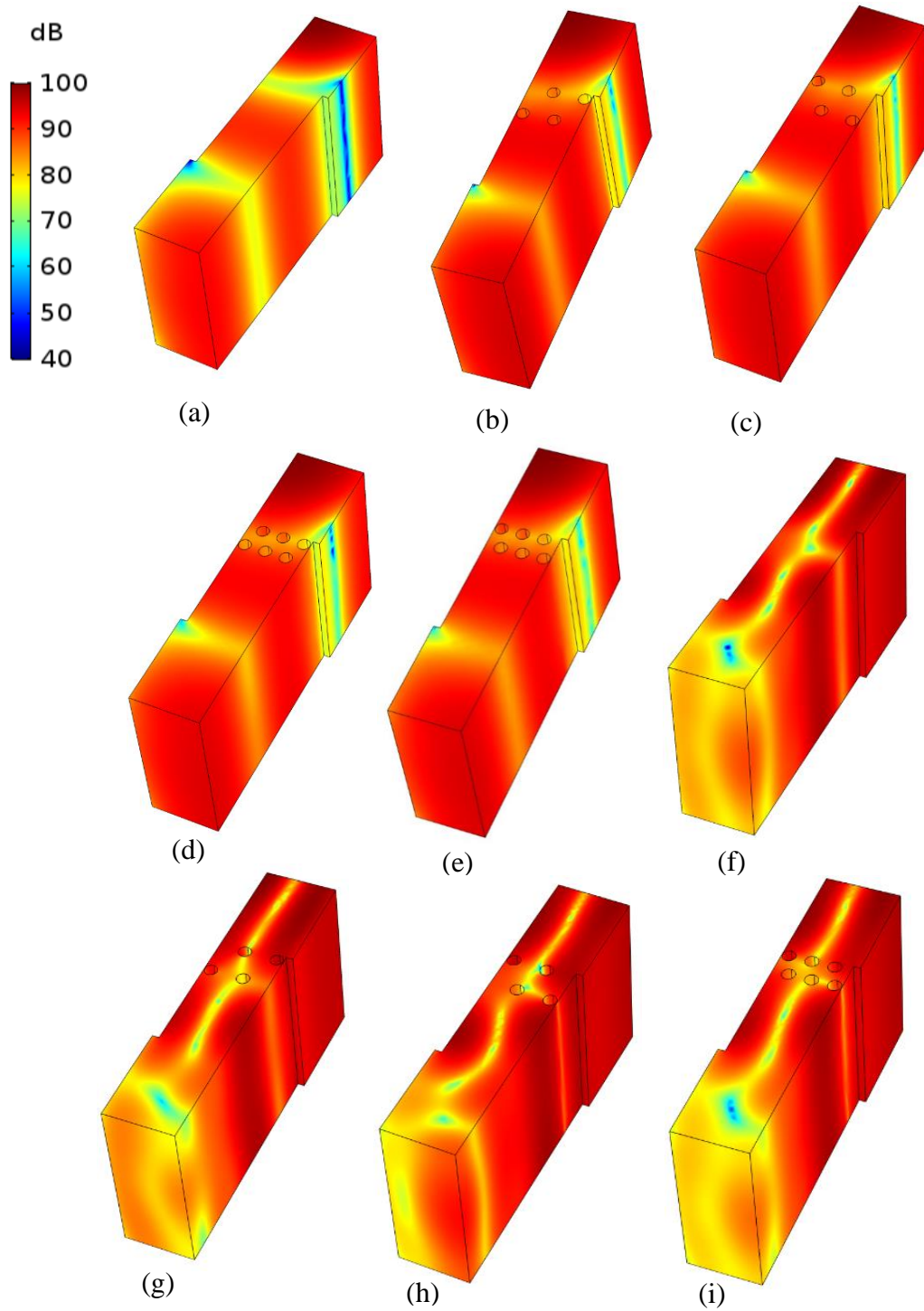


Figure 5.19 Sound field of plenum windows installed with dual staggered rows rigid cylinder array.

- (a). $V(0,0)$, frequency=200 Hz; (b). $V(2,2)^{ds}$, frequency=200 Hz;
(c). $V(2,2)_{ds}$, frequency=200 Hz; (d) $V(2,3)^{ds}$, frequency=200 Hz;
(e) $V(2,3)_{ds}$, frequency=200 Hz; (f) $V(0,0)$, frequency=500 Hz;
(g) $V(2,2)^{ds}$, frequency=500 Hz; (h) $V(2,2)_{ds}$, frequency=500 Hz;
(i) $V(2,3)_{ds}$, frequency=500 Hz;

Around the 200 Hz one-third octave band, there are peaks for all cases installed with dual staggered rows rigid cylinder array as shown in Figure 5.18. The sound field of $V(0,0)$ is shown in Figure 5.19(a). After the installment of the rigid cylinder array $V(2,2)^{ds}$, $V(2,2)_{ds}$, $V(2,3)^{ds}$ and $V(2,3)_{ds}$, the sound field changes slightly as shown in Figure 5.19(b)-(e). Compared to the sound field of $V(0,0)$ in Figure 5.19(a), the SPL at the outlet increases slightly in Figure 5.19(b)-(e). It results in small ΔTL dips for the cases installed with the rigid cylinder array $V(2,2)^{ds}$, $V(2,2)_{ds}$, $V(2,3)^{ds}$, $V(2,3)_{ds}$. Similar phenomenon as mentioned above is observed in the plenum window installed with $V(2,2)^{ds}$, $V(2,2)_{ds}$, $V(2,3)_{ds}$ as shown in Figure 5.19 (f)-(i). Compared to the reference case $V(0,0)$ shown in figure 5.19 (f), the installment of $V(2,2)^{ds}$, $V(2,2)_{ds}$, $V(2,3)_{ds}$ inside the plenum window has an effect on the original sound field of $V(0,0)$ which can reduce the sound energy from passing into the window cavity, thus result in lower ΔTL or slight negative ΔTL around 500 Hz.

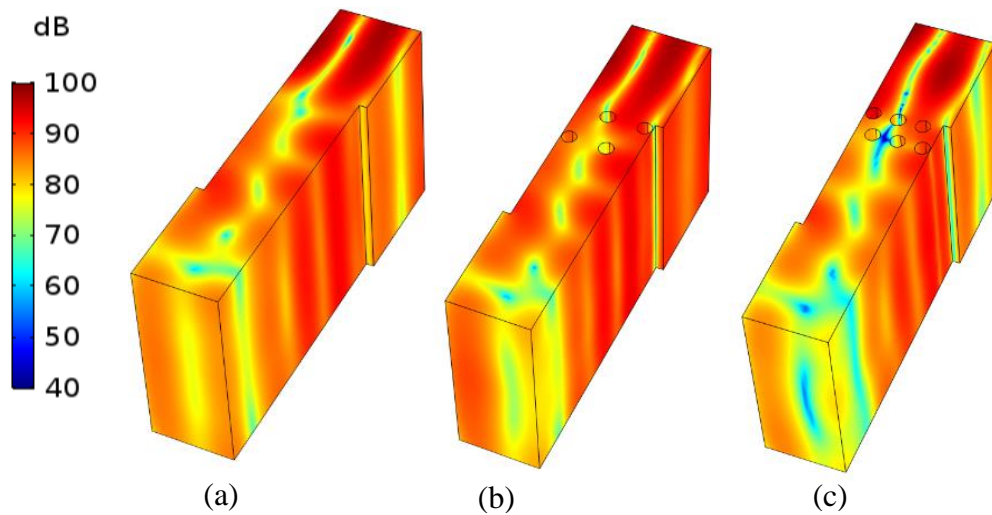


Figure 5. 20 Sound field of plenum windows installed with dual staggered rows rigid cylinder array at 630 Hz.

(a). $V(0,0)$; (b). $V(2,2)_{ds}$; (c). $V(2,3)_{ds}$.

Figure 5.18 shows that, there are peaks for the plenum window installed with $V(2,2)_{DS}$ and $V(2,3)_{DS}$ around 630 Hz. Figure 5.20 shows the sound field inside the plenum window for $V(0,0)$, $V(2,2)_{DS}$ and $V(2,3)_{DS}$. It is apparent that the after the installment of $V(2,2)_{DS}$ and $V(2,3)_{DS}$, the sound field near the outlet of the plenum window has changed. More lower SPL regions appear at the outlet cavity of the plenum window. Compared with Figure 5.20 (b) and (c), one can find that the more sound energy pass into the outlet opening in $V(2,2)_{DS}$, which results in lower ΔTL than in the case of $V(2,3)_{DS}$, as shown in Figure 5.18.

The peaks around 1250 Hz and 3150 Hz is also caused by the resonances along the plenum window gap as mentioned in above sections.

5.6.5 Effect of the gap of plenum window and the diameter of cylinder.

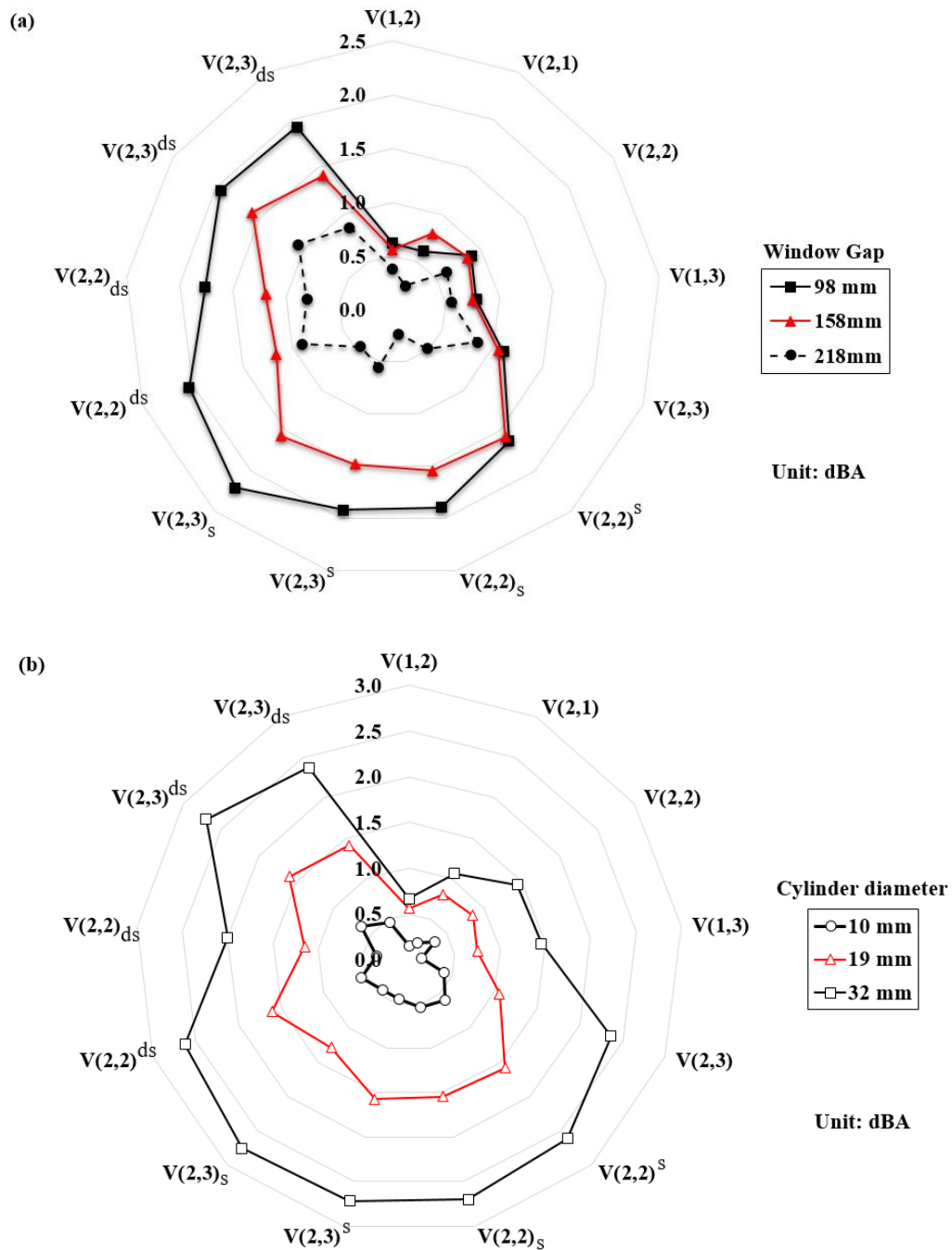


Figure 5. 21 ΔTL_{EN1793} of the plenum widows installed with rigid cylinder array.

(a) ΔTL_{EN1793} of plenum windows with different gaps installed with rigid cylinder arrays with diameter of 19mm;

(b) ΔTL_{EN1793} of plenum window with gap of 158mm installed rigid arrays with

different cylinder diameters.

Figure 5.21 shows that rigid cylinder arrays with single or dual staggered rows have better acoustic performance than the regular rigid cylinder arrays. However, the ΔTL_{EN1793} difference between the cases of $V(2,2)_s$, and $V(2,2)^s$ are comparable (shown in Figure 5.21), which also applies to the ΔTL_{EN1793} of plenum windows installed with rigid cylinder array $V(2,3)_s$, and $V(2,3)^s$. For the same type of rigid cylinder array, $V(2,2)^{DS}$ can always provide a considerable ΔTL as $V(2,2)_{DS}$. This also applies to other cases with same cylinder number and array type. Similar trend can be found for plenum windows with a gap width of 158mm and 218 mm.

It is apparent that for the same arrangement of cylinder array, the $\Delta TL_{EN1793S}$ of plenum window increases with the decreasing gap width when the diameter of the cylinder is 19 mm, as shown in Figure 5.21 (a). A wider gap weakens the acoustical performance of the plenum window, resulting in lower spectral ΔTL and ΔTL_{EN1793} , as shown in table 5.1, table 5.2 and table 5.3. As increasing the gap results in larger distance and space between adjacent cylinders, it leads to weaker reflection of sound back into the inlet cavity of the plenum window and more sound energy goes into the plenum window cavity, reducing the noise reduction. And larger gap means more leakage of the sound energy into the main window cavity.

Table 5. 1 Sound transmission loss of the plenum windows. (Gap=98 mm, cylinder diameter= 19 mm)

| Rigid cylinder array | ΔTL (dB) | | | | | | | | | | | | | | | | | | |
|----------------------------|---|------|------|-------|------|-------|-------|-------|-------|-------|-------|------|-------|------|------|------|------|------|--------|
| | One-third octave band centre frequency (Hz) | | | | | | | | | | | | | | | | | | EN1793 |
| | 100 | 125 | 160 | 200 | 250 | 315 | 400 | 500 | 630 | 800 | 1000 | 1250 | 1600 | 2000 | 2500 | 3150 | 4000 | 5000 | |
| V(1,2) | 0.17 | 0.25 | 0.68 | 0.04 | 0.19 | 0.16 | -0.05 | -0.37 | 0.09 | 0.52 | 1.45 | 1.29 | -0.14 | 1.22 | 1.14 | 1.69 | 0.59 | 1.28 | 0.62 |
| V(2,1) | 0.10 | 0.18 | 0.16 | 0.02 | 0.23 | 0.15 | -0.23 | -0.53 | 0.39 | -0.06 | -0.24 | 2.73 | 1.99 | 1.28 | 1.17 | 2.25 | 0.51 | 1.42 | 0.61 |
| V(2,2) | 0.76 | 0.80 | 0.67 | 0.29 | 0.65 | 0.10 | -0.07 | 0.02 | 0.20 | 0.69 | 0.85 | 1.91 | 0.60 | 2.53 | 1.98 | 3.21 | 0.98 | 1.91 | 0.89 |
| V(1,3) | 0.30 | 0.30 | 1.29 | 0.05 | 0.42 | 0.08 | 0.37 | 0.07 | -0.60 | 0.67 | 1.55 | 0.94 | 1.35 | 0.60 | 1.78 | 1.57 | 1.85 | 2.43 | 0.79 |
| V(2,3) | 0.61 | 1.08 | 1.08 | 0.97 | 1.20 | 0.20 | -0.01 | 0.63 | 0.26 | 0.48 | 0.63 | 2.61 | 1.00 | 2.80 | 2.20 | 3.35 | 1.08 | 2.78 | 1.11 |
| V(2,2) ^s | 0.51 | 0.93 | 1.12 | 0.55 | 0.70 | 0.19 | -0.18 | -0.09 | 0.23 | 1.65 | 1.47 | 5.19 | 2.51 | 2.77 | 3.09 | 3.30 | 0.90 | 2.48 | 1.63 |
| V(2,2) _s | 0.75 | 0.98 | 0.76 | 0.25 | 0.79 | -0.07 | -0.18 | 0.41 | 0.02 | 1.79 | 2.86 | 5.14 | 2.51 | 3.69 | 2.94 | 3.58 | 1.15 | 2.56 | 1.90 |
| V(2,3) ^s | 1.17 | 1.85 | 1.98 | 1.21 | 0.94 | 0.53 | 0.43 | -0.44 | -0.58 | 1.92 | 2.84 | 2.42 | 3.67 | 5.22 | 5.27 | 3.29 | 2.22 | 1.99 | 1.92 |
| V(2,3) _s | 1.57 | 2.08 | 1.55 | 1.16 | 0.96 | 0.46 | 0.38 | 0.06 | -0.47 | 2.14 | 3.51 | 2.72 | 5.16 | 4.85 | 5.73 | 3.97 | 2.53 | 1.99 | 2.22 |
| V(2,2) ^{ds} | 1.00 | 0.77 | 0.11 | -0.24 | 0.92 | 0.06 | -0.12 | -1.20 | 2.15 | 1.68 | 3.95 | 6.81 | 2.45 | 3.15 | 1.66 | 2.99 | 2.88 | 2.33 | 2.03 |
| V(2,2) _{ds} | 1.13 | 0.90 | 0.41 | 0.29 | 1.20 | 0.15 | 0.11 | -0.97 | 0.93 | 2.40 | 3.04 | 3.47 | 3.11 | 1.59 | 1.51 | 3.02 | 2.92 | 3.22 | 1.76 |
| V(2,3) ^{ds} | 1.08 | 2.38 | 1.71 | 0.02 | 1.88 | 0.23 | 0.27 | 0.52 | 1.04 | 1.64 | 1.74 | 4.34 | 3.48 | 1.77 | 2.35 | 4.68 | 3.72 | 4.13 | 1.95 |
| V(2,3) _{ds} | 1.30 | 2.14 | 1.45 | -0.55 | 1.68 | 0.21 | 0.09 | -0.87 | 2.75 | 1.75 | 2.90 | 3.86 | 2.77 | 1.58 | 3.30 | 4.70 | 3.33 | 2.22 | 1.92 |

Table 5. 2 Sound transmission loss of the plenum windows tested. (Gap=158 mm, cylinder diameter= 19 mm)

| Rigid cylinder array | ΔTL (dB) | | | | | | | | | | | | | | | | | | |
|----------------------------|---|-------|------|-------|-------|-------|-------|-------|-------|-------|------|------|------|------|------|------|------|-------|--------|
| | One-third octave band centre frequency (Hz) | | | | | | | | | | | | | | | | | | EN1793 |
| | 100 | 125 | 160 | 200 | 250 | 315 | 400 | 500 | 630 | 800 | 1000 | 1250 | 1600 | 2000 | 2500 | 3150 | 4000 | 5000 | |
| V(1,2) | 0.26 | 0.29 | 0.88 | -0.06 | -0.03 | 0.34 | 0.44 | 0.43 | 0.22 | -0.34 | 1.14 | 0.40 | 1.17 | 0.43 | 2.02 | 0.94 | 2.09 | 0.36 | 0.56 |
| V(2,1) | 0.20 | -0.20 | 1.03 | 0.10 | -0.01 | 0.19 | 0.76 | 0.45 | 0.44 | 0.30 | 1.18 | 0.56 | 2.01 | 1.24 | 2.28 | 0.26 | 1.72 | -0.30 | 0.80 |
| V(2,2) | 0.14 | 0.17 | 1.55 | 0.39 | 0.33 | 0.28 | 0.73 | 0.78 | 0.48 | -0.20 | 0.86 | 0.10 | 2.98 | 2.26 | 2.96 | 1.35 | 2.26 | -1.30 | 0.85 |
| V(1,3) | 0.77 | 0.45 | 1.33 | -0.08 | 0.15 | 0.38 | 0.64 | 0.47 | 0.32 | -0.13 | 1.16 | 0.79 | 1.82 | 0.71 | 2.47 | 0.69 | 2.28 | -0.56 | 0.75 |
| V(2,3) | 0.33 | 0.10 | 0.72 | 0.53 | 0.38 | 0.16 | 0.39 | 0.34 | 0.20 | 0.01 | 1.28 | 1.09 | 3.16 | 2.24 | 3.00 | 2.26 | 2.45 | -0.02 | 1.06 |
| V(2,2) ^s | 0.83 | 0.44 | 1.75 | 0.35 | 0.30 | 0.28 | 0.82 | 1.09 | 1.08 | 0.73 | 2.06 | 1.80 | 4.03 | 2.77 | 3.63 | 1.57 | 2.49 | -1.49 | 1.58 |
| V(2,2) _s | 0.19 | 0.42 | 1.61 | 0.36 | 0.06 | 0.44 | 0.79 | 0.87 | 1.38 | 1.29 | 2.47 | 1.48 | 3.34 | 2.47 | 2.52 | 0.86 | 2.06 | -1.52 | 1.54 |
| V(2,3) ^s | 0.68 | 0.90 | 1.16 | 0.40 | 0.29 | 0.29 | 0.74 | 0.58 | 0.59 | 0.05 | 2.09 | 2.40 | 3.35 | 3.02 | 4.21 | 1.66 | 3.07 | -0.55 | 1.48 |
| V(2,3) _s | 0.89 | 0.48 | 1.64 | 0.29 | 0.19 | 0.52 | 0.90 | 0.47 | 1.06 | 0.25 | 1.99 | 2.61 | 4.40 | 2.52 | 4.10 | 1.45 | 3.19 | -1.71 | 1.57 |
| V(2,2) ^{ds} | 0.72 | 0.64 | 0.49 | -0.13 | 0.13 | -0.18 | -0.01 | -0.02 | 0.98 | 2.18 | 2.09 | 1.30 | 1.82 | 0.69 | 1.86 | 2.09 | 1.65 | -0.38 | 1.16 |
| V(2,2) _{ds} | 0.21 | 0.54 | 0.52 | 0.32 | 0.24 | -0.49 | -0.18 | -0.06 | 0.12 | 3.15 | 1.78 | 2.29 | 1.05 | 1.08 | 1.59 | 2.02 | 2.20 | 0.50 | 1.19 |
| V(2,3) ^{ds} | 0.99 | 0.95 | 0.70 | -0.16 | 0.11 | -0.27 | 0.14 | -0.69 | 1.22 | 1.11 | 2.66 | 3.02 | 3.68 | 1.84 | 2.59 | 3.46 | 3.08 | 1.26 | 1.60 |
| V(2,3) _{ds} | 1.07 | 0.52 | 0.79 | 0.23 | 0.23 | -0.55 | 0.19 | -0.12 | -0.67 | 1.31 | 2.01 | 3.43 | 4.06 | 1.84 | 1.99 | 2.65 | 3.00 | 0.84 | 1.41 |

Table 5. 3 Sound transmission loss of the plenum windows tested. (Gap=218 mm, cylinder diameter= 19 mm)

| Rigid cylinder array | ΔTL (dB) | | | | | | | | | | | | | | | | | | |
|----------------------------|---|-------|-------|-------|-------|-------|-------|-------|-------|-------|------|-------|------|-------|------|------|------|-------|--------|
| | One-third octave band centre frequency (Hz) | | | | | | | | | | | | | | | | | | EN1793 |
| | 100 | 125 | 160 | 200 | 250 | 315 | 400 | 500 | 630 | 800 | 1000 | 1250 | 1600 | 2000 | 2500 | 3150 | 4000 | 5000 | |
| V(1,2) | -0.04 | -0.04 | -0.25 | 0.25 | -0.63 | -0.30 | -0.44 | -0.17 | -0.08 | 0.18 | 0.58 | 0.56 | 0.10 | 2.10 | 1.89 | 1.07 | 0.83 | 0.54 | 0.38 |
| V(2,1) | -0.13 | -0.46 | -0.03 | -0.12 | -0.72 | -0.60 | -0.29 | 0.12 | -0.97 | -0.21 | 0.32 | 0.21 | 0.66 | 2.30 | 1.83 | 0.94 | 0.98 | 2.63 | 0.25 |
| V(2,2) | 0.14 | 0.02 | -0.02 | 0.28 | -0.45 | -0.31 | -0.46 | -0.59 | -0.98 | 0.38 | 0.96 | 1.05 | 0.86 | 3.09 | 2.25 | 1.81 | 1.71 | 3.53 | 0.61 |
| V(1,3) | 0.27 | -0.12 | 0.05 | 0.12 | -0.38 | -0.19 | 0.08 | 0.20 | -0.36 | 0.33 | 0.65 | -0.12 | 1.50 | 2.25 | 1.91 | 1.48 | 1.70 | 2.33 | 0.55 |
| V(2,3) | 0.10 | -0.57 | -0.19 | 0.19 | -0.02 | -0.18 | -0.38 | -0.01 | -0.39 | 0.06 | 1.04 | 0.89 | 2.42 | 3.13 | 2.62 | 2.25 | 2.82 | 3.25 | 0.85 |
| V(2,2) ^s | -0.29 | 0.45 | -0.40 | 0.18 | -1.09 | -0.41 | 0.90 | 0.00 | 0.95 | 0.59 | 0.76 | 0.02 | 0.26 | 0.83 | 1.66 | 2.47 | 1.50 | -0.41 | 0.48 |
| V(2,2) _s | -0.48 | 0.43 | -0.07 | 0.05 | -1.20 | -0.56 | 0.12 | 0.02 | 0.04 | -0.06 | 0.10 | 0.21 | 0.56 | 0.41 | 1.45 | 2.20 | 2.07 | 1.16 | 0.23 |
| V(2,3) ^s | 0.06 | 0.62 | -0.31 | -0.07 | -0.60 | -0.59 | 0.89 | -1.14 | 1.00 | 1.08 | 1.15 | -0.35 | 1.08 | 0.65 | 1.84 | 3.14 | 1.35 | 0.19 | 0.55 |
| V(2,3) _s | -0.26 | 0.29 | -0.11 | 0.07 | -0.79 | -1.03 | 0.74 | -1.28 | 0.12 | 1.17 | 1.07 | 0.28 | 1.21 | -0.79 | 2.87 | 2.98 | 1.86 | 0.81 | 0.46 |
| V(2,2) ^{ds} | 0.31 | 0.29 | 0.09 | -0.22 | 0.49 | 0.16 | 0.10 | 0.98 | 0.33 | 0.51 | 1.18 | 1.21 | 1.34 | 2.00 | 1.93 | 1.26 | 0.97 | 0.48 | 0.91 |
| V(2,2) _{ds} | -0.06 | 0.07 | 0.05 | -0.36 | 0.21 | 0.32 | 0.19 | 0.79 | 0.06 | 0.66 | 1.16 | 1.19 | 1.04 | 1.73 | 1.20 | 1.27 | 1.12 | 0.61 | 0.81 |
| V(2,3) ^{ds} | -0.21 | 0.82 | -0.02 | -0.29 | 0.00 | -0.30 | -0.33 | 0.68 | 0.77 | 1.18 | 1.26 | 1.26 | 1.93 | 2.06 | 2.57 | 2.02 | 1.71 | 0.56 | 1.07 |
| V(2,3) _{ds} | -0.72 | 0.42 | 0.08 | -0.38 | 0.04 | -0.13 | -0.41 | -0.16 | -0.10 | 0.98 | 1.57 | 0.87 | 1.68 | 1.70 | 2.54 | 2.05 | 2.17 | 0.78 | 0.87 |

When the gap of the plenum window is constant, increasing the diameter of the cylinder leads to higher ΔTL_{EN1793} , as shown in Figure 5.21 (b). Plenum windows installed with staggered rigid cylinder arrays perform better. When the gap width is constant, increasing the diameter of the cylinder has the similar effect as the situation mentioned above. Larger cylinders will reduce the space between adjacent cylinders, which results in stronger reflection of the sound energy back into the inlet cavity and can improve the ΔTL . Thus larger cylinder will increase the transmission loss of the plenum window. And the improvement is more obvious at frequencies above 1000 Hz according ΔTL variation in one-third octave band data shown in table 5.2, table 5.4 and table 5.5.

Figure 5.21 (b) shows that with the same plenum window with gap of 158 mm, when the cylinder diameter is 10 mm, the ΔTL_{EN1793} of the plenum window is near to 0 dB. Cylinder array with diameter of 19mm and 32 mm can provide significant ΔTL_{EN1793} up to 2.8 dBA. Results show that increasing the cylinder diameter can enhance the acoustic performance of the plenum window in term of traffic noise reduction. When the ratio between cylinder diameter and plenum window gap is beyond 0.1, ΔTL s are significant in present study.

In present measurements, the ΔTL_{EN1793} of plenum windows installed with single staggered row rigid cylinder array can be as large as ~2.8 dBA and the highest ΔTL_{EN1793} of the plenum window installed with dual staggered rows rigid cylinder array

reaches ~ 2.7 dBA, as shown in table 5.4 . The combination of plenum window with gap of 158 mm and add-in cylinder diameter with 32mm give the best acoustic performance, where the ratio between cylinder diameter and the plenum gap is the highest and about 0.2. In other cases, the ratio between cylinder diameter and the plenum window gap is lower than 0.2. Furthermore, the results suggest that increasing the ratio of r/d helps enhance the acoustical performance of the plenum window after the placement of rigid cylinder array. Thus, the performance of the plenum window will be improved as the ratio of d/G increases.

Table 5. 4 Sound transmission loss of the plenum windows tested. (Gap=158 mm, cylinder diameter= 10 mm)

| Rigid cylinder array | ΔTL (dB) | | | | | | | | | | | | | | | | | | |
|----------------------------|---|-------|-------|-------|------|------|-------|-------|------|-------|------|-------|-------|-------|------|-------|------|-------|--------|
| | One-third octave band centre frequency (Hz) | | | | | | | | | | | | | | | | | | EN1793 |
| | 100 | 125 | 160 | 200 | 250 | 315 | 400 | 500 | 630 | 800 | 1000 | 1250 | 1600 | 2000 | 2500 | 3150 | 4000 | 5000 | |
| V(1,2) | 0.33 | -0.10 | -0.03 | -0.02 | 0.68 | 0.41 | -0.33 | 0.17 | 0.77 | 1.09 | 0.74 | -1.56 | -0.02 | -0.68 | 1.28 | 0.60 | 1.86 | 2.19 | 0.15 |
| V(2,1) | -0.01 | 0.34 | 0.48 | 0.25 | 0.14 | 0.07 | 0.36 | 0.25 | 0.36 | -0.23 | 0.16 | -0.27 | 0.87 | 0.39 | 0.99 | -0.06 | 1.07 | -0.75 | 0.20 |
| V(2,2) | 0.07 | 0.30 | 0.68 | 0.00 | 0.11 | 0.30 | 0.38 | 0.26 | 0.44 | -0.52 | 0.49 | -0.30 | 1.39 | 0.99 | 1.83 | -0.04 | 1.61 | -0.84 | 0.35 |
| V(1,3) | 0.28 | 0.08 | 0.01 | -0.10 | 0.48 | 0.28 | -0.27 | 0.13 | 1.19 | 1.07 | 0.45 | -1.73 | -0.21 | -0.28 | 1.30 | 1.22 | 1.91 | 2.85 | 0.14 |
| V(2,3) | 0.18 | 0.30 | 0.48 | 0.20 | 0.34 | 0.35 | 0.18 | 0.37 | 0.47 | -0.24 | 0.64 | -0.13 | 1.23 | 0.61 | 1.48 | 0.97 | 1.37 | -1.13 | 0.41 |
| V(2,2) ^s | 0.29 | 0.27 | 0.86 | 0.10 | 0.17 | 0.26 | 0.39 | 0.41 | 0.57 | -0.17 | 0.62 | 0.33 | 1.63 | 1.44 | 2.03 | 0.50 | 1.38 | -0.84 | 0.59 |
| V(2,2) _s | 0.18 | -0.23 | 1.15 | 0.14 | 0.28 | 0.28 | 0.33 | 0.43 | 0.58 | -0.22 | 0.78 | 0.12 | 1.58 | 1.32 | 1.28 | 0.28 | 1.33 | -0.75 | 0.54 |
| V(2,3) ^s | 0.20 | 0.18 | -0.05 | 0.31 | 0.46 | 0.08 | -0.23 | 0.26 | 0.55 | 0.02 | 0.09 | 0.33 | 1.15 | 1.81 | 1.65 | 1.19 | 0.40 | -1.12 | 0.45 |
| V(2,3) _s | 0.43 | 0.38 | 0.66 | 0.33 | 0.16 | 0.28 | 0.21 | 0.05 | 0.46 | -0.33 | 0.82 | 0.33 | 0.83 | 0.92 | 1.51 | 1.03 | 0.87 | -1.32 | 0.44 |
| V(2,2) ^{ds} | 0.59 | 0.21 | 0.09 | -0.29 | 0.56 | 0.56 | -0.21 | 0.00 | 1.65 | 1.64 | 0.93 | -0.97 | 0.78 | -0.05 | 1.46 | 1.48 | 2.24 | 2.42 | 0.56 |
| V(2,2) _{ds} | 0.19 | 0.40 | -0.07 | -0.17 | 0.28 | 0.31 | -0.25 | 0.16 | 1.25 | 1.16 | 0.73 | -0.81 | 0.51 | -0.06 | 1.40 | 1.11 | 0.92 | -1.36 | 0.36 |
| V(2,3) ^{ds} | 0.43 | 0.30 | 0.22 | -0.23 | 0.42 | 0.49 | -0.09 | -0.02 | 1.02 | 1.18 | 1.07 | -0.53 | 0.83 | 0.96 | 1.62 | 1.59 | 2.03 | 0.64 | 0.64 |
| V(2,3) _{ds} | 0.26 | 0.27 | -0.03 | 0.18 | 0.46 | 0.28 | -0.43 | 0.23 | 1.19 | 1.27 | 0.88 | -1.12 | 0.47 | 0.06 | 1.76 | 1.86 | 2.31 | 2.55 | 0.46 |

Table 5. 5 Sound transmission loss of the plenum windows tested. (Gap=158 mm, cylinder diameter= 32 mm)

| Rigid cylinder array | <i>ATL</i> (dB) | | | | | | | | | | | | | | | | | | EN1793 |
|----------------------------|---|------|-------|-------|-------|-------|-------|-------|------|-------|------|-------|------|------|------|------|------|------|--------|
| | One-third octave band centre frequency (Hz) | | | | | | | | | | | | | | | | | | |
| | 100 | 125 | 160 | 200 | 250 | 315 | 400 | 500 | 630 | 800 | 1000 | 1250 | 1600 | 2000 | 2500 | 3150 | 4000 | 5000 | |
| V(1,2) | 1.60 | 0.98 | 0.06 | 0.28 | 0.51 | 0.08 | 0.89 | -0.50 | 0.10 | -0.17 | 0.56 | 0.17 | 2.36 | 0.98 | 2.38 | 2.57 | 3.48 | 2.74 | 0.67 |
| V(2,1) | 1.26 | 0.36 | -0.07 | 0.43 | -0.03 | -1.95 | -0.15 | 0.45 | 3.10 | 2.38 | 0.43 | 1.02 | 1.62 | 0.89 | 2.67 | 2.13 | 3.48 | 3.35 | 1.06 |
| V(2,2) | 2.45 | 0.64 | 0.00 | 0.43 | 0.60 | 0.01 | 0.64 | -1.39 | 0.06 | 0.87 | 1.92 | 1.56 | 3.54 | 3.70 | 3.97 | 4.00 | 5.43 | 4.92 | 1.44 |
| V(1,3) | 2.52 | 1.31 | 0.02 | 0.23 | 0.68 | -0.14 | 1.06 | 0.33 | 2.34 | 2.16 | 2.22 | -0.58 | 2.19 | 1.65 | 3.68 | 4.71 | 5.19 | 3.81 | 1.46 |
| V(2,3) | 4.11 | 1.59 | 0.16 | 0.75 | 0.68 | -0.17 | 0.82 | -0.34 | 2.27 | 4.28 | 2.97 | 0.89 | 3.80 | 4.20 | 5.71 | 6.73 | 7.00 | 7.19 | 2.36 |
| V(2,2) ^s | 3.63 | 1.44 | -0.06 | 0.42 | 0.72 | 0.13 | 1.00 | -0.58 | 7.49 | 5.42 | 4.81 | 0.59 | 3.71 | 2.15 | 4.69 | 4.99 | 6.54 | 5.61 | 2.62 |
| V(2,2) _s | 2.31 | 0.62 | -0.09 | 0.49 | 0.80 | 0.13 | -0.05 | -0.35 | 4.28 | 6.58 | 5.28 | 0.92 | 3.82 | 3.20 | 5.66 | 5.35 | 5.72 | 5.44 | 2.7 |
| V(2,3) ^s | 5.80 | 1.74 | 0.18 | 0.39 | 0.86 | 0.77 | 1.69 | -0.39 | 2.27 | 4.50 | 5.32 | 0.63 | 4.95 | 3.43 | 5.43 | 5.72 | 8.09 | 7.23 | 2.72 |
| V(2,3) _s | 4.39 | 1.71 | -0.02 | 0.67 | 0.99 | 0.54 | 0.40 | 0.24 | 0.74 | 4.59 | 5.51 | 1.44 | 5.01 | 3.94 | 5.90 | 6.39 | 8.08 | 7.52 | 2.76 |
| V(2,2) ^{ds} | 1.62 | 0.54 | 0.77 | -0.81 | 0.18 | -0.48 | 0.46 | -0.91 | 4.44 | 4.36 | 4.45 | 5.24 | 4.26 | 3.47 | 3.21 | 2.77 | 2.93 | 0.50 | 2.62 |
| V(2,2) _{ds} | 2.14 | 0.63 | 0.65 | 0.53 | 0.14 | -1.73 | 1.03 | 0.18 | 0.70 | 4.71 | 2.95 | 4.15 | 1.88 | 2.82 | 2.10 | 3.16 | 3.22 | 1.82 | 2 |
| V(2,3) ^{ds} | 3.81 | 1.40 | 0.79 | -0.25 | 0.10 | -0.54 | 1.55 | -1.04 | 3.48 | 2.98 | 4.70 | 3.97 | 4.89 | 4.27 | 3.93 | 4.52 | 4.38 | 2.65 | 2.7 |
| V(2,3) _{ds} | 3.64 | 2.11 | 0.88 | 0.39 | 0.18 | -1.29 | 1.00 | 0.12 | 0.14 | 2.80 | 3.73 | 4.20 | 3.82 | 5.06 | 4.44 | 4.68 | 5.20 | 2.35 | 2.37 |

5.7 Summary

In present study, a 1:4 scale down model was established to study the sound transmission losses of plenum windows installed with different types of rigid cylinder array. Reverberation time inside the model box with and without rigid cylinder arrays was first tested to make sure the reverberation inside the model box had no effect on the TL of the plenum window. A series of measurements were conducted in this study. Three plenum windows with the same length, height but different gaps were included. Different cylinder diameters were studied for acoustical performance improvement inside the plenum window. Δ TL of plenum window installed with different types of rigid cylinder arrays were obtained.

Owing to the placement of rigid cylinder array, there is improvement of the sound transmission loss of the plenum window. The placement of rigid cylinder array increases the sound energy reflections out of the plenum window inlet and decreases the sound energy that passes through the plenum window cavity. At the same time, the resonances inside the window cavity are also contributing to the sound transmission loss of the plenum window. It is noticed that in present study, the main resonances inside the plenum window take place on the horizontal plane and along the gap and length of the plenum window. The resonances along the gap near the inlet opening play an important role in the sound transmission loss.

However, the installment of rigid cylinder array is not always help improve the acoustical protection for the plenum window. The locations of the cylinders have

significant effects on the TL. When the rigid cylinder array is placed on the nodal positions inside the window cavity, the noise reduction will decrease.

Results show that the placement of rigid cylinder array can significantly enhance the acoustical attenuation by as high as ~2.8 dBA in term of traffic noise reduction. As for the arrangement of rigid cylinder arrays, ΔTL_{EN1793} in the presence of regular cylinder array can be up to ~2.3dBA. For the case of single staggered row rigid cylinder array, ΔTL_{EN1793} of the plenum window has been raised by as high as ~2.8dBA. Rigid cylinder arrays with dual staggered rows tend to produce a similar level of sound reduction as the single staggered row rigid cylinder array with the same derived array. Increasing the ratio of r/G helps increase the ΔTL of the plenum window.

The installation of the rigid cylinder array into the plenum window can further improve the sound reduction of the plenum window, thus enhancing traffic noise attenuation of the plenum window. It provides an effective and simple option for the improvement of traffic noise reduction of the plenum window.

Chapter 6 Conclusions and Recommendations

This thesis presents the prediction work for the noise transmission losses across façade with single plenum window, dual plenum windows and triple plenum windows. Besides, experimental and computational study have been conducted on the acoustic performance of the plenum window installed with rigid cylinder array. The main findings and conclusions are summarized in this section. Limitations of present study and future research recommendations are also presented.

6.1 Main Conclusions

Based on the plenum theory in existing literature, Chapter 3 presents a parametric study in an attempt to develop a simple empirical prediction model for the traffic noise transmission loss across plenum windows. Laboratory data and the site measurement results of Tong (2015) were used for the analysis of prediction model validation.

Results suggest that the reverberant field inside the plenum windows is very much weaker than those assumed inside normal plenum chambers studied in existing literature. The diffracted field also has a directivity factor lower than those adopted in plenum chamber theory except at low frequencies.

Three empirical prediction models are proposed and their traffic noise transmission loss prediction performances are compared. The first one is simply the plenum chamber model in existing literature augmented with a constant. A regression analysis using experimental data suggests that this constant is approximately 6 dB. The second one

assumes frequency-independent diffracted field directivity and reverberant field attenuation in the plenum chamber model without any artificial constant. The last one is basically the same as the second model, except that the diffracted field directivity and reverberation field attenuation are obtained in one-third octave bands. The second model gives the best prediction with a standard error of 0.5 dB. Similar error is observed when the independent field mockup data of Tong (2015) are compared with predictions. The third model performs the worst with standard error of 0.7 dB and an overestimation of nearly 1 dB is observed for most of the plenum windows tested.

In Chapter 4, on-site measurement of the traffic noise transmission across plenum windows was carried out in a high-rise residential building located next to a busy trunk road in an opened environment. This building is the first residential public housing block equipped with plenum windows for the acoustical protection of the residents against the very strong traffic noise from the busy trunk road nearby the building.

It is observed that the measured sound levels at the building façades and the shapes of their one-third octave band spectra do not vary much with increasing elevation from the trunk road. The variation of equivalent sound pressure levels from the fifth to the thirtieth floor appears to be just around 2 dBA.

For the flat units with a single plenum window, the results of the present site measurement further validate directly the empirical model developed in Chapter 3. The corresponding discrepancy is within engineering tolerance. The generalized prediction method developed in Chapter 3 also performs well for the cases of multiple plenum windows with a root-mean-square deviation of about 0.8 dBA for the dual plenum window cases and that for the triple plenum window cases is much smaller.

An attempt to improve the sound transmission loss across a plenum window is presented in Chapter 5. A series of laboratory measurements were carried out with a 1:4 scale down model to study the acoustic performance of the plenum window installed with rigid cylinder array. Also, numerical simulations were conducted to explore the sound fields inside the plenum windows. The parametric effect of gap of the plenum window, diameter of the rigid cylinder, arrangement of the rigid cylinder array were studied in detail.

Results showed that the placement of rigid cylinder array inside the central cavity of the plenum window can significantly enhance the acoustical attenuation as high as ~2.8 dBA. As for the arrangement of rigid cylinder array, the best ΔTL that the regular cylinder array can provide is ~2.3 dBA. For the case of the rigid cylinder array with a single stagger row, the best ΔTL that plenum window can give is ~2.8 dBA. In conclusion, dual staggered row rigid cylinder arrays produce similar level of sound reduction as the rigid cylinder array with a single staggered row in general. Results suggest that increasing the ratio of r/g will increase the noise reduction and the installation of the rigid cylinder array inside the plenum window could provide acceptable noise reduction.

6.2 Limitations of this study

Though much efforts has been made for the prediction of plenum window performance and for improving its acoustical performance, there are still few

limitations that need to be pointed out as reference for subsequent studies.

For the work presented in Chapter 4, owing to the dimensions of the plenum windows adopted, the traffic noise transmission losses of the flat unit façades measured in the present study varies over a very narrow range of 10.6 to 13.0 dBA. It is better that large number of plenum windows with totally different dimensions providing wider noise reduction range can be included in future studies.

In Chapter 5, due to the limitations of computer resources, the corresponding 3D simulation at higher frequencies was not carried out. For the present simulation study, the sound source is set as a plane wave incidents normally onto the inlet opening of the plenum window. The case of oblique incidence is not taken into consideration in present computational study. In chapter 5, hollow aluminum tube is adopted as the rigid cylinder in experiment. In order to achieve the ideal performance, Blu Tack was used to seal up the gap between cylinder and top and bottom window frame to prevent possible the sound leakage through these cracks. In present study, the placement position of the cylinder array is not always on the exact position due to the human error as shown in Figure 5.8. To reduce the human error, the exact position of every cylinder has been marked on the top and bottom plane of plenum window in advance to lock cylinders' position. And for every case, the measurements will be repeat for 3 times to reduce the interference of errors.

6.3 Recommendations for future work

For an in-depth understanding the mechanism of the rigid cylinder array installed inside the plenum window, theoretical study is recommended. Due to the limitation of computer resources, the sound field distribution at higher frequencies in 3D simulation is still unclear.

Furtherly, the modification of the plenum window configuration and shape is a potential research for higher noise reduction, especially for the noise reduction at low frequencies. Also, there are some potential work on the modification of the add-in cylinder. Changing the material of cylinder with micro-perforated absorbers may be an interesting option. Both simulation and experiment study on the ventilation performance of the plenum window are also advised.

References

- Asdrubali, F., & Buratti, C. (2005). Sound intensity investigation of the acoustics performances of high insulation ventilating windows integrated with rolling shutter boxes. *Applied Acoustics*, 66(9), 1088-1101.
- Bajraktari, E., Lechleitner, J., & Mahdavi, A. (2015). Estimating the sound insulation of double facades with openings for natural ventilation. *Energy Procedia*, 78, 140-145.
- Basner, M., Babisch, W., Davis, A., Brink, M., Clark, C., Janssen, S., & Stansfeld, S. (2014). Auditory and non-auditory effects of noise on health. *The Lancet*, 383(9925), 1325-1332.
- BS EN ISO 10140-2. Acoustics – Laboratory measurement of sound insulation of building elements. Measurement of airborne sound insulation. BSI : London; 2011.
- BS EN ISO 16283-1. 2014. Acoustics – Field measurement of sound insulation in buildings and of building elements – Part 1: Airborne sound insulation, BSI, London.
- BS EN ISO 16283-3. Acoustics – Field Measurement of sound insulation in buildings and of building elements. Façade sound insulation. London: BSI; 2016.
- BS EN ISO 3382-2. 2008. Acoustics – Measurement of room acoustic parameters – Part 2: Reverberation time in ordinary rooms, BSI, London.

- BS EN1793-3. 1998. Road traffic noise reduction devices – Test methods for determining the acoustic performance, Part 3. Normalized traffic noise spectrum, BSI, London.
- Buratti, C. (2002). Indoor noise reduction index with open window. *Applied Acoustics*, 63(4), 431-451.
- Cheng, W. F., Ng, C. F., & Fung, K. C. (2000). The theoretical model to optimize noise barrier performance at the window of a high-rise building. *Journal of sound and vibration*, 238(1), 51-63.
- Cheung, K. M. C., Wong, H. Y. C., Hung, W. C. T., Lau, K. K., Yim, Y. C. S., & Lee, Y. C. R. (2019, September). Development and application of specially designed windows and balconies for noise mitigation in Hong Kong. In *INTER-NOISE and NOISE-CON Congress and Conference Proceedings* (Vol. 259, No. 2, pp. 7458-7469). Institute of Noise Control Engineering.
- Cummings, A. (1978). The attenuation of lined plenum chambers in ducts: I. Theoretical models. *Journal of sound and vibration*, 61(3), 347-373.
- Cummings, A., & Wing-King, A. M. (1979). The attenuation of lined plenum chambers in ducts, II: Measurements and comparison with theory. *Journal of Sound and Vibration*, 63(1), 19-32.

- El Dien, H. H., & Woloszyn, P. (2004). Prediction of the sound field into high-rise building facades due to its balcony ceiling form. *Applied Acoustics*, 65(4), 431-440.
- El Dien, H. H., & Woloszyn, P. (2005). The acoustical influence of balcony depth and parapet form: experiments and simulations. *Applied Acoustics*, 66(5), 533-551.
- Environmental Protection Department. 2006. A comprehensive plan to tackle road traffic noise in Hong Kong, Hong Kong Special Administration Region, Hong Kong.
- Ford, R. D., & Kerry, G. (1973). The sound insulation of partially open double glazing. *Applied Acoustics*, 6(1), 57-72.
- Fritschi, L., Brown, L., Kim, R., Schwela, D., & Kephelopoulos, S. (2011). Burden of disease from environmental noise: Quantification of healthy life years lost in Europe. *WHO regional office for Europe*.
- Fry, A. (1988) *Noise Control in Building Services*, Pergamon, Oxford.
- Garai, M., & Guidorzi, P. (2000). European methodology for testing the airborne sound insulation characteristics of noise barriers in situ: Experimental verification and comparison with laboratory data. *The Journal of the Acoustical Society of America*, 108(3), 1054-1067.

- Gierke V. (1990). *Acoustics: Determination of occupational noise exposure and estimation of noise-induced hearing impairment*. International Organization for Standardization. ISO/DIS 1999[J]. *American Journal of Hospice & Palliative Care*, 1990, 38(9):1001-8.
- Hammad, R. N. S., & Gibbs, B. M. (1983). The acoustic performance of building façades in hot climates: Part 2—Closed balconies. *Applied Acoustics*, 16(6), 441-454.
- Hammad, R. N. S., & Gibbs, B. M. (1983). The acoustic performance of building façades in hot climates: Part 1—Courtyards. *Applied Acoustics*, 16(2), 121-137.
- Hänninen, O., Knol, A. B., Jantunen, M., Lim, T. A., Conrad, A., Rappolder, M., & Torfs, R. (2014). Environmental burden of disease in Europe: assessing nine risk factors in six countries. *Environmental health perspectives*, 122(5), 439-446.
- Hardy, H. C. (1952). Design Characteristics for Noise Control of Jet Engine Test Cells. *The Journal of the Acoustical Society of America*, 24(2), 185-190.
- Hart, C. R., & Lau, S. K. (2012). Active noise control with linear control source and sensor arrays for a noise barrier. *Journal of sound and vibration*, 331(1), 15-26.
- Hong Kong Planning Standard and Guidelines. (1990). Environmental Protection Department, the HKSAR Government.

- Hothersall, D. C., Horoshenkov, K. V., & Mercy, S. E. (1996). Numerical modelling of the sound field near a tall building with balconies near a road. *Journal of Sound and Vibration*, *198*(4), 507-515.
- Huang, H., Qiu, X., & Kang, J. (2011). Active noise attenuation in ventilation windows. *The Journal of the Acoustical Society of America*, *130*(1), 176-188.
- Hughes, T. L., & Mabry, J. E. (1976). The relationship between aircraft noise annoyance and duration above specified noise levels. *The Journal of the Acoustical Society of America*, *60*(S1), S84-S84.
- Hygge, S. (2011). Noise and cognition in children. *Encyclopedia of Environmental Health*, 146-151.
- Ih, J. G. (1992). The reactive attenuation of rectangular plenum chambers. *Journal of Sound and Vibration*, *157*(1), 93-122.
- Ishizuka, T., & Fujiwara, K. (2012). Traffic noise reduction at balconies on a high-rise building façade. *The Journal of the Acoustical Society of America*, *131*(3), 2110-2117.
- Jafari, Z., Kolb, B., & Mohajerani, M. (2019). Noise exposure accelerates the risk of cognitive impairment and Alzheimer's disease: Adulthood, gestational, and prenatal mechanistic evidence from animal studies. *Neuroscience & Biobehavioral Reviews*.

- Janczur, R., Walerian, E., & Czechowicz, M. (2011). Façade shaping as local means protecting against traffic noise. *Acta Acustica united with Acustica*, 97(5), 769-778.
- Jean, P. (2009). Sound transmission through opened windows. *Applied acoustics*, 70(1), 41-49.
- Kang, J., & Brocklesby, M. W. (2005). Feasibility of applying micro-perforated absorbers in acoustic window systems. *Applied Acoustics*, 66(6), 669-689.
- Kang, J., & Li, Z. (2007). Numerical simulation of an acoustic window system using finite element method. *Acta acustica united with acustica*, 93(1), 152-163.
- Khan, J., Ketzler, M., Kakosimos, K., Sørensen, M., & Jensen, S. (2018). Road traffic air and noise pollution exposure assessment – A review of tools and techniques. *Science Of The Total Environment*, 634, 661-676.
- Kinsler, L. E., Frey, A. R., Coppens, A. B., & Sanders, J. V. (2000). Fundamentals of acoustics, 560. *New York: Wiley*.
- Ko, N. W. M. (1978). Traffic noise in a high-rise city. *applied acoustics*, 11(3), 225-239.
- Ko, N. W. M., NWM, K., & CP, T. (1978). REVERBERATION TIME IN A HIGH-RISE CITY.

- Kropp, W., & Brillon, J. (1998). A theoretical model to investigate the acoustic performance of building facades in the low and middle frequency range. *Acta Acustica united with Acustica*, 84(4), 681-688.
- Kurze, U. J., & Anderson, G. S. (1971). Sound attenuation by barriers. *Applied Acoustics*, 4(1), 35-53.
- Lau, S. K., & Tang, S. K. (2000). Sound fields in a slightly damped rectangular enclosure under active control. *Journal of sound and vibration*, 238(4), 637-660.
- Lee, H. M., Haris, A., Lim, K. M., Xie, J., & Lee, H. P. (2019). Environmental Noise Mitigation by Plenum Window with Sonic Crystals and Jagged Flap. *Fluctuation and Noise Letters*, 18(01), 1950001.
- Lee, H. M., Wang, Z., Lim, K. M., Xie, J., & Lee, H. P. (2020). Novel plenum window with sonic crystals for indoor noise control. *Applied Acoustics*, 167, 107390.
- Li, K. M., & Tang, S. H. (2003). The predicted barrier effects in the proximity of tall buildings. *The Journal of the Acoustical Society of America*, 114(2), 821-832.
- Li, X., & Hansen, C. H. (2005). Comparison of models for predicting the transmission loss of plenum chambers. *Applied Acoustics*, 66(7), 810-828.

- Liu, Z. S., Lee, H. P., & Lu, C. (2006). Passive and active interior noise control of box structures using the structural intensity method. *Applied Acoustics*, 67(2), 112-134.
- May, D. N. (1979). Freeway noise and high-rise balconies. *The Journal of the Acoustical Society of America*, 65(3), 699-704.
- Meissner, M. (2012). Acoustic energy density distribution and sound intensity vector field inside coupled spaces. *The Journal of the Acoustical Society of America*, 132(1), 228-238.
- Miedema, H. M., & Vos, H. (2007). Associations between self-reported sleep disturbance and environmental noise based on reanalyses of pooled data from 24 studies. *Behavioral sleep medicine*, 5(1), 1-20.
- Mohsen, E. A., & Oldham, D. J. (1977). Traffic noise reduction due to the screening effect of balconies on a building façade. *Applied Acoustics*, 10(4), 243-257.
- Morse, P. M. (1968). KU Ingard, Theoretical Acoustics. *Princeton University Press*, 949p, 4, 150.
- Munjal, M. L. (1987a). A simple numerical method for three-dimensional analysis of simple expansion chamber mufflers of rectangular as well as circular cross-section with a stationary medium. *Journal of Sound and Vibration*, 116(1), 71-88.

- Munjal, M. L. (1987b). *Acoustics of ducts and mufflers with application to exhaust and ventilation system design*. John Wiley & Sons.
- Öhrström, E., Skånberg, A., Svensson, H., & Gidlöf-Gunnarsson, A. (2006). Effects of road traffic noise and the benefit of access to quietness. *Journal Of Sound And Vibration*, 295(1-2), 40-59.
- Okubo, T., & Fujiwara, K. (1998). Efficiency of a noise barrier on the ground with an acoustically soft cylindrical edge. *Journal of Sound and Vibration*, 216(5), 771-790.
- Oldham, D. J., & Mohsen, E. A. (1979). The acoustical performance of self-protecting buildings. *Journal of Sound and Vibration*, 65(4), 557-581.
- Peters, R. J. (2013). *Acoustics and noise control*. Routledge.
- Sabine, W.C. (1964). *Collected Papers in Acoustics*, Dover, New York.
- Sakamoto, S., Ito, K., & Asakura, T. (2008, October). Experimental study on the noise shielding effects of eaves attached on building façade. In *INTER-NOISE and NOISE-CON Congress and Conference Proceedings* (Vol. 2008, No. 6, pp. 3379-3386). Institute of Noise Control Engineering.
- Sharland, I., & Ltd Woods of Colchester. (1972). *Woods practical guide to noise control*. Woods of Colchester Limited.

- Søndergaard, L. S., & Legarth, S. V. (2014, November). Investigation of sound insulation for a supply air window—Field measurements and occupant responses. In *Proceedings of the 43rd International Congress and Exposition on Noise Control Engineering, Melbourne, Australia* (pp. 16-19).
- Tadeu, A. J., & Mateus, D. M. (2001). Sound transmission through single, double and triple glazing. Experimental evaluation. *Applied Acoustics*, 62(3), 307-325.
- Tadeu, A., Ant ́nio, J., Mendes, P. A., & Godinho, L. (2007). Sound pressure level attenuation provided by thin rigid screens coupled to tall buildings. *Journal of sound and vibration*, 304(3-5), 479-496.
- Takagi, K., Miyake, T., Yamamoto, K., & Tachibana, H. (2000, August). Prediction of road traffic noise around tunnel mouth. In *Proc. InterNoise* (Vol. 2000, pp. 3099-3104).
- Tang, S. K. (2005). Noise screening effects of balconies on a building facade. *The Journal of the Acoustical Society of America*, 118(1), 213-221.
- Tang, S. K. (2010). Scale model study of balcony insertion losses on a building facade with non-parallel line sources. *Applied acoustics*, 71(10), 947-954.
- Tang, S. K. (2015, August). Acoustical protection of a plenum window installed with sound absorptions. In *Proceedings of the 44th International Congress and Exposition on Noise Control Engineering, San Francisco, CA, USA*.

- Tang, S. K. (2016, August). Sound transmission across plenum windows with non-parallel glass panes. In *INTER-NOISE and NOISE-CON Congress and Conference Proceedings* (Vol. 253, No. 7, pp. 1326-1330). Institute of Noise Control Engineering.
- Tang, S. K. (2017). A review on natural ventilation-enabling façade noise control devices for congested high-rise cities. *Applied Sciences*, 7(2), 175.
- Tang, S. K. (2018). Reduction of sound transmission across plenum windows by incorporating an array of rigid cylinders. *Journal of Sound and Vibration*, 415, 25-40.
- Tang, S. K., Tong, Y. G., & Tsui, K. L. (2016). Sound transmission across a plenum window with an active noise cancellation system. *Noise Control Engineering Journal*, 64(4), 423-431.
- The European Environment Agency (EEA). 2013. Air Pollutant Emission Inventory Guidebook. Retrieved from. <http://www.eea.europa.eu/publications/emep-eeaguidebook-2013>.
- Tong, Y. G., & Tang, S. K. (2013). Plenum window insertion loss in the presence of a line source—A scale model study. *The Journal of the Acoustical Society of America*, 133(3), 1458-1467.

- Tong, Y. G., Tang, S. K., & Yeung, M. K. L. (2011). Full scale model investigation on the acoustical protection of a balcony-like facade device (L). *The Journal of the Acoustical Society of America*, *130*(2), 673-676.
- Tong, Y. G., Tang, S. K., Kang, J., Fung, A., & Yeung, M. K. L. (2015). Full scale field study of sound transmission across plenum windows. *Applied acoustics*, *89*, 244-253.
- Vienneau, D., Schindler, C., Perez, L., Probst-Hensch, N., & Rössli, M. (2015). The relationship between transportation noise exposure and ischemic heart disease: a meta-analysis. *Environmental research*, *138*, 372-380.
- Wallas, A., Ekström, S., Bergström, A., Eriksson, C., Gruzieva, O., Sjöström, M., ... & Pershagen, G. (2019). Traffic noise exposure in relation to adverse birth outcomes and body mass between birth and adolescence. *Environmental research*, *169*, 362-367.
- Wells, R. J. (1957). Acoustical Plenum Chambers. *The Journal of the Acoustical Society of America*, *29*(1), 186-186.
- Wells, R. J. (1958). Acoustical plenum chambers. *Noise Control*, *4*(4), 9-15.
- World Health Organization. (2018). Environmental noise guidelines for the European region.

Yu, X., Lau, S. K., Cheng, L., & Cui, F. (2017). A numerical investigation on the sound insulation of ventilation windows. *Applied Acoustics*, 117, 113-121.

Zuccherini Martello, N., Fausti, P., Santoni, A., & Secchi, S. (2015). The use of sound absorbing shading systems for the attenuation of noise on building façades. An experimental investigation. *Buildings*, 5(4), 1346-1360.